UNIVERSITY OF LONDON THESIS

Degree PhD Year 2006 Name of Author McHUGH Patrick Michael

Precipitation of Nucleic Acids for Selective Recovery of Plasmid DNA

by

Patrick M. McHugh

A thesis submitted for the degree of

Doctor of Philosophy

in

The Department of Biochemical Engineering

University College London

June 2006

ProQuest LLC
789 East Eisenhower Parkway
P.O. Box 1346
Ann Arbor, MI 48106-1346

ABSTRACT

Nucleic acids are being targeted more commonly as pharmaceutical therapeutic agents, and consequently the ability to purify these biological macromolecules at large scale has taken on increased importance. Although precipitation of nucleic acids plays a key role in existing purification processes, the effects of different process variables are not well understood. In recovery processes, typically supercoiled plasmid DNA is the form of interest, however because other nucleic acid forms (chromosomal DNA, RNA, relaxed plasmid DNA) are very similar to plasmid DNA both structurally and chemically, separation of plasmid DNA from these forms represents a significant challenge.

This project studied the precipitation behaviour of different nucleic acids forms in typical clarified lysate streams from *E. coli* fermentation. Solubilities of individual forms were studied, investigating effects of process variables such as salt type, salt concentration, organic solvents, and polymers. Key findings from single-component studies showed monovalent cations alone to be relatively ineffective agents for precipitation of any of the nucleic acid forms studied. Divalent cations alone were relatively ineffective for precipitation of double-stranded DNA, however they were effective agents for precipitation of RNA and single-stranded DNA, suggesting these salts may be effective for fractional precipitation of these forms. Inclusion of organic solvents or polymers decreased solubilities of all forms in the presence of either monovalent or divalent cations.

Single-component findings were extended to investigation of multi-component clarified lysate process streams. To aid in this effort, an analytical anion-exchange HPLC method was developed to quantify different nucleic acid forms from multi-component streams. This analytical method was used to show divalent cations were effective for the fractional precipitation of the majority of single-stranded nucleic acid impurities in clarified lysate, leaving most of the plasmid DNA plus small quantities of chromosomal DNA and RNA impurities in solution.

Single-component results were further extended through the development of a novel controlled thermal-denaturation step prior to divalent cation precipitation. This step converted double-stranded DNA forms, with the exception of supercoiled plasmid, to the single-stranded form. Performing thermal denaturation on clarified lysate streams prior to divalent cation precipitation resulted in improved separation of chromosomal and relaxed plasmid DNA forms, leaving highly-purified supercoiled DNA in solution following precipitation. A non-chromatographic purification process for recovery of supercoiled plasmid DNA is proposed based on these results. Findings were further characterised through kinetics of precipitation studies, investigation of precipitation mechanisms, comparison to solubility models, and investigation of plasmid stability.

ACKNOWLEDGMENTS

I am very grateful to Mike for his guidance and patience throughout this project. Thanks to Susana and Markus for their warm introduction to the department and helpful discussions. To Misti, Fran, and Julia for the fond memories from our UCL experience together. I'm also appreciative of Ann and Barry for helping to make this experience possible. Finally, special thanks to Lya for her love and support throughout and to my parents Brian and Maryellen.

CONTENTS

LIST OF FIGURES

LIST OF TABLES

1 INTRODUCTION

1.1 Motivation for the project

Due to the continuing advances in gene therapy and DNA vaccination, there is a growing need to manufacture large quantities of highly purified plasmid DNA vectors. One of the biggest challenges in purifying plasmid DNA is separating the desired supercoiled plasmid DNA form from other nucleic acids, including host-cell chromosomal DNA and RNA as well as non-supercoiled plasmid DNA forms. Traditional laboratory techniques, including cesium chloride density gradients, are scale-limited. Current large-scale purification protocols rely heavily on chromatography to achieve these separations. Because of the large size of nucleic acids, traditional chromatographic resins have a much lower capacity for nucleic acids compared to other biomolecules such as proteins; hence at manufacturing scale large and/or multiple columns are needed, making chromatography an expensive unit operation in the recovery process.

Laboratory plasmid DNA purification protocols typically use RNAse A to digest the high impurity load of RNA prior to chromatographic separation. Although effective for RNA clearance, the use of mammalian-derived enzymes such as RNase A in the manufacture of human products is undesirable because of concerns over the introduction of pathogens into the process stream; furthermore extensive testing is required to demonstrate their absence in the final product.

Improvements in upstream plasmid DNA purification steps without the use of RNAse A could reduce or even eliminate the reliance on downstream

chromatography at large scale. One of the upstream steps typically used during plasmid purification is precipitation. Existing precipitation steps have generally been developed from empirical laboratory studies or existing protein purification methods, and the precipitation of different forms of nucleic acids, in particular RNA and single-stranded DNA, have not been studied in detail. The studies carried out in this project used different nucleic acid forms and mixtures to provide an improved understanding of their precipitation properties, which could ultimately lead to process improvements for plasmid DNA purification.

1.2 Aims of the project

The overall objective of the project was to develop an improved understanding of nucleic acid precipitation properties, to underpin the specification of bioprocesses for plasmid DNA purification and recovery. Specific aims included:

i. Identifying suitable precipitating agents for further detailed characterisation

ii. Performing single-component solubility experiments for different types of nucleic acids (plasmid DNA, double-stranded chromosomal DNA, denatured single-stranded chromosomal DNA, RNA) to assess the effect of process variables including different counter-ions, pH, starting nucleic acid concentration, added organic anti-solvents, added neutral polymer (PEG), and nucleic acid size

iii. Using results from single-component experiments and follow-up experiments to draw conclusions about trends and mechanisms involved in the precipitation of different types of nucleic acids

iv. Characterising kinetics of precipitation for nucleic acids to assess the impact of initial contacting conditions on solubilities

v. Developing an HPLC assay so that different forms of nucleic acids can be quantified from multi-component streams, in order to assess effectiveness of precipitation on these streams

vi. Developing novel methods related to precipitation to improve fractionation of plasmid DNA from other nucleic acids in a complex process stream

vii. Assessing the scalability of precipitation methods developed

viii. Assessing existing solubility / precipitation models for predicting nucleic acid behaviour

1.3 Background on gene therapy and DNA vaccination

Recent advances in molecular biology have led to the introduction of gene therapy and nucleic acid vaccination for the treatment and prevention of disease. Gene therapy involves the introduction of genes to specific types of cells in a patient, causing these cells to produce therapeutic proteins or other biomolecules targeted against disease in the patient. DNA vaccination involves a similar introduction of genes to cells, however in this case the biomolecules produced serve as antigens to enhance the immune response against a target pathogen.

Using genes for the treatment and prevention of disease offers several potential advantages over traditional therapies. Some of these include the potential for long-term expression of therapeutic biomolecules, straightforward adaptability for expression of new biomolecules once their genes have been identified, the potential for co-delivery of multiple genes for multiple forms of therapy, and the potential to use the same manufacturing process for the production of many different therapeutic products.

Various delivery vectors have been successful in introducing therapeutic genes to cells in animal studies, and studies are ongoing to determine which vectors will be most appropriate for humans. Most of the initial work in the early 1990s used either viral DNA or plasmid DNA injected into mice to demonstrate expression of foreign genes (Wolff et al., 1990;Tang et al., 1992). Using recent recombinant DNA techniques, foreign DNA was modified to contain therapeutic genes of interest; successful expression of the therapeutic genes was also obtained in mice, but at lower levels than would be needed to treat disease. Gene delivery systems are intended mainly to enhance uptake of these therapeutic genes by a patient's cells and thereby improve expression levels. Other than plasmid DNA alone, delivery systems currently under study include plasmid DNA complexed with cationic liposomes (Gao and Huang, 1995), bacteria containing plasmid DNA (Sizemore et al., 1997), adenoviruses (Rosenfeld et al., 1992), retroviruses (Vile and Russell, 1995), and other viruses (Jolly, 1994). To date, each vector has shown certain advantages and disadvantages. Some studies are now underway using more than one type of delivery vector. Considering the current state of development, it is likely that plasmid DNA will be used in one form or another in the future for gene delivery to humans.

1.4 Background on existing plasmid processes

1.4.1 Vector and host-cell selection

The vast majority of existing methods for non-viral gene therapy or vaccination are based on plasmid DNA propagated in *Escherichia coli* bacteria. *E. coli* is a gram-negative bacteria which may contain naturally occurring plasmids. The choice of *E. coli* as the system for plasmid propagation was a natural extension of many years of study and characterisation of this organism. Recombinant DNA techniques make possible the construction of many different types of plasmids, so the first consideration is the design of the plasmid itself. Of primary importance is the inclusion of the therapeutic gene(s) of interest and other elements to regulate gene expression. There are other considerations from a manufacturing perspective, including the size of the plasmid, its origin of replication (which plays a major role in determining the copy number in a given bacterial host), stability during fermentation, and inclusion of a selectable marker gene in the plasmid (Imanaka and Aiba, 1981;Seo and Bailey, 1985). An example of a selectable marker typically used is an antibiotic-resistance gene, which when used in conjunction with the corresponding antibiotic during fermentation, ensures that plasmid-free cells do not overwhelm the growth of the plasmid-containing cells during fermentation.

Once the full nucleotide sequence of a plasmid has been designed and constructed through recombinant techniques (Cohen et al., 1973), it is typically established in a chosen strain of *E. coli* bacteria. Many different strains have been used, and there is currently no clear choice for the best strain to use. Desirable characteristics of the strain include compatibility with high plasmid copy number

and high cell density during fermentation, minimal generation of plasmid-free cells, minimal genetic changes to the plasmid, and compatibility with downstream purification (Eastman and Durland, 1998). Once the plasmid has been established in the chosen bacterial strain, a master cell bank is established and extensively characterised in accordance with regulatory guidelines (USFDA Center for Biologics Evaluation and Research, 1993). The master cell bank is divided into many vials, which are stored frozen until needed to seed a fermentation batch.

1.4.2 Fermentation

The fermentation process begins with the thawing of one of the master cell bank vials. The contents are typically added to fresh fermentation medium in a shake flask and grown at 37 °C to produce a primary seed culture. This primary culture is introduced directly to the fermentation vessel or in some cases (e.g. for large fermentation volumes) used as an inoculum for a secondary seed. The fermentation medium, whether complex or fully defined (by blending of purified components), is the source of carbon, nitrogen, phosphate, and other nutrients that are essential for cell propagation. The media composition along with temperature, pH, dissolved oxygen concentration, and agitation all have effects on the cell growth, plasmid yield, and plasmid form. Fermentation can be performed as either a batch process or fed-batch process, whereby additional nutrients are added during growth. Fermentations typically proceed for approximately 12-24 hours to obtain a target cell density that has been empirically determined to optimise plasmid yield and quality. Published examples cite plasmid yields of anywhere from about 5 to 250 mg per L of fermentation broth, depending on the type of plasmid, the *E. coli* strain and the

fermentation conditions (Horn et al., 1995;Lahijani et al., 1996;Eastman and Durland, 1998). Following fermentation, bacterial cells are harvested by centrifugation or filtration, and the cell paste is either immediately processed or frozen for future use.

1.4.3 Cell lysis

Bacterial cell lysis is necessary to release plasmid DNA to the extracellular environment prior to purification. Cell lysis is a critical processing step, in that it (along with initial clarification) defines the upper limits on the final recoverable plasmid, and it also has a large impact on achievable purity level for a given purification process. Many different methods are available including mechanical disruption, enzymatic treatment, osmotic lysis, heat lysis, and various chemical methods. The most widely used approach is a variation of an alkaline lysis method first described by Birnboim and Doly (Birnboim and Doly, 1979), as described briefly below.

The bacterial cell paste is resuspended in a Tris/EDTA buffer. It should be noted that in laboratory methods, RNAse A is typically included in the resuspension buffer such that digestion of RNA occurs during the lysis procedure; this is an effective way to clear the majority of RNA, however as mentioned previously the use of mammalian-derived enzymes in the manufacture of human parenteral products is undesirable (Eastman and Durland, 1998;Prazeres et al., 1999). After fully resuspending the cells, lysis buffer containing sodium hydroxide and sodium dodecyl sulphate (SDS) is added. In addition to disrupting the *E. coli* cell walls/membranes, the alkaline environment during this step is thought to denature both host-cell chromosomal DNA and plasmid DNA into single-stranded forms to

a certain extent, although plasmids are thought to remain closed-circular. Many cellular proteins and lipids are also denatured and solubilised. After incubating in the lysis conditions for a short period, potassium acetate neutralisation buffer is added. Addition of this buffer reduces the pH such that most of the plasmid DNA renatures to its original double-stranded form while leaving much of the chromosomal DNA denatured. Addition of this neutralisation buffer also causes a co-precipitation/flocculation of SDS, denatured chromosomal DNA, proteins, lipids, and cell debris into a curd-like substance. Mixing is a key parameter during the entire lysis procedure, since local pH extremes are known to cause irreversible denaturation of plasmids (Rush and Warner, 1970); however, excessive shear from over-mixing also tends to solubilise chromosomal DNA. Thus mixing speed is set to balance the need for fast dispersion of NaOH with that of chromosomal DNA insolubility.

1.4.4 Clarification

The precipitated material is typically removed by filtration or centrifugation. Filtration is preferred because some of the precipitate has a lower density than the buffer, making clearance by centrifugation difficult. A relatively large pore size is typically used allowing for fast filtration, since precipitate flocs are large; for example, Varley et al. (Varley et al., 1999) describe the use of a 50 μm nylon bag filter to remove the precipitated material from the plasmid-containing solution.

1.4.5 Intermediate purification

Following clarification, of the total nucleic acid content in the process stream, roughly 80% is RNA, 2-20% is chromosomal DNA, and only 1-2% is plasmid DNA (Bhikhabhai, 1999). Intermediate purification is typically intended

primarily to remove additional amounts of nucleic acid and protein impurities prior to chromatography, but it can also be used to concentrate the process stream. Because most chromatographic resins do not have a high capacity for nucleic acids, impurities removed during intermediate purification can reduce the amount of chromatographic resin required. A number of approaches have been used at this stage, although most published examples have involved a precipitation step.

In a number of cases, the first step after initial clarification is an isopropanol or ethanol precipitation (Horn et al., 1995;Prazeres et al., 1999). Here the plasmid DNA itself is usually precipitated and collected by centrifugation or filtration; this method serves primarily as a concentration and buffer exchange step and there is little fractionation from nucleic acid impurities. The precipitate pellet is normally redissolved to the desired concentration in TE buffer (10 mM Tris-Cl / 1 mM EDTA/ pH 8.0) or a similar low salt buffer for further processing.

A number of different precipitation methods have been used at this stage, the majority of these methods having been adapted from protein purification methods. Addition of ammonium acetate, ammonium sulphate, or lithium chloride to high concentrations has been used to precipitate impurities while keeping plasmid DNA in solution (Yang and Henley, 1991;Horn et al., 1995;Eastman and Durland, 1998;Prazeres et al., 1999). Polyethylene glycol (PEG) in combination with a salt has also been used (Marquet et al., 1995;Lahijani et al., 1996;Eastman and Durland, 1998). PEG/salt precipitation is often performed as a two-step method, whereby a first precipitation is used to

precipitate impurities while leaving plasmid in solution, then additional PEG is added to the supernatant to precipitate the plasmid while leaving some remaining impurities in solution. The plasmid pellet is collected by centrifugation and re-dissolved prior to chromatography. These methods have proven effective for protein clearance but less effective and less consistent for nucleic acid impurity clearance. Some small-scale studies have demonstrated the potential for fractional precipitation using polyamines such as spermine, spremidine, and cobalt hexamine (Hoopes and McClure, 1981;Murphy et al., 1999), but like PEG precipitation re-dissolution of plasmid DNA is necessary and the precipitating agent must be cleared (e.g. by diafiltration). A selective method using the detergent CTAB was recently introduced (Lander et al., 2002) which uses precipitation of plasmid DNA as well as selective re-dissolution. Greater clearance of nucleic acid impurities can often be achieved by using multiple precipitations (as in the PEG example) or by using multiple precipitating agents, but the use of additional steps, especially when the plasmid itself is precipitated, is generally less desirable from a yield and manufacturing standpoint.

1.4.6 Chromatography

Chromatography is typically the final purification step in the plasmid purification process. The major impurities typically found at this stage include chromosomal DNA fragments, RNA, plasmid variants, and endotoxins (Prazeres et al., 1999). The most common method used at this stage is anion exchange chromatography; other chromatographic methods that have been used with some success include size exclusion, reversed phase, and hydrophobic interaction chromatography (Ferreira et al., 1997;Prazeres et al., 1998;Diogo et al., 1999;Lee and Sagar,

2001). Often two chromatographic purification steps are included using different interaction mechanisms.

Existing chromatographic resins generally have low capacities for DNA; the media pores are often inaccessible to DNA because of its large size. Although chromatography generally provides higher degrees of resolution compared to other purification methods, plasmid DNA is still difficult to separate from nucleic acid impurities by chromatography because plasmids are very similar to other nucleic acids both chemically and structurally. High levels of impurities in the feed-stream decrease the efficiency of chromatographic separations by taking up binding sites on the chromatographic resin; since chromatography is typically the most expensive unit operation in the purification process, it is important that upstream purification steps be optimised to provide as much purification as possible. If upstream steps could be improved such that chromatography could be eliminated, this would represent a significant cost savings to the manufacturer.

After chromatography, a buffer exchange to the formulation buffer is typically performed using alcohol precipitation or tangential flow filtration. The final plasmid-containing stream is sterile filtered before filling.

1.5 Physico-chemical aspects of nucleic acids

Nucleotides are the basic building blocks of nucleic acids, the molecules which store and transfer genetic information in virtually all forms of life. One nucleotide unit is made up of a sugar group (ribose), a nitrogenous base, and a phosphate group. Nucleic acids are linear polymers of nucleotides linked by phosphodiester bridges. Polymers of ribonucleotides are called ribonucleic acid (RNA) while polymers of deoxyribonucleotides (ribonucleotides lacking an oxygen atom at the 2' position) are called deoxyribonucleic acid (DNA).

1.5.1 Double-stranded DNA

Crick, Franklin, Gosling, Stokes, Wilkins and Watson determined that the naturally occurring form of DNA consists of two polynucleotide strands wound around each other in a long helical molecule (Watson and Crick, 1953;Wilkins et al., 1953;Franklin and Gosling, 1953a;Franklin and Gosling, 1953b); this form has been termed the double helix or double-stranded DNA (dsDNA). Since this double-stranded form is the naturally occurring form, most references to 'DNA' refer to this form. The strands are held together by hydrogen bonds between specific nitrogenous bases (adenine bonds with thymine using two hydrogen bonds, guanine bonds with cytosine using three hydrogen bonds). This causes the hydrophobic nitrogenous bases to be somewhat shielded on the inside of the double helix, while the polar sugar-phosphate 'backbone' of each strand is located on the outside of the molecule (see Figure 1.1). Because the nitrogenous bases are hydrophobic, this also causes the molecule to 'twist' to its normal helix conformation in solution, known as the B conformation (B-DNA). Two other

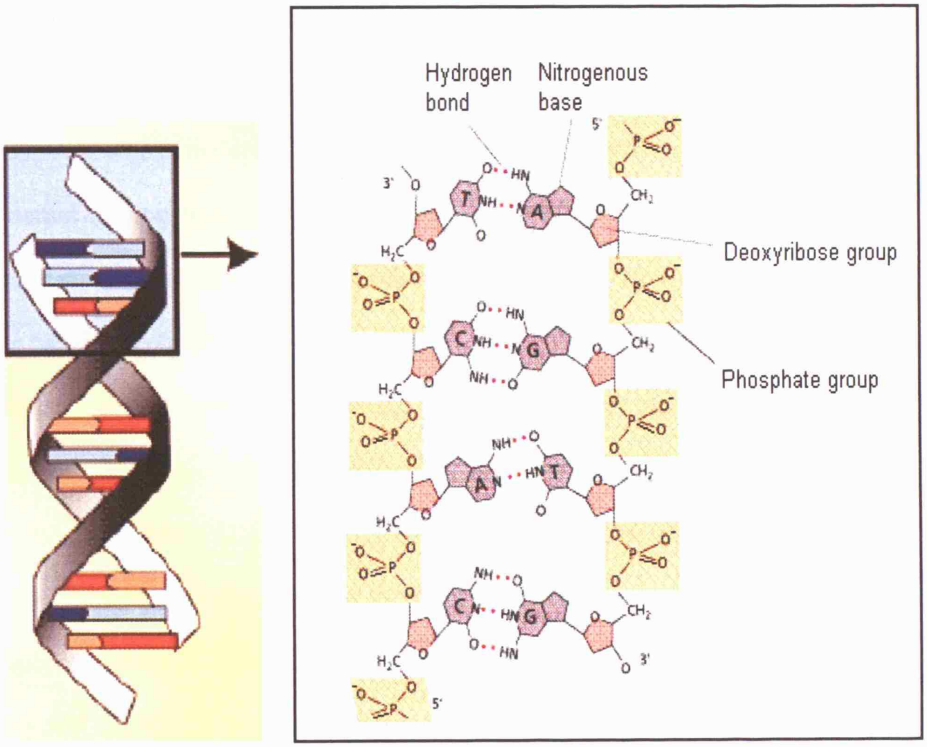

Figure 1.1 Schematic of double-stranded DNA repeating structure. In this figure, A, T, C, and G represent the nitrogenous bases adenine, thymine, cytosine, and guanine respectively.

conformations (termed A and Z) of the double helix have also been observed under special conditions. In this thesis 'dsDNA' will refer to double-stranded DNA in the B conformation unless stated otherwise. A number of factors make dsDNA a stable molecule in solution: internal hydrogen bonds between bases, external hydrogen bonds between the polar backbone atoms and surrounding water molecules, accessibility of stabilising counterions from a buffer solution to the backbone phosphate groups, and hydrophobic and van der Waals interactions between adjacent nitrogenous bases causing them to 'stack' on top of one another. The basic repeating structure of the chains and these stabilising forces permit very large DNA molecules, often millions of base pairs in length. Although DNA has considerable local ordered structure there is little long-range structure, hence in solution these long macromolecules behave as semi-flexible polymer coils. Also worth noting is that because each phosphate group contributes a negative charge, DNA is highly anionic.

1.5.1.1 *E. coli* chromosomal DNA

In cells, DNA is organised into chromosomes, which are very large discrete DNA molecules. *E. coli* contains a single double-stranded circular covalently-closed chromosome, made up of approximately 4,720,000 base pairs (4,720 kilobase pairs or kb), which would extend linearly to roughly 2 mm in length; since the longest dimension of the *E. coli* cell is only 2 μm in length, the chromosome exists as a highly folded structure inside the cell. This *E. coli* chromosome is thought to contain approximately 2800 – 3000 genes, hence chromosomal DNA is often referred to as genomic DNA. The molecular weight of the *E. coli* chromosome is roughly 3 x 10^6 kilodaltons (kDa). Unlike eukaryotes (such as

human cells), prokaryotes such as *E. coli* have little protein associated with the chromosome, and although the chromosome is compacted to the middle area of the cell there is no nucleus to contain it. Once the *E. coli* cell membrane and wall have been disrupted, the chromosome is quickly extruded to the exterior solution where it becomes extended. Because it is less compacted and less protected than in the cellular environment, the chromosome becomes susceptible to shear damage, and normally breaks into linear double-stranded fragments once in solution, with greater shear forces resulting in smaller fragments. Indeed it is very difficult to isolate intact chromosomes from *E. coli* even under the gentlest of laboratory conditions. As mentioned previously, during plasmid purification the majority of *E. coli* chromosomal DNA is cleared during the lysis/initial clarification steps, but even after these steps the ratio of chromosomal DNA to plasmid DNA may be as high 20:1. The remaining chromosomal DNA is in the form of sheared fragments which are often in the same size range as plasmid DNA, leading to increased purification challenge.

1.5.1.2 Plasmid DNA

Plasmids are circular, self-replicating, extrachromosomal dsDNA molecules found naturally in bacteria cells. Plasmids can have a range of sizes, but they are typically on the order or 1-100 kb (~700 – 70,000 kDa). Because of their smaller size plasmids are less susceptible to shear damage than chromosomal DNA which is advantageous from a processing standpoint. Because of their stability and ability to propagate in bacteria such as *E. coli*, plasmids make ideal cloning vectors for therapeutic genes; these genes are introduced into plasmids through recombinant DNA techniques.

A number of different structural conformations are possible for plasmids. Bacterial enzymes known as topoisomerases cause plasmid molecules to become twisted or 'supercoiled' while retaining a covalently closed circular conformation. Supercoiling makes plasmid molecules more compact and thus even less susceptible to shear damage than the 'relaxed' conformation (i.e. covalently closed circular without supercoiling). Supercoiling can be either negative (right-handed) or positive (left-handed), but the majority of plasmids are found in the negative configuration. Negative supercoiling introduces a torsional stress on the double helix. Current opinion holds that the supercoiled conformation is the most desirable plasmid form for gene delivery to humans (Schorr et al., 1995;Middaugh et al., 1998).

Certain denaturing conditions can cause duplex base pairings of plasmid DNA to be lost while not introducing breaks in either of the backbone strands. In this conformation, the molecule may be partially or completely single-stranded although the strands are still intertwined. In this conformation it is possible for the strands to 're-anneal' to the duplex form once the denaturing conditions are removed.

If one or both strands of a plasmid DNA molecule becomes 'nicked' (cut to form two loose ends), the molecule typically reverts to the *relaxed conformation* (i.e. circular but not twisted upon itself). This conformation is also often referred to as 'open-circular' plasmid DNA. If the molecule is exposed to denaturing conditions, the two stands will separate to the single-stranded form, producing either two linear strands or one circular strand and one linear strand; in this case,

if the two strands are no longer intertwined, the strands will not renature after the denaturing conditions are removed.

1.5.2 Single-stranded DNA

As previously mentioned, denaturing conditions can disrupt hydrogen bonding and other intermolecular stabilising forces, causing the strands of dsDNA to separate and form single-stranded molecules (ssDNA). Some of these denaturing conditions include thermal denaturation, pH extremes (roughly less than pH 2 or greater than pH 12), and the presence of strong hydrogen-bonding solutes such as formamide or urea. High pH is preferable to low pH for the preservation of the length of single strands, since high pH results primarily in deprotonation of the bases only (causing the two strands to separate), while low pH can result in hydrolysis of glycosidic linkages in the sugar-phosphate backbone, as well as disruption of base pairing due to excessive protonation. The conversion of dsDNA to ssDNA can be characterised by a concomitant increase in the absorbance at 260 nm, due to a greater exposure of the aromatic bases to transmitted light through the solution. Since guanine-cytosine base pairing incorporates three hydrogen bonds compared to two in adenine-thymine base pairing, dsDNA which has higher guanine-cytosine content is more difficult to denature. As a result, different types of DNA will exhibit different 'melting curves' - plots of relative absorbance at 260 nm versus increasing temperature during thermal denaturation.

Although the chemical composition is the same, ssDNA has some different properties than dsDNA. First, because the nitrogenous bases are not shielded internally but are instead exposed to the solution environment, ssDNA can

participate in hydrophobic interactions to a greater extent than dsDNA. Also, since the local structure is less ordered, some of the atoms that make up ssDNA are believed to pack together through van der Waals interactions, compacting the molecule into a smaller volume and making it more dense overall than dsDNA. However less local ordered structure also results in ssDNA being more extended locally than dsDNA, with an axial spacing between the nitrogenous bases of 4.0 angstroms compared to 3.4 angstroms in dsDNA (Record, Jr. et al., 1976). It should be noted that nucleic acid charge neutralisation under the counterion condensation theory (described in section 0) is very dependent on the *average axial charge spacing*, b. The relation of this parameter to axial spacing between the bases for dsDNA and ssDNA is shown in Figure 1.2.

1.5.3 RNA

As mentioned previously, *E. coli* RNA is a major impurity in the plasmid DNA process stream, present in clarified lysate at levels on the order of 50 times the level of plasmid DNA. The majority of RNA in *E. coli* cells is one of three types: ribosomal RNA (rRNA) which comprises approximately 80-90% of the total RNA, transfer RNA (tRNA) which comprises about 10-15%, and messenger RNA (mRNA) which is present transiently and comprises less than 2% at any time. All three types of RNA are synthesised by transcription of DNA

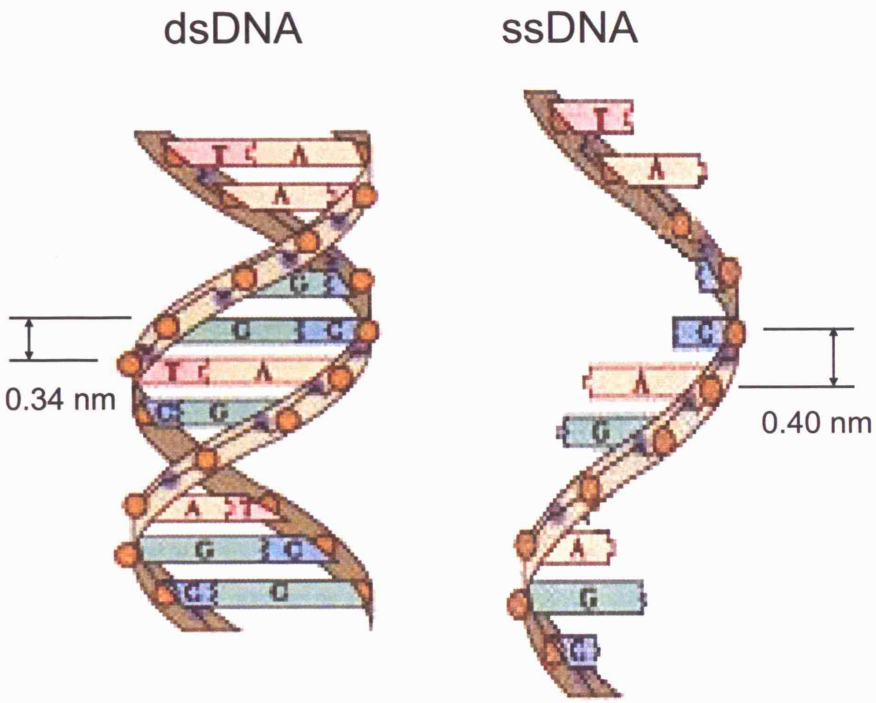

Figure 1.2 Axial spacing between bases and average axial charge spacing, b, for dsDNA and ssDNA. In the schematics above, the nitrogenous bases adenine, thymine, cytosine, and guanine are represented by A, T, C, and G respectively. Charged phosphate groups are represented by circles. Schematics show axial spacing between bases, i.e. axial spacing between phosphate groups of 0.34 nm for dsDNA and 0.40 nm for ssDNA. For dsDNA, b = 0.34 nm charge spacing divided by 2 phosphate groups per level (1 from each strand) = 0.17 nm. For ssDNA, b = 0.40 nm charge spacing divided by 1 phosphate group per level = 0.40 nm. Schematics not to drawn to scale.

sequences. rRNA makes up about 65% of the ribosomes, where protein synthesis takes place. mRNA acts as a template for specific polypeptide chains which are translated by the ribosomes, and tRNA serves as a carrier of amino acids during the synthesis process.

RNA has two fundamental chemical differences from DNA. First, it contains ribose instead of 2-deoxyribose as its sugar group. Second, RNA uses the uracil nitrogenous base instead of thymine. These differences help to guard against genetic mutations propagating in an organism but also render RNA less stable locally than DNA.

RNA molecules are smaller than most DNA molecules, but larger RNA molecules may approach the size of some plasmids and small chromosomal DNA fragments. In *E. coli* the largest type of RNA (the 23s rRNA subunit) contains 2904 nucleotides, with a molecular weight of roughly 1,000 kDa. RNA is synthesised as single-stranded nucleic acid polymers, however given some degree of base complementarity, RNA molecules tend to fold to form a number of intramolecular base pairs. This creates complex structures containing double-stranded regions with conformations similar to A-DNA, connected by single-stranded loops or 'hairpin turns', resulting in highly folded and branched molecules.

1.5.4 Summary

Table 1.1 lists some of the fundamental structural parameters for different nucleic acids forms, and Table 1.2 shows a comparison of the different nucleic acids predominantly found in an *E. coli* lysate stream.

1.6 Background on precipitation of nucleic acids

1.6.1 The electrical double layer

Biomolecules in solution can be considered colloidal dispersions, and it is useful to review the basis of stability for all colloidal dispersions before introducing specific factors for nucleic acids. The ability of electrolytes to cause instability in colloidal dispersions was first recorded around 1900, although the mechanisms involved were largely unknown at this time (Hardy, 1900;Smoluchowski, 1917).. Particles in an aqueous solution are usually charged. Through the early work of many individuals such as Gouy, Chapman, Stern, Grahame, Debye, and Hückel, the interaction of a charged particle in aqueous solution was described by an *electrical double layer* model. In this model, the surface charges on a particle make up the first layer; these surface charges are balanced by an adjacent second layer with an accumulation of oppositely charged *counterions* from the bulk solution, and a deficit of equally charged *co-ions* from the bulk. The distribution of ions near the particle surface can be determined by the Poisson-Boltzmann equation.

Table 1.1 Structural parameters for different forms of nucleic acids. Parameters shown for RNA are for double-stranded stretches only, but note that RNA contains both single-stranded and double-stranded regions. Axial charge spacing data for DNA from Record (Record, Jr. et al., 1976), for dsRNA from others (Arnott et al., 1973;Dock-Bregeon et al., 1989;Porschke et al., 1999). ξ was calculated using Equation 1.14, assuming an aqueous solution at 25°C, and V was calculated using Equation 1.18.

Nucleic acid type	b Average Axial charge spacing (nm)	ξ Axial charge density parameter	V Counterion binding volume (mL / mole P)
dsDNA (B-form)	0.17	4.2	646
ssDNA	0.40	1.8	2104
dsRNA stretches	0.14	5.1	462

Table 1.2. Major nucleic acids in *E. coli* clarified lysate process streams

Nucleic Acid Type	Structural Forms	Size	M_r (kDa)	Amt. Rel. to Plasmid
plasmid DNA	supercoiled (ds) relaxed (ds/ss) linear (ds/ss)	~ 1 –100 kb	~ 700 – 70,000	1 x
chromosomal DNA	linear (ss/ds) (usually in fragments)	~ 4,720 kb unbroken	~3 x 10^6 unbroken	~1-10 x
rRNA	folded (generally ss)	2904 nucleotides (23s subunit) 1541 nucleotides (16s subunit) 120 nucleotides (5s subunit)	~1000 (23s) ~ 500 (16s) ~ 40 (5s)	~ 45 x (includes all forms)
tRNA	folded (generally ss)	75 nucleotides	~ 30	~ 5x
mRNA	folded (generally ss)	75 - 3000 nucleotides	~30 - 1,000	< 1x

1.6.1.1 Ion distribution based on the Poisson-Boltzmann equation

In the early 1900s Gouy and Chapman independently proposed a model to determine the ionic distribution away from a charged surface. Assumptions for this model include an infinitely long flat charged surface, that ions are point charges which can contact but not penetrate the surface, that surface charge and potential are uniformly spread across the surface, and that the solvent has a constant dielectric constant. The distribution of counterions is determined by electrostatic attraction toward the particle surface charges, balanced by diffusion away from the particle surface back to the bulk solution. This establishes an *electrostatic potential* gradient from the surface of the particle to bulk solution. The distribution of ions away from the particle surface can be described by the *Boltzmann distribution*:

$$\rho(x)_i = \rho(\infty)_i \exp(-z_i e \psi(x) / kT)$$

Equation 1.1

where:

$\rho(x)_i$ is the number density of ion i at distance x from the particle surface

$\rho(\infty)_i$ is the known number density of ion i in the bulk solution (far the from particle surface)
z_i is the valency of ion i
e is the elementary electronic charge (1.602×10^{-19} C)
$\psi(x)$ is the electrostatic potential at distance x from the particle surface
k is the Boltzmann constant
T is absolute temperature

The *Poisson equation* relates the charge density of ion i to the potential gradient:

$$\rho(x)_i = \frac{-\varepsilon_0 \varepsilon}{z_i e} \frac{d^2\psi(x)}{dx^2}$$

Equation 1.2

where

ε_0 = vacuum permittivity = 8.854×10^{-12} $C^2J^{-1}m^{-1}$
ε = medium dielectric constant = 80 for water at 20°C

Equation 1.1and Equation 1.2 can be combined to obtain the *Poisson-Boltzmann equation* :

$$\frac{d^2\psi(x)}{dx^2} = \frac{-\rho(x)_i z_i e}{\varepsilon_0 \varepsilon} = \frac{-\rho(\infty)_i z_i e}{\varepsilon_0 \varepsilon} \exp(-z_i e \psi(x) / kT)$$

Equation 1.3

Two boundary conditions are needed for this second-order differential equation. One is defined at $x = \infty$ where conditions are known from the bulk solution. Another boundary condition is determined for $x = 0$ at the surface. Given a particle with known surface charge density σ, and recognising that the concentration of counterions at the particle surface depends only on σ and $\rho(\infty)_i$, the *Grahame equation* can be used to calculate the electrostatic potential $\psi(0)$ at the particle surface:

$$\sigma^2 = 2 \varepsilon_0 \varepsilon k T \left(\sum_i \rho(0)_i - \sum_i \rho(\infty)_i \right)$$

Equation 1.4

$\rho(0)_i$ and $\rho(\infty)_i$ in Equation 1.4 are defined in terms of $\psi(0)$ and $\psi(\infty)$ respectively using Equation 1.1, then substituting $\psi(\infty) = 0$. For dsDNA, σ has been estimated at -0.15 C / m^2 (Harries et al., 2003). Once $\psi(0)$ is known, Equation 1.1 can be used to calculate $\rho(0)_i$ for each ion i.

Once the boundary conditions are defined, Equation 1.3 can be solved either numerically (e.g. through Monte Carlo simulations) or in some cases analytically (e.g. for symmetrical electrolytes such as 1:1 or 2:2), to determine the electrostatic potential and ion densities at any distance x from the particle surface. The boundary conditions which apply are:

at $x = 0$, $\psi(x) = \psi(0)$ and $\rho(x)_i = \rho(0)_i$

at $x = \infty$, $\psi(x) = 0$ and $\rho(x)_i = \rho(\infty)_i$

1.6.1.2 Effects of cation valence

For DNA in an electrolyte solution containing a single counterion species (e.g. from NaCl or $CaCl_2$) Figure 1.3 shows how the electrostatic potential at the molecule surface varies as a function of bulk counterion concentration, based on solution of the Grahame equation (Equation 1.4). We see that surface potential falls progressively as the counterion concentration is increased. Also evident is that divalent cations have a much greater effect on surface potential reduction compared to monovalent cations at the same bulk concentration. For example, surface potential in a 10 mM solution of NaCl is calculated as -167 mV,

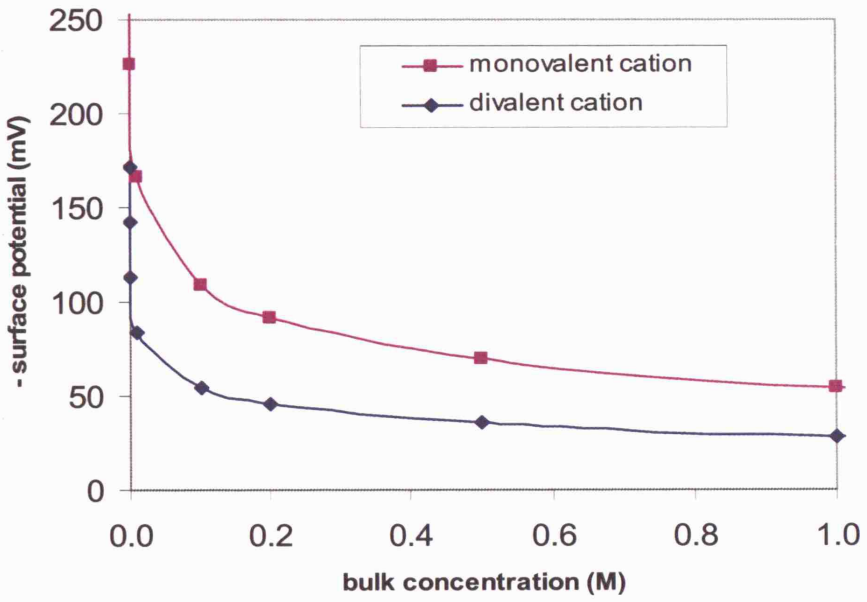

Figure 1.3 Surface potential versus bulk counterion concentration based on the Poisson-Boltzmann equation, for dsDNA in electrolyte solution containing a single species of either monovalent (e.g. Na^{+}) or divalent (e.g. Ca^{2+}) counterion. Surface potentials were determined from Equation 1.4 assuming a surface charge density of -0.15 C / m^2 and temperature of 25°C.

compared to -83 mV in a 10 mM solution of $CaCl_2$. Another way to look at this effect is by bulk concentrations needed to obtain equivalent surface potentials. For example, to reach the same surface potential as in a 10 mM $CaCl_2$ solution, a NaCl concentration of approximately 250 mM would be needed.

As shown in Figure 1.4, the counterion concentrations at the particle surface can be much higher than those of the bulk solution, especially at low bulk electrolyte concentrations. For example, even for bulk counterion concentrations less than 1 mM, the concentrations at the surface of a dsDNA molecule are calculated to be 6.6 M. Surface counterion concentrations are calculated to be nearly equal regardless of whether the counterions are monovalent or divalent (although note that divalent ions are doubly charged). Furthermore note that there is little increase in surface counterion concentration predicted for increasing bulk concentrations; this led to the approximation under the counterion condensation theory (to be discussed further in Section 0) that charge neutralisation of the DNA surface is the same for a given valence of counterion, regardless of the bulk concentration, as long as counterions are present in excess. Hence the distribution of counterions around the particle is influenced to a large extent by the type and concentration of ions in the bulk solution. In a stable dispersion, the surfaces of two particles approaching each other do not contact and this is primarily due to the repulsion between the diffuse counterion layers of each particle.

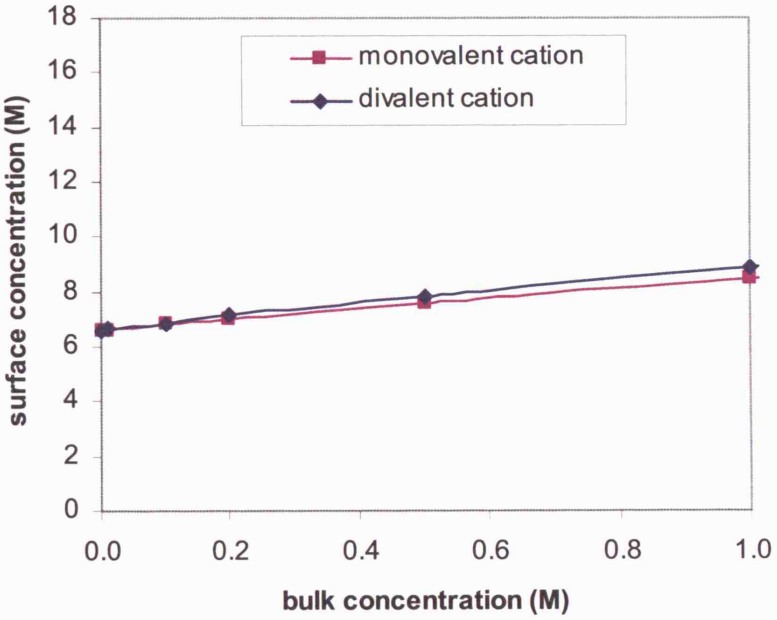

Figure 1.4 Surface counterion concentration versus bulk counterion concentration based on the Poisson-Boltzmann equation, for dsDNA in electrolyte solution containing a single species of either monovalent (e.g. Na^{+}) or divalent (e.g. Ca^{2+}) counterion. Surface counterion concentrations were determined from Equation 1.1 using the potential data from Figure 1.3 and temperature of 25°C.

1.6.2 van der Waals forces

It has also long been recognised that an attractive force exists between colloidal particles. In 1837 the Dutch physicist J.D. van der Waals included a term (a / V^2) in his famous equation of state for gases and liquids to account for these forces, and over time these forces came to be known as van der Waals forces. These forces are relatively weak, long-range, intermolecular attractive forces made up of an induction force, an orientation force, and a dispersion or London force (London, 1937). For many colloidal systems the London force is the dominant of the three, but for cases involving highly polar molecules such as water, the orientation force dominates. These forces will not be reviewed further here, but it is important to note that van der Waals forces typically dominate particle interactions at very close separation distances (typically on the order of 2 nm or less).

1.6.3 DLVO theory

In the 1940's, two groups developed similar theories to explain observations of dispersion instability, which were combined into what is now known as DLVO theory (Derjaguin and Landau, 1941;Verwey and Overbeek, 1948). In this model, interaction energies due to both repulsive electrical double layer forces and attractive van der Waals forces are summed to obtain a total energy of interaction between particles as a function of separation distance. As shown by Figure 1.5 curve a, a stable dispersion is characterised by long-range net positive interaction energy resulting in particle repulsion, as well as a significant *energy*

barrier peak at closer separation distances (typically on the order of 2-3 nm) which normally prevents particle surfaces from contacting. However if solution conditions change, this energy barrier can be decreased such that particles may approach close enough to overcome the barrier, resulting in fast progression to the deep *primary minimum* where van der Waals forces dominate and surfaces contact during precipitation. Another possible scenario, depending on the surface and solution properties, is the formation of a *secondary minimum*, where particles may form stable loose aggregates without surface contact. At a certain higher electrolyte concentration, the height of the energy barrier will be reduced to zero (see Figure 1.5 curve d); this is referred to as the *critical coagulation concentration* (CCC), above which aggregation/precipitation is inevitable.

Depending on the particular particle and electrolyte type, the CCC may or may not be impacted by particle concentration. If particle concentration is observed to impact the CCC (i.e. solubility is dependent on initial particle concentration), this is usually an indication of specific adsorption of counterions to the particle surface (Elimelech et al., 1995). In this case very high electrolyte concentrations could actually have the effect of restabilisation due to complete surface charge reversal.

1.6.4 Non-DLVO Forces

DLVO theory provides a model which reasonably predicts dispersion stability behaviour in many cases. However it should be noted that DLVO theory does

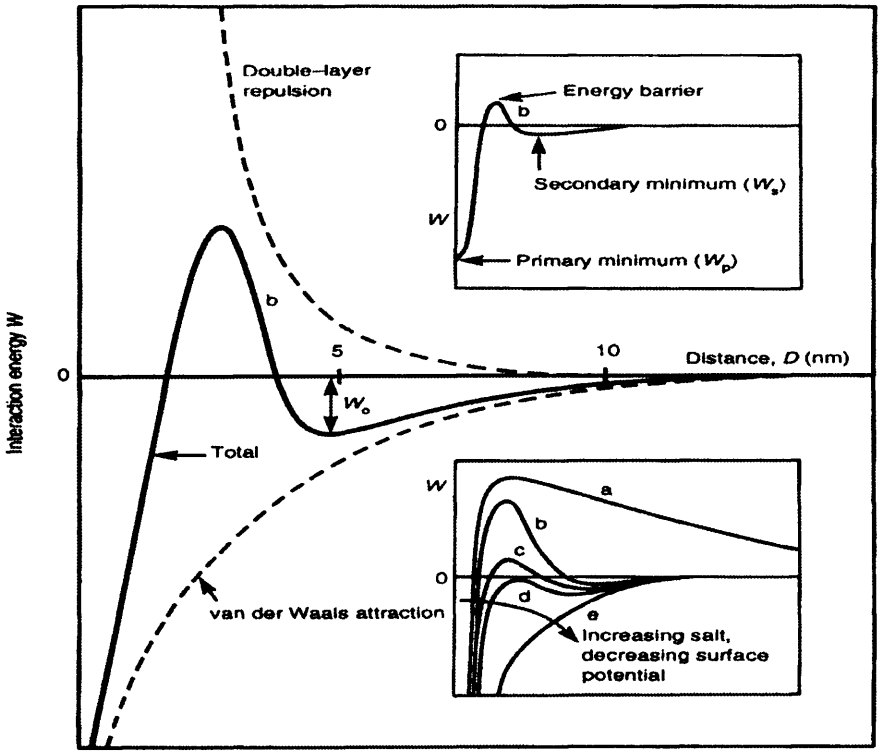

Figure 1.5 DLVO interaction energy versus distance (Israelachvili, 1992). Positive interaction energy indicates particle repulsion, negative interaction energy indicates attraction. Main plot shows summation of double layer repulsion and van der Waals attraction energies (dashed lines) to obtain total interaction energy (solid line). Examples of different interaction energy profiles include a) highly charged particle in dilute electrolyte solution; stable dispersion b) in higher ionic strength solution, a secondary minimum is formed; 'kinetically stable' c) lower charged particle surfaces in higher ionic strength solution; slow aggregation or flocculation d) ionic strength increased further such that *critical coagulation concentration* is reached; rapid coagulation, 'unstable' e) uncharged or minimally charged particle surfaces attract at all separation distances; very rapid precipitation.

not account for all types of interaction forces. Some of the so-called 'non-DLVO' forces include Born repulsion, solvation or hydration forces, hydrophobic interactions, steric interactions, and polymer bridging. The most relevant of these to nucleic acid stability include hydration forces, hydrophobic forces and steric exclusion forces.

1.6.4.1 Hydration forces

Hydration forces, also known as structural forces, are present when water molecules strongly bind to hydrophilic surfaces, including certain ionic, zwitterionic, and hydrogen bonding groups. For example the phosphate groups on the backbone of nucleic acids participate in hydrogen binding with water; at separation distances less than about 1 nm, interactions between DNA molecules are thought to be governed more by hydration forces than by van der Waals forces (Schneider et al., 1998). This results in greater repulsion between colloidal particles than predicted by standard DLVO theory, due to the additional energy required to disrupt hydrogen bonding and dehydrate the particle surfaces.

1.6.4.2 Hydrophobic forces

Attractive hydrophobic forces can be thought of as the opposite of the repulsive hydration forces. A hydrophobic or non-polar surface is a surface that does not bind water by ionic or hydrogen bonds. Water in contact with a hydrophobic surface is entropically unfavourable, and when two such surfaces come into contact in an aqueous solution this results in rejection of water molecules and a reduction in free energy of the system beyond that from van der Waals forces alone; this potential to reduce free energy results in the attractive hydrophobic

force. The hydrophobic force can be much stronger than the van der Waals force for highly non-polar surfaces, and it is generally of longer range as well, sometimes covering surface separation distances up to 80 nm (Christenson.H.K. et al., 1990).

1.6.4.3 Steric exclusion forces

Interactions between neutral polymers such as polyethylene glycol and most biomolecules, including proteins and nucleic acids, are thermodynamically unfavourable. When these polymers are added to a solution of biomolecules, the polymers are strongly excluded from the biomolecule surfaces, a phenomenon is known as *steric exclusion* (Ogston, 1962). This results in shells around the biomolecules which contain water and counterions if present, but no polymer. This *preferential hydration* in turn creates a discontinuity between the biomolecule shells and the bulk solution, which contains a high polymer concentration (Arakawa and Timasheff, 1985). Preferential hydration can also be thought of in terms of *osmotic stress* or *crowding* approaches, however all three approaches have essentially the same thermodynamic basis (Parsegian et al., 2000). The discontinuity created is entropically unfavourable, and is resolved by the biomolecules associating to share their hydration shells, liberating some water back to the bulk solution. Higher polymer concentrations lead to stronger entropically driven attraction leading to self-association of the biomolecules. With high enough polymer concentration, multiple biomolecules self-associate forming aggregates or precipitates, freeing even more water back to the bulk solution.

1.6.4.4 Polymer or Ion Bridging

Charged polymers such as polyethyleneimine (PEI) have been used as a means to flocculate or precipitate nucleic acids, cell debris, and other biomolecules from lysate solutions (Atkinson and Jack, 1973;Milburn et al., 1990;Cordes et al., 1990;Salt et al., 1995). PEI is a highly charged cationic polymer. Unlike non-ionic polymers that do not generally interact with the surfaces of biomolecules, cationic polymers would be expected to interact electrostatically with anionic polymers such as DNA. Based on previous experimental studies, solubility of nucleic acids have been observed to drop very quickly above a certain threshold PEI concentration. Although electrostatic charge neutralisation is clearly involved and steric exclusion may also be involved, the full mechanism of flocculation / formation of precipitates by charged polymers is somewhat unclear, and likely involves more complex aspects such as polymer bridging. Bridging has also been proposed as a possible mechanism involved in the precipitation of dsDNA by smaller polyamines such as spermidine^{3+} and spermine^{4+} (Olvera de la Cruz et al., 1995;Raspaud et al., 1998).

1.6.5 Condensation versus aggregation/precipitation

Condensation is the collapse of extended-coil biomolecules to a much more compact form, yielding discrete particles of distinct morphology containing only one or a few molecules (Bloomfield, 1991;Bloomfield, 1997). Condensation is an important aspect of many naturally occurring biological processes, and indeed in its natural environment most DNA is present in its compact form. For example, in eukaryotic cells, histones and other proteins complex with DNA

resulting in condensation as part of the formation of chromosomes. In viruses, proteins and polyamines condense DNA allowing packaging into the small internal volume of a capsid. *In vitro* condensation of DNA was first reported by Lerman using combination of polyethylene oxide and dissolved salt (Lerman, 1971). This was followed by condensation using the polyamine spermidine^{3+} (Gosule and Schellman, 1976). During this period it was noted that most attempts at DNA condensation were unsuccessful, resulting in the formation of amorphous aggregates or precipitates. Follow up work by Post and Zimm (Post and Zimm, 1982) predicted phase diagrams which showed three different possible states of DNA depending on solution conditions: 1) extended random coils, 2) collapsed or condensed individual coils, and 3) aggregated random coils. They and a few others (Lis, 1980;Arscott et al., 1990;Flock et al., 1996) showed that for unstable solution conditions with very low DNA concentrations (less than ~1 μg/mL) the intramolecular condensation state was preferentially obtained, while at high DNA concentrations (greater than ~10 μg/mL) condensation was largely replaced by intermolecular aggregation and precipitation.

1.6.6 Kinetic factors

Once a colloidal dispersion becomes unstable, aggregation and precipitation reactions do not occur instantaneously, but occur over time depending on properties of both the dispersed particles and the solution environment. Precipitation reactions occur in two successive regimes. The first regime, perikinetic growth, is governed by particle diffusion without impact from fluid dynamics. The second regime, orthokinetic aggregation, becomes important once

the aggregate size exceeds roughly 1 μm, and is governed to a large extent by the shear rate of the fluid.

1.6.6.1 Perikinetic growth

For an unstable dispersion of spherical particles, Smoluchowski determined that the initial decrease in dispersed particle concentration due to aggregate growth is a second order process (Smoluchowski, 1917), described by:

$$-\frac{d\,N(t)}{dt} = K_A\,N(t)^2$$

Equation 1.5

where:

N(t) is the dispersed (soluble) particle concentration at time t

and

K_A = the rate constant = $8\,\pi\,D\,d$

Equation 1.6

and

d = the dispersed particle diameter

D = the particle diffusivity = $\frac{kT}{3\,\pi\,\mu\,d}$ (Stokes-Einstein equation)

Equation 1.7

k = Boltzmann constant
T = absolute temperature
μ = solution viscosity

Equation 1.5 predicts that the aggregate growth rate will be directly proportional to particle diffusivity and concentration squared, however independent of particle size. Equation 1.5 assumes that all particle collisions add to the forming

aggregate, however this may not hold for dispersions which are unstable but do not have complete charge neutralisation of particles. These cases can be modelled using the Fuchs modification to Smoluchowksi theory (Fuchs, 1934), where Equation 1.5 becomes:

$$-\frac{d\,N(t)}{dt} = \frac{K_A N(t)^2}{W}$$

Equation 1.8

where W = stability ratio = 1 / collision efficiency, calculated according to

$$W = d \int_0^{\infty} \frac{\exp(\varphi(h) / kT)}{(h + d)^2}\, dh$$

Equation 1.9

where

h = separation distance between particles
$\varphi(h)$ = interaction energy, determined from DLVO theory

The most important implications from Equation 1.8 are that higher dispersed particle concentration, greater temperature, and higher collision efficiency result in faster aggregate growth, and that the aggregate mass increases linearly with time. Note that neither Equation 1.5 nor Equation 1.8 account for the removal of water molecules from particles during aggregation, and this hydration barrier may be an additional factor to slow aggregation kinetics, especially at the very start of a precipitation reaction.

1.6.6.2 Orthokinetic aggregation

Once aggregate particle sizes exceed roughly 1 μm in diameter, further aggregation is governed largely by fluid transport during orthokinetic aggregation. In this regime, also first studied by Smoluchowski (Smoluchowski, 1917), the aggregate growth rate is approximated as

$$-\frac{dN(t)}{dt} = -\frac{2}{3}\alpha G d^3 N(t)^2 = \frac{4}{\pi}\alpha \varphi_v(t) G N(t)$$

Equation 1.10

where

N(t) is the dispersed particle concentration at time t

α = collision efficiency factor
G = shear rate (assumed uniform)
d = the dispersed particle diameter (e.g. aggregate size after perikinetic aggregation)
$\varphi_v(t)$ = volume fraction of particles = $\pi (d^3/6) N(t)$

If $\varphi_v(t)$ is assumed to be a constant equal to the initial volume fraction , Equation 1.10 can be integrated to obtain

$$N(t) = N(0) \exp(-4 \alpha \varphi_v(0) G t / \pi)$$

Equation 1.11

Equation 1.10 predicts that the aggregate growth rate during perikinetic aggregation will be proportional to shear rate and particle concentration. Equation 1.11 predicts that dispersed particle concentration will decrease exponentially with time, and likewise that average aggregate size should increase

exponentially with time. Although $\varphi_v(t)$ is assumed to be constant in Equation 1.11 from a mass balance standpoint, in reality aggregates typically adopt a fairly open structure, such that the volume occupied by aggregates may be significantly larger than the total volume of dispersed particles prior to orthokinetic aggregation; this leads to larger aggregates and faster kinetics than that predicted by Equation 1.11. The 'G t' term in Equation 1.11, a dimensionless parameter called the Camp number (Camp, 1953), is often kept constant during scaling of precipitation/flocculation systems.

1.6.6.3 Aggregate break-up

The preceding sections on perikinetic and orthokinetic aggregation essentially assume that aggregation processes are irreversible. In reality this is not the case, as many of the same forces that promote aggregation of dispersed particles may also act to break-up aggregates once formed. Modelling of aggregate break-up is difficult, however in practice it has been found that aggregates often obtain a limiting maximum size proportional to aggregate strength, and inversely proportional to shear rate, power dissipation, or impeller speed in a vessel.

$$d_{max} = c\, X^{-n}$$

Equation 1.12

where

d_{max} is maximum aggreagte diameter
c is proportional to aggregate strength
X is shear rate, power dissipation or impeller speed
n is proportional to aggregate size

The strength of an aggregate depends on the attractive forces between the primary particles making up the aggregate and the number of particle-particle contacts. For an aggregate with a given number of primary particles, one that is smaller and more compact is considered stronger than a larger aggregate, since the compact aggregate is better able to resist shearing forces. For a turbulent flow field, one approach assumes that the limiting size is roughly the same as the Kolmogoroff length scale (η_K), given by

$$\eta_K = (\nu^3 / \varepsilon)^{0.25}$$

Equation 1.13

where

ν is the kinematic viscosity of the fluid
ε is power input per mass of fluid

1.7 Solubility models

Various models have been put forth to describe the solubility behaviour of biological molecules. Following are some of these models that may be useful for modelling solubility behaviour of different nucleic acid forms.

1.7.1 Counterion condensation theory

1.7.1.1 Description

The phenomenon of condensation or collapse of a charged polymer in solution due to counterions was first introduced by Manning as part of polyelectrolyte theory (Manning, 1969), based on a statistical mechanics analysis. This was later extended to more specifically describe the behaviour of polynucleotides in ionic

solutions (Manning, 1978). Counterion condensation theory has been widely applied over the years and found to predict dsDNA solution behaviour with reasonable accuracy.

DNA is modelled as an infinite line of charges and characterised by a dimensionless axial charge density parameter ξ, where ξ is calculated as

$$\xi = q^2 / (4\pi \varepsilon_0 \varepsilon kTb) \quad = \quad 4.2 \text{ for dsDNA in water at } 25°C$$

Equation 1.14

where:

ε_0 = vacuum permittivity = 8.854×10^{-12} $C^2J^{-1}m^{-1}$
ε = medium dielectric constant = 80 for water at 20°C
q = protonic charge
k = Boltzmann constant
b = average axial charge spacing
T = absolute temperature

Counterions are considered point charges with non-specific binding to the DNA polymer. The extent of binding is determined by balancing the minimisation of electrostatic free energy due to charge neutralisation with the maximisation of entropy through counterion dissociation and diffusion. For the case of a single counterion species with valence z, as long as counterions are present in excess (which is easily satisfied), the fractional neutralisation (F) of phosphate groups along the DNA backbone is predicted to be

$$F = \text{fractional charge neutralisation for one z-valent counterion} = 1 - 1 / (z \xi)$$

Equation 1.15

For the case of two counterion species in excess, one monovalent and one multivalent (z-valent), the system is described by the following set of equations:

$$\ln \left(\frac{\theta_1}{V (C_1 - \theta_1 C_p) \gamma_1} \right) + \phi = -2 (1 - \theta_1 - z\,\theta_n)\, \xi \ln(1 - e^{-Kb})$$

Equation 1.16

$$\ln \left(\frac{\theta_n}{V (C_z - \theta_z C_p) \gamma_z} \right) + \phi = -2z (1 - \theta_1 - z\,\theta_z)\, \xi \ln(1 - e^{-Kb})$$

Equation 1.17

where unknown parameters include :

θ_1 = fraction of phosphate groups associated with monovalent counterions
θ_z = fraction of phosphate groups associated with z-valent counterions

and known parameters include :

C_1 = bulk concentration of monovalent cations
C_z = bulk concentration of z-valent cations
C_p = bulk concentration of polynucleotide
ϕ = osmotic coefficient
γ_1 = activity coefficient of unassociated monovalent counter-ions
γ_z = activity coefficient of unassociated z-valent counter-ions

V = surrounding volume within which counter-ions are bound
= $8000\, \pi\, e\, N_{av}\, (\xi - 1)\, b^3$ (per mole of phosphate)

Equation 1.18

K = Debye screening parameter = sq. rt. ($2000\, N_{av}\, (q^2 / \varepsilon_0 \varepsilon_r k\, T)\, I$)

Equation 1.19

where

N_{av} is Avogadro's number (6.02×10^{23})
e is elementary electronic charge (1.602×10^{-19} C)

and

$$I = \text{ionic strength} = 0.5 \sum_i (z_i^2 [x_i])$$

Equation 1.20

where z_i is the charge of ion i at molar concentration x_i
(note that both counterions and co-ions are included in ionic strength calculation)

Equation 1.16 and Equation 1.17 represent a coupled system of equations with two unknowns, which can be solved iteratively for θ_1 and θ_z. At equilibrium, the total fraction of phosphate charge neutralisation (F) is calculated as:

$$F = \text{charge neutralisation for monovalent and z-valent counterions} = \theta_1 + z\theta_z$$

Equation 1.21

1.7.1.2 Application to dsDNA

As discovered experimentally by Wilson and Bloomfield (Wilson and Bloomfield, 1979) and confirmed many times since, *collapse of dsDNA molecules almost always occurs when the fraction of phosphate charge neutralisation (F) exceeds 89-90% according to the counterion condensation theory*. This has been found to hold regardless of the number and types of counterion species present, and for both aqueous solvents and aqueous/non-aqueous mixtures. This finding suggested that collapse of dsDNA is governed by net charge neutralisation rather than by the number fraction of phosphate groups 'bound' by counterions.

As discussed previously, at low dsDNA concentrations collapse leads to condensation, while at high concentrations condensation is replaced by aggregation/precipitation. Since condensed biomolecules typically remain in solution, and the intent of this project was to investigate precipitation as a means of purification, experiments for this thesis were carried at higher nucleic acid concentrations, typically 40 μg/mL or greater. A review of the literature shows that although many fundamental studies on condensation have been performed over the years using low dsDNA concentrations, only a few such studies have investigated the higher concentration regime where aggregation/precipitation occurs. Furthermore, previous studies have primarily focused on pure dsDNA solutions, with very few investigating other nucleic acid forms, and no reports of application of counterion condensation theory to multi-component process streams.

Although counterion condensation theory has been found to predictive of condensation of dsDNA in most situations, it should be noted that is still an approximation in that it only distinguishes between counterions by charge, does not take into account steric or geometrical considerations, and does not take hydration or other non-DLVO forces into account.

1.7.1.3 Effect of cation valence

For dsDNA in aqueous solution with a single species of counterion present, application of Equation 1.15 predicts charge neutralisation as shown in Table 1.3. It is important to note that according to the theory the predicted charge

neutralisation holds as long as the cationic counterion is present in excess; for example for dsDNA in solution at 100 μg/mL, a monovalent cation would need to be present at only ~300 μM or greater to be in excess. As long as this condition is satisfied, *the predicted charge neutralisation is the same, regardless of the bulk counterion concentration.* This is probably a reasonable approximation in most cases, since as shown in Figure 1.4, Gouy-Chapman theory predicts that for particles with a high surface charge density like DNA, the counterion distribution very near the particle surface is largely independent of the bulk ion concentration. Therefore referring to Table 1.3, for dsDNA in a sodium chloride buffer, charge neutralisation is predicted to be 76%, regardless of whether the sodium chloride concentration is 10 mM or 1 M. A consequence of this is that the theory is normally used to predict the onset of collapse or aggregation, but does not predict a solubility profile.

As mentioned previously, collapse or aggregation/precipitation of DNA is predicted when charge neutralisation exceeds 89-90%. Referring to Table 1.3, for a single species of counterion in aqueous solution, this level of neutralisation does not occur unless the counterion is a cation with valence 3 or higher. Therefore monovalent and even divalent cations, even at high concentrations, would not be expected to result in collapse or precipitation of double-stranded DNA in aqueous solution. A review of the literature shows that experimentally this has held true with very few exceptions. This was also a basis for the investigation of divalent cations for precipitation of other nucleic acid

Table 1.3 Counterion condensation theory predictions for dsDNA in aqueous solution at 25°C (ξ = 4.2), with a single counterion species present in excess. Charge neutralisation fractions were calculated from Equation 1.15. Collapse/ precipitation prediction based on Wilson & Bloomfield extension (Wilson and Bloomfield, 1979)

Cation valence	Charge neutralization fraction	Counterions per phosphate	Collapse / Pptn. predicted?
1	0.762	0.762	no
2	0.881	0.440	no
3	0.921	0.307	yes
4	0.940	0.235	yes

Table 1.4 Counterion condensation theory predictions for dsRNA stretches in aqueous solution at 25°C (ξ = 5.1) with a single counterion species present in excess. Charge neutralisation fractions were calculated from Equation 1.15.

Cation valence	Charge neutralization fraction	Counterions per phosphate
1	0.804	0.804
2	0.902	0.451
3	0.935	0.312
4	0.951	0.238

Table 1.5 Counterion condensation theory predictions for ssDNA in aqueous solution at 25°C (ξ = 1.8), with a single counterion species present in excess. Charge neutralisation fractions were calculated from Equation 1.15.

Cation valence	Charge neutralization fraction	Counterions per phosphate
1	0.444	0.444
2	0.722	0.361
3	0.815	0.272
4	0.861	0.215

components as part this project.

For cases of two species of counterions, with one of these at higher valence, DNA charge neutralisation is predicted to be lower than if the higher valence cation were the only counterion species in solution. This is a result of competition between the two species for sites along the DNA backbone; with more sites occupied by the lower valence cation, the overall charge neutralisation is lower. This might be expected, but it is interesting to note that the theory predicts that an increase in the ionic strength of the solution could result in a decrease in DNA charge neutralisation, if the ionic strength increase were due to higher concentration of a lower valence counterion. Other interesting trends also occur for two counterion species; for example with appropriate adjustment of the dielectric constant, precipitation then resolubilisation of DNA can occur as the concentration of the higher valence counterion is increased from low to higher levels (Flock et al., 1996).

1.7.1.4 Effect of dielectric constant

Note that both the axial charge density parameter (ξ) as defined in Equation 1.14, and the Debye screening parameter (K) from Equation 1.19, are dependent on the *dielectric constant* (ε) of the solution. Given the same bulk concentrations of DNA and counterions, solutions with lower dielectric constants result in greater DNA fractional charge neutralisation and a shift toward condensation / precipitation. Just as in aqueous solution, if charge neutralisation exceeded 89-90% under this scenario, collapse or precipitation would be predicted, and this

has also been shown to hold experimentally. For example divalent cations, which do not normally provide sufficient charge neutralisation for condensation in aqueous solution, have been used to condense dsDNA in water-methanol and water-ethanol mixtures (Wilson and Bloomfield, 1979;Votavova et al., 1986). Another study reported the condensation of dsDNA with only monovalent counterions (Na^+) in ethanol/water mixtures where the ethanol fraction was greater than 40% (Roy et al., 1999). Likewise solutions with higher dielectric constants result in lower DNA charge neutralisation. For example, addition of 1.5 M glycine to aqueous solution was used to *prevent* the precipitation of dsDNA by spermidine^{3+} (Flock et al., 1995).

1.7.1.5 Application to other nucleic acids

Counterion condensation theory has not been widely applied to nucleic acid forms other than dsDNA. Table 1.4 and Table 1.5 show the theoretical charge neutralisation calculated for stretches of double-stranded RNA and single-stranded DNA, respectively, in aqueous solution at 25°C in the presence of a single counterion type. However to date few experimental studies have been reported which have investigated the relevance of these calculations to condensation/precipitation behaviour for these other nucleic acid forms.

Unlike dsDNA, a significant difficulty in applying counterion condensation theory and other models to RNA behaviour is due to the high degree of irregularity in RNA tertiary structure, resulting in inconsistencies in the surrounding counterion environment (Draper, 2004). One numerical study of RNA has reported local phosphate charge densities that drastically exceed that of

dsDNA, for example 24 excess counterions were predicted to be present at an RNA branch junction in a 1:1 electrolyte solution (Olmsted and Hagerman, 1994). Another study has proposed that counterion condensation is largely responsible for the intramolecular folding typically observed for RNA in solution (Murthy and Rose, 2000), resulting in partially condensed molecules. It is interesting to note that if stretches of dsRNA behaved similarly to dsDNA and collapsed when charge neutralisation exceeded 89-90% according to counterion condensation theory, these dsRNA stretches would be predicted to collapse in the presence of divalent cations, due to the slightly higher linear charge density of dsRNA compared to dsDNA (see Table 1.4). Also note that trace amounts of divalent cations are thought to be more prevalent in typical buffers and biological fluids than trivalent or higher cations.

For single-stranded DNA, although calculations and experiments are relatively straightforward, very few studies have investigated the collapse/precipitation of this nucleic acid form. Due to the lack of base pairing, ssDNA molecules are much more extended than dsDNA. Referring to Table 1.5, counterion condensation theory predicts a maximum fractional phosphate charge neutralisation of 86% for ssDNA in the presence of tetravalent cations in aqueous solution; if ssDNA behaved as dsDNA, cations with valence even as high as 4 would not be predicted to result in ssDNA condensation/precipitation.

It should be noted however that unlike dsDNA, for ssDNA and RNA many of the nitrogenous bases are exposed to the solution environment, which likely results in more intermolecular hydrophobic interactions than for dsDNA, although the

extent to which these interactions govern solubility behaviour is unclear. Another interesting analysis suggests that the sharp collapse predicted by counterion condensation may only be applicable to stiffer molecules such as dsDNA, whose persistence length (the characteristic distance along which the chain retains direction) is greater than the range of attractive forces (Diamont and Andelman, 2005).

1.7.2 Cohn solubility equation

Cohn empirically derived an equation to describe the solubility of proteins in higher concentration electrolyte solutions (Cohn and Ferry, 1943) which is still widely used:

$$\log S = \beta - K I$$

Equation 1.22

where:

S = protein solubility, defined as concentration in the supernatant phase
β is a constant that depends on temperature, pH and specific protein
K is a constant that depends on specific salt and specific protein
I = ionic strength (see Equation 1.20)

For a given protein the K term is dependent on salt type, according the well-known lyotropic series first identified by Hoffmeister (Hoffmeister, 1888). Equation 1.22 is typically used to model protein solubility, however it has also been used to model solubility behaviour of other polymers and dissolved gases which may be salted-out by electrolytes (Dixon and Webb, 1961). Further investigation of the basis of this equation led to the conclusion that electrolytes affect protein solubility largely by modifying electrostatic and hydrophobic interactions, and that the type of salt impacts hydrophobic interactions according

to differences in molal surface tension increments (Melander and Horvath, 1977). More recent studies also showed that for some proteins the final concentration in the supernatant is dependent upon the initial protein concentration, while for other proteins it is independent of initial concentration (Shih et al., 1992). Equation 1.22 has not typically been used to describe the solubility of nucleic acids in electrolyte solutions. As described earlier, double-stranded nucleic acids are highly charged with little hydrophobic surface area exposed to an aqueous solvent; therefore they remain soluble in high monovalent salt concentrations, and Equation 1.22 might not be expected to be a good solubility model for these macromolecules. It is unclear whether Equation 1.22 may be more predictive of solubility behaviour for single-stranded DNA or RNA, which have greater exposure of hydrophobic surfaces to the solvent.

1.7.3 Solubility change due to dielectric constant change

Following the development of the Cohn equation, an equation was derived to describe the change in solubility of a protein at its isoelectric point due to a change in the solution dielectric constant, based on electric dipole moment interactions (Frigerio and Hettinger, 1962):

$$\log S = K \frac{\varepsilon_0^2}{\varepsilon^2} + \log S_0$$

Equation 1.23

where

S = solubility at new dielectric constant
S_0 = known solubility for reference dielectric constant
ε = new dielectric constant
ε_0 = reference dielectric constant

K = constant, dependent on specific protein, ionic strength, and temperature

Dielectric constant is typically adjusted by varying the ratio of organic solvent to water in solution. Note that the K term in Equation 1.23 is very sensitive to solution temperature. Organic solvents have also been used under various protocols for precipitation of highly charged polymers such as polysaccharides and nucleic acids; similar forms of Equation 1.23 have been developed empirically to describe the solubility behaviour for these molecules due to changing dielectric constant.

1.7.4 Effect of non-ionic polymers

Non-ionic polymers such as polyethylene glycol have been long used for the fractional precipitation of proteins (Polson et al., 1964). Juckes derived a semi-empirical model to describe solubility behaviour of proteins and viruses in the presence of non-ionic polymers (Juckes, 1971) :

$$\log S = K' - \beta' \omega$$

Equation 1.24

where

S = solubility
ω = concentration of polymer
K' = constant dependent on pH, ionic strength, temperature
β' = constant dependent on specific protein and polymer properties (especially size)

Note that the form of this equation is the same as that of the Cohn equation (Equation 1.22). Experimental work confirmed that protein solubility is inversely proportional to both polymer size and protein size; otherwise solubility in the presence of non-ionic polymers is as expected based on electrostatic theory, with

lower solubility at higher ionic strength or near a protein's isoelectric point (for examples see (Foster et al., 1973), (Atha and Ingham, 1981), (Mahadevan and Hall, 1992a). As described in Section 1.6, work by Timasheff showed that in the presence of non-ionic polymers, proteins are strerically excluded from the polymer surfaces and hence preferentially hydrated, leading to reduced solubility (Arakawa and Timasheff, 1985).

Non-ionic polymers have also been used in a few studies for the precipitation and fractionation of nucleic acids (Lis and Schleif, 1975;Lis, 1980;Paithankar and Prasad, 1991). Other studies have been carried out at low nucleic acid concentrations to investigate DNA condensation by non-ionic polymers (Lerman, 1971;Vasilevskaya et al., 1995). Although not as exhaustively investigated as proteins, based on these studies the same trends were observed for the effect of non-ionic polymers on nucleic acid solubility as for protein solubility.

1.8 Analytical background

Lysate from an *E. coli* fermentation typically contains various forms of nucleic acids including RNA (primarily ribosomal), chromosomal DNA (both single- and double-stranded), and potentially plasmid DNA (relaxed and supercoiled). Because these forms are chemically and structurally similar, they are difficult to separate during purification and are therefore important to monitor during processing. Various analytical techniques have been developed to quantify these nucleic acid forms. Absorbance measurements on bulk samples without prior separation can give some relative information about DNA and RNA but is only

quantitative for pure streams. Fluorescent dyes can be used to quantitate double-stranded DNA, single-stranded DNA, and RNA to low levels (Labarca and Paigen, 1980;Singer et al., 1997), however binding is not entirely specific and some sample buffers cause signal interference. Electrophoretic techniques are useful tools for separating and visualising various nucleic acid components from mixed samples, however these techniques are labour intensive and quantifying different forms can be difficult. PCR has been developed recently for sensitive detection of specific nucleic acids (Livak et al., 1995), but this technique can also be labour intensive and does not provide information about the form of the nucleic acid in the original sample. Some HPLC methods have already been reported including those based on reversed-phase, anion exchange, and hydrophobic interactions (for examples see Colote et al., 1986;Ferreira et al., 1998;Diogo et al., 1999), although the majority of existing methods do not support RNA and DNA quantitation nor resolve plasmid variants.

1.9 Summary

There is a growing need to purify large quantities of plasmid DNA from clarified *E. coli* lysate streams for gene therapy and vaccine applications. The great load of nucleic acid impurities in the clarified lysate stream combined with the limited capacity of chromatographic resins for nucleic acids makes optimisation of upstream purification steps important. A review of the literature suggests that there is room for improvements to existing intermediate purification methods prior to chromatography. Specifically, few studies have been performed to characterise the precipitation behaviour of the different forms of DNA and RNA

typically present in a clarified lysate stream. Furthermore, existing precipitation models and knowledge of nucleic acid structure suggest that under certain solution conditions, differences in precipitation behaviour may be achievable, which would form the basis for fractional precipitation.

In this project single-component experiments were performed to gather fundamental data on precipitation properties of different forms of nucleic acids. *E. coli* chromosomal DNA (both double-stranded and single-stranded), *E. coli* RNA, and a representative 7 kb plasmid DNA were be used. A number of precipitating agents were tested including polymers and monovalent, divalent, and trivalent cations. Data gathered from single-component experiments were used to develop methods for fractional precipitation from complex mixture solution, and these methods were investigated on process streams of clarified lysate. Single-component precipitation data were also used to assess the ability of existing models to predict precipitation behaviour for different nucleic acids.

2 MATERIALS AND METHODS

2.1 Materials

E. coli DH5α cells were obtained from Gibco-Life Technologies (Gaithersburg, MD, USA). pSVβ plasmid DNA (6.9 kb) and pQR150 plasmid DNA (20 kb) were obtained from Promega (Madison, WI, USA). Tryptone, yeast extract, agar were obtained from Oxoid (Basingstoke, UK). Isopropanol and ethanol were obtained from Merck (Dorset, UK). Celpure® diatomaceous earth media was obtained from Advanced Minerals Corp. (Santa Barbara, CA, USA). Plasmid-Safe ATP Dependent DNase was purchased from Epicentre (Madison, WI, USA). Chromosomal DNA (from type VIII from *E. Coli* strain B or from calf-thymus), ribosomal and transfer RNA from *E. coli* (strain W), RNase A (E.C. 3.1.27.5), lysozyme, ampicillin, and other chemicals were obtained from Sigma (Poole, UK). All salts were of analytical grade.

Bacterial cell lysis, clarification and plasmid purifications were performed using Endofree Mega kits from Qiagen (Venlo, Netherlands). A Beckman (Palo Alto, CA, USA) J2-M1 centrifuge was also used during cell harvest and purification operations. Precipitation experiments were carried out in 1.5 mL and 2.2 mL Eppendorf tubes, with mixing using a vortexer and shaker plate. Sample heating was performed using a water bath. Centrifugation was carried out using either a Beckman J2-21 centrifuge with a JA17 rotor or a Heraeus (Longton, UK) microcentrifuge.

1 mL Q Sepharose HP HiTrap columns were obtained from Amersham Pharmacia Biotech AB (Uppsala, Sweden). Q Sepharose HP is a strong anion exchange resin with quaternary amine groups bound to highly cross-linked agarose in 34 μm spherical particles. Poros PI resin, 20 μm, cat # P6253, was obtained from PerSeptive Biosystems, Inc. (Framingham, MA, USA). A PEEK column with 4 mm I.D. x 10 cm was packed with Poros PI resin. Analytical HPLC was performed using a Dionex HPLC system (Sunnyvale, CA, USA) with a GP40 gradient pump, AD20 UV absorbance detector, AS3500 auto sampler, and controlled via Dionex Peaknet software on a Dell personal computer. A water bath with a digital controller from Grant Instruments (Cambridge, UK) was used for pre-treating some samples prior to chromatography.

Agarose gels were run with a 7 cm tray horizontal system from Merck (Dorset, UK) and a Gibco BRL power source (Paisley, UK). Imaging was performed using an Ultraviolet Products (Cambridge, UK) 5000 Gel Documentation System, and densitometry was performed using Scion Image software. Absorbance readings were taken with a Beckman DU70 UV/visible spectrophotometer using a quartz cuvette with a 1 cm pathlength.

2.2 Bacterial cultures

Plasmids were transformed and propagated in DH5α *E. coli* using a method from Sambrook (Sambrook et al., 1989). Plasmid-free cultures were prepared in LB medium (Sambrook et al., 1989) in 2 L shake flasks and incubated at 37 °C with agitation. Large-scale plasmid-containing cultures were prepared in LB medium containing ampicillin in an Inceltech (Reading, UK) Series 2000 LH 75 L

bioreactor. Cells were harvested by centrifugation at 7000 rpm for 30 minutes at 4 °C using the Beckman centrifuge with a JA10 rotor, and stored at –70 °C until lysis.

2.3 Preparation of clarified lysate

Alkaline lysis of plasmid-containing cells was performed using a modification of a procedure described by Qiagen (Qiagen, 1998) using materials from a Qiagen Endofree Mega kit. Harvested DH5α *E. coli* cell paste was resuspended in 50 mM Tris-Cl / 10 mM EDTA / pH 8.0 buffer at a concentration of 0.12g cell paste per mL of buffer. One volume of lysis buffer (200 mM NaOH / 1% SDS) was added, mixed gently, and incubated at room temperature for 5 minutes. An equal volume of 4 °C neutralisation buffer (3.0 M potassium acetate / pH 5.5) was then added, mixed gently, then incubated on ice for 30 minutes with intermittent gentle mixing every five minutes. Precipitated cell debris was removed by filtration. Clarified lysate was either forwarded immediately to isopropanol precipitation or stored frozen for later use at -20 °C.

2.4 Isopropanol precipitation/resuspension of clarified lysate

For most experiments isopropanol precipitation was performed after clarification to perform a buffer exchange. This was performed by adding 0.75 volumes of isopropanol to the clarified lysate, mixing gently for 30 minutes, then centrifuging at 13,000 rpm for 30 minutes at 4 °C in the Beckman centrifuge. The supernatants were discarded and the nucleic-acid-containing pellet was washed gently with 70% ethanol to remove additional salts, then re-centrifuged using the same conditions. These supernatants were also discarded; the pellets

were allowed to dry and then resuspended in TE buffer (10 mM Tris-Cl / 1 mM EDTA / pH 8.0), followed by capillary shear to fragment chromosomal DNA using the method outlined in Section 2.6. Aliquots were stored at –20 °C until further use.

2.5 Preparation of purified nucleic acid solutions

2.5.1 Plasmid DNA

Plasmid DNA (mainly supercoiled form) was purified using a procedure and materials from Qiagen (Qiagen, 1998). Briefly, DH5α *E. coli* cells were resuspended as described above but with 100 μg/mL RNase A in the resuspension buffer. The same lysis and clarification procedures were followed as described above. Following filtration, endotoxin removal buffer was added to inhibit binding of endotoxin by the Qiagen column. The clarified lysate was then applied to the Qiagen column, a wash buffer was applied, and purified plasmid was recovered by applying an elution buffer. An isopropanol precipitation and ethanol wash were performed as described above and the purified plasmid was resuspended in TE buffer. Aliquots were stored at –20 °C until further use.

2.5.2 Relaxed plasmid DNA

Purified plasmid DNA was converted primarily to relaxed form using a method from Levy (Levy et al., 2000) by incubating purified plasmid in TE buffer in a 60°C water bath for 67 hours. These samples were then stored at –70 °C until further use.

2.5.3 Chromosomal DNA

Chromosomal DNA (mainly double-stranded form) was purified from wild-type DH5α *E. coli* non-plasmid-containing cells using a modification of a method by Carter (Carter and Milton, 1993). Cells were resuspended in TE buffer with 100 μg/mL RNase A and 1 mg/mL lysozyme with light agitation to disrupt the cells. Sodium chloride was added to a final concentration of 4M and diatomaceous earth was added at approximately 70g per g of wet cell weight. This solution was mixed to allow DNA adsorption to diatomaceous earth then centrifuged at 13,000 rpm for 30 minutes at 4 °C using the Beckman centrifuge with a JA17 rotor. The pellet was collected, washed with 100% ethanol, then washed with 70% ethanol. The diatomaceous earth/DNA pellet was resuspended in TE buffer, sodium chloride was again added to 4M, mixed and centrifuged again. The pellet was again washed with 100% ethanol followed by 70% ethanol, then resuspended again in TE buffer without sodium chloride. The diatomaceous earth was removed from the stream by centrifuging again, followed by capillary shear to fragment the chromosomal DNA (described in Section 2.7).

2.5.4 Single-stranded chromosomal DNA

Purified chromosomal DNA from DH5α *E. coli* was converted to the single-stranded form by incubating samples in an 85 °C water bath for 3 minutes. The conversion was verified by an increase in absorbance at 260 nm and by gel electrophoresis.

2.5.5 RNA

Lyophilised *E. coli* ribosomal or transfer RNA from Sigma was dissolved in TE buffer and stored at –20 °C until further use.

2.6 Analytical methods

2.6.1 Ultraviolet (UV) spectrophotometry

Nucleic acid concentration was determined for each purified solution by measuring the absorbance at 260 nm (A260) in a quartz cuvette. Samples were diluted with TE buffer or 10 mM Tris buffer to obtain absorbance readings between 0.2 and 0.7 absorbance units. Concentrations were calculated using extinction coefficient assumptions from Qiagen (Qiagen, 1998): for double-stranded DNA (chromosomal or plasmid) concentration was determined as A260 x 50 μg/mL x dilution factor; for RNA concentration was determined as A260 x 40 μg/mL x dilution factor; and for single-stranded DNA concentration was determined as A260 x 33 μg/mL x dilution factor. Absorbance at 320 nm was used to monitor sample turbidity.

2.6.2 Agarose gel electrophoresis

Various samples were analyzed using 0.5% agarose gels, which were run at 60 V for 2.5 hours in 2X TBE buffer (180 mM Tris-borate / 4 mM EDTA). Gels were stained using 0.5 μg/mL ethidium bromide for a minimum of ten hours and imaged under ultraviolet light. Negative images were produced for easier viewing and densitometry was performed on these.

2.6.3 HPLC

Analytical HPLC was used to characterise and quantify different forms of nucleic acids from multi-component solutions. Two methods were developed and used for this purpose: one that utilises Q Sepharose HP strong anion-exchange resin and one that utilises POROS-PI weak anion-exchange resin. The development of these methods is described in detail in Section 3.

2.6.3.1 Shear fragmentation of chromosomal DNA

Samples containing chromosomal DNA were generally fragmented using shear prior to precipitation experiments or HPLC analysis. This was accomplished using a variation of a technique which recirculated DNA through capillary tubing (Oefner et al., 1996). Samples were placed into a syringe and pushed by hand through a 2 cm length of 0.018 cm diameter PEEK capillary tubing into a clean receptacle, then pulled through the same capillary tubing back into the syringe. This was repeated 10 times.

2.6.3.2 Chromosomal DNA denaturation by heating

During method development it was found that denaturing chromosomal DNA to single-stranded form aided in the resolution of supercoiled plasmid DNA. For the Q Sepharose HPLC method, this procedure was carried out by heating and cooling: 150 μL of sample was added to a screw top vial followed by incubation in a water bath at 85°C for 3 minutes, then cooled in an ice-bath for a minimum of 20 minutes prior to RNase pre-treatment and injection to the column.

2.6.3.3 Chromosomal DNA denaturation by plasmid-safe DNase treatment

An alternative method for chromosomal DNA denaturation using ATP-Dependent Plasmid-Safe DNase pre-treatment was investigated during Q Sepharose HPLC method development. 100 µL samples containing clarified lysate were prepared in TE Buffer, with 0.625 - 50 units of supplied Plasmid-Safe DNase, 4 µL of supplied ATP solution, and 10 µL of supplied 10X reaction buffer. Samples were incubated for 1 hour at 37 °C before sample analysis.

2.6.3.4 Chromosomal DNA denaturation by pH shift

Another alternative method of chromosomal DNA denaturation using a pH shift was developed as part of the Poros PI method development: one volume of sample was rapidly mixed with 1/3rd volume of 0.2 M NaOH. After 2 minutes at room temperature, one volume of 500 mM Tris pH 8.0 was then added to each sample to lower the sample pH. Chromosomal DNA denaturation was carried out on samples only when it was desired to quantify supercoiled plasmid DNA content.

2.6.3.5 RNase pre-treatment

It was found that pre-treating samples with RNase improved resolution of nucleic acid components. A stock solution of 10 mg/mL RNase A (DNase-free) was prepared according to Sambrook (Sambrook et al., 1989) and added to samples at 100 µg/mL. Samples were incubated at room temperature for a minimum of 30 minutes prior to injecting to the column. RNase treatment was carried out for all samples.

2.6.3.6 Q Sepharose HP method

A flow rate of 0.3 mL/minute was used and temperature maintained at 30°C throughout HPLC. The column was equilibrated with 0.64 M NaCl / 10 mM Tris-Cl / pH 8.0 for a minimum of 6 column volumes. 100 µL of RNase-treated sample was injected 3 minutes after the start of data collection and followed by 17 minutes of equilibration buffer. A linear elution gradient was then applied to increase NaCl concentration from 0.64 M to 0.84 M over 30 minutes. NaCl concentration was then increased linearly to 2.0 M over 3 minutes and maintained at 2.0 M for 5 minutes, followed by 10 minutes of 0.8 M NaCl / 0.1 M NaOH / 10 mM Tris-Cl to remove residual components and regenerate the column. Absorbance at 260 nm was recorded throughout the operation.

2.6.3.7 Poros PI method

This method was carried out at 25 °C. Buffer A was 10 mM Tris, pH 8.0. Buffer B was 10 mM Tris, pH 8.5, 4M NaCl. The column was equilibrated for 5 minutes at 80% buffer A, 20% buffer B, followed by 100 µl of sample injection. Injection of IPA precipitated nucleic-acid samples usually required a 15 to 20 minute column wash to clear digested RNA. Bound DNA was eluted using a gradient from 20% to 45 % buffer B over 25 minutes. The column was then washed for 5 minutes with 0.2 M NaOH to remove residual DNA and proteins bound to the column. A flowrate of 0.3 ml/min was used throughout, with absorbance monitored at 260 nm.

2.7 Experimental methods

2.7.1 Solubility experiments

Solubility experiments were performed on either clarified lysate, iPA-precipitated/resuspended clarified lysate in TE buffer, or purified nucleic acid solutions in TE buffer. Calculations were first performed using a spreadsheet to determine appropriate amounts of precipitating agent and 10 mM Tris diluent stock solutions to add in order to achieve target concentrations of both nucleic acids and precipitating agent (see Appendix I). These experiments were carried out at room temperature by first adding equal-volume aliquots of a given nucleic acid solution to Eppendorf tubes, then adding appropriate volumes of precipitating agent solution and 10 mM Tris diluent to each tube to achieve target final concentrations, followed by immediate vortexing (except for reverse-order-of addition experiments). In each experiment the target initial nucleic acid concentration was maintained constant and the precipitating agent concentration varied; for purified single-component experiments, initial nucleic acid concentrations were in the range 50 - 100 μg/mL. As a non-precipitated control, an equal volume of 10 mM Tris buffer was added to one aliquot instead of the precipitating agent solution. Solubility experiments were performed at pH 8 unless indicated otherwise. Samples were mixed gently using a shaker plate at room temperature for a minimum of 2 hours to ensure the precipitation reaction had come to equilibrium. The precipitate suspension samples were then centrifuged at 13,000 rpm (16,000 x g) in a microcentrifuge for 20 minutes to pellet the precipitated phase. Samples of the supernatant phase were then collected for analysis using either agarose gel electrophoresis or UV

spectrophotometry. 10 mM Tris buffer was added immediately to supernatant samples to dilute them to appropriate nucleic acid concentrations for analysis, and this dilution factor was accounted for in the solubility calculation. A blank sample was also prepared, using TE buffer instead of nucleic acid solution with the highest concentration of precipitating agent, to ensure that the impact of the precipitating agent on UV absorbance was minimal.

2.7.2 Kinetics of precipitation experiments

Kinetics experiments were carried out using the same technique as in solubility experiments, except after vortexing, instead of mixing samples by shaker plate, samples were immediately transferred to a quartz cuvette and monitored for increasing turbidity at 320 nm using a spectrophotometer. Samples to investigate effects of initial contacting conditions during precipitation were prepared slightly differently. High-mixing samples were prepared by adding a precipitating agent solution drop-wise to nucleic acid solutions while vortexing; minimal-mixing samples were prepared by adding nucleic acid solutions drop-wise to precipitating agent solutions without vortexing, and holding static for 2 minutes. Both high-mixing and mnimal-mixing samples were then agitated slowly by shaker plate for 5 hours before centrifuging and recovering the supernatant for analysis as described above.

2.7.3 Sample pre-treatment methods

Typically precipitation experiments were performed on clarified lysate, iPA-precipitated/resuspended clarified lysate, or purified nucleic acid solutions without pre-treatment prior to introduction of the precipitating agent. However

pre-treatment of the nucleic acid solution samples was performed in some cases, for example when investigating mechanisms of precipitation. Pre-treatment methods for precipitation experiments included heat denaturation and addition of RNase.

2.7.3.1 Heat denaturation of nucleic acids

A heating step was included in some experiments as a means to denature nucleic acids. Samples in 1.5 mL eppendorf tubes were immersed in a water bath that was controlled to maintain a given temperature from 70-95 °C, depending on the desired nucleic acids for denaturation. Samples were incubated for a desired time period, then immediately immersed in an ice bath for a minimum of 20 minutes.

2.7.3.2 RNase pre-treatment

RNase treatment of clarified lysate samples was carried out prior to some precipitation experiments, using the same method as for the HPLC assay sample pre-treatments. A stock solution of 10 mg/mL RNase A (DNase-free) was prepared (Sambrook et al., 1989), and added to clarified lysate samples at 100 μg/mL. Samples were incubated at room temperature for a minimum of 30 minutes for RNA digestion, then either input directly to precipitation experiments or frozen at -20 °C for later use.

3 HPLC ASSAY DEVELOPMENT

3.1 Introduction

HPLC methods were pursued to quantify different forms of nucleic acids in multi-component samples, for example before and after precipitation of a clarified lysate process stream. Agarose gel electrophoresis can provide semi-quantitative information on plasmid DNA for these types of samples, however cannot be used to quantify other nucleic acid forms such as chromosomal DNA or RNA. Therefore, better analytical methods were needed for multi-component samples, and a review of the literature suggested that HPLC methods, in particular those based on anion exchange, held promise for this purpose. HPLC method development was pursued in conjunction with another UCL graduate student, Francis Meacle, who was studying the effects of *E. coli* lysis conditions on plasmid DNA recovery and thus also had a need for analysis of multi-component streams. Two main HPLC methods were developed, one that used Poros PI weak anion-exchange resin for overall process stream analysis, and one that used Q Sepharose HP strong anion-exchange resin for more detailed analysis of DNA structure. This author's responsibility was for the Q Sepharose HP method, therefore details will be provided on this work along with a summary of the Poros PI assay.

3.2 Q Sepharose HP HPLC assay

3.2.1 Method summary

As described in detail in the Materials and Methods section, this method used a 1 mL Q Sepharose HP HiTrap column containing quaternary amine groups bound to spherical agarose particles. A linear NaCl gradient at pH 8 was used to separate nucleic acid forms through the column. Nucleic acids were detected by monitoring UV absorbance at 260 nm.

3.2.2 Characterisation of starting materials

Agarose gel electrophoresis was used to characterise starting materials for HPLC assay development (Figure 3.1). Note that no pre-treatment was performed on these samples prior to electrophoresis except for addition of gel loading solution. Figure 3.1 lanes 1 and 9 contain supercoiled and linear DNA ladders respectively; prominent bands are marked adjacent to the image for reference. Buffer-exchanged clarified lysate was loaded to lane 2, purified pSVβ plasmid was loaded to lane 3, purified high-supercoiled-content pSVβ was loaded to lane 4, and purified high-relaxed-content pSVβ was loaded to lane 5. Comparison of these samples to the marker lanes 1 and 9 confirms the presence of the 6.9 kb supercoiled plasmid in lanes 2-4 and the presence of the relaxed plasmid form (corresponding to ~14.2 kb position on the supercoiled ladder) in lanes 2-5. *E. coli* RNA (lane 6) appears as a smear at the bottom of the gel due to its size range. Purified chromosomal DNA (lane 7) also appears as a smear due to a range of fragment sizes, and comparison of the purified single-stranded

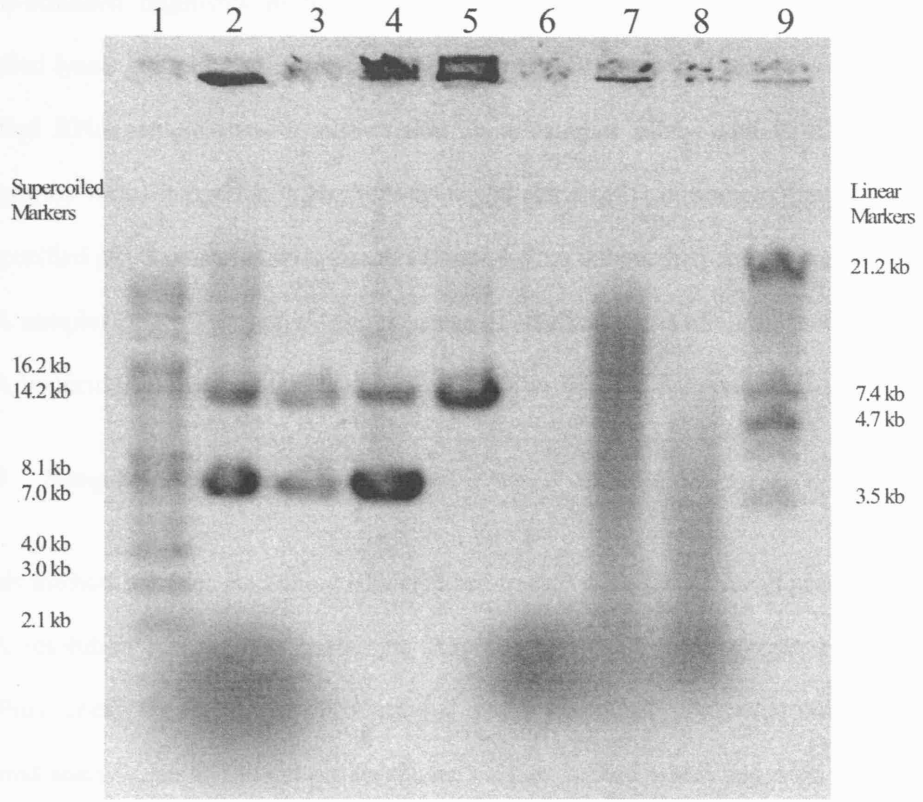

Figure 3.1. Agarose gel analysis of samples used for assay development. Lane 1: supercoiled ladder; Lane 2: clarified lysate (isopropanol-precipitated/ resuspended in TE); Lane 3: purified pSVβ plasmid; Lane 4: purified high-supercoiled-content pSVβ plasmid; Lane 5: purified high-relaxed-content pSVβ plasmid; Lane 6: purified *E. coli* ribosomal RNA; Lane 7: purified *E. coli* chromosomal DNA; Lane 8: single-stranded purified *E. coli* chromosomal DNA; Lane 9: Lambda DNA EcoR1 digest linear DNA ladder.

chromosomal DNA sample (lane 8) to lane 7 shows the conversion to smaller single-stranded fragments in this sample. Comparing the buffer-exchanged clarified lysate and purified chromosomal DNA samples (lanes 2, 7 and 8) to the purified RNA sample (lane 6) shows that these samples likely contain RNA impurities. Also, comparing the buffer-exchanged clarified lysate sample (lane 2) and purified pSVβ plasmid DNA samples (lanes 4-5) to the purified chromosomal DNA samples (lanes 7-8) suggest the presence of small amounts of chromosomal DNA impurities in these samples.

3.2.3 Sample pre-treatment

In this method, samples containing RNA are pre-treated with RNase for improved RNA resolution and samples containing chromosomal DNA are pre-treated by capillary shear for improved chromosomal DNA recovery. For supercoiled plasmid analysis, an additional pre-treatment method is used which relies on the stability of supercoiled plasmid under controlled heating that irreversibly denatures linear DNA fragments.

3.2.4 Assay development

The different purified starting materials were analyzed by the HPLC method. Chromatograms from each of the runs are shown in Figure 3.2. Comparison of chromatograms for purified pSVβ plasmid DNA samples (Figure 3.2 panels A, B, and C) demonstrates the capability for separation of different forms of plasmid DNA by the HPLC method. A relaxed form of plasmid DNA is seen to

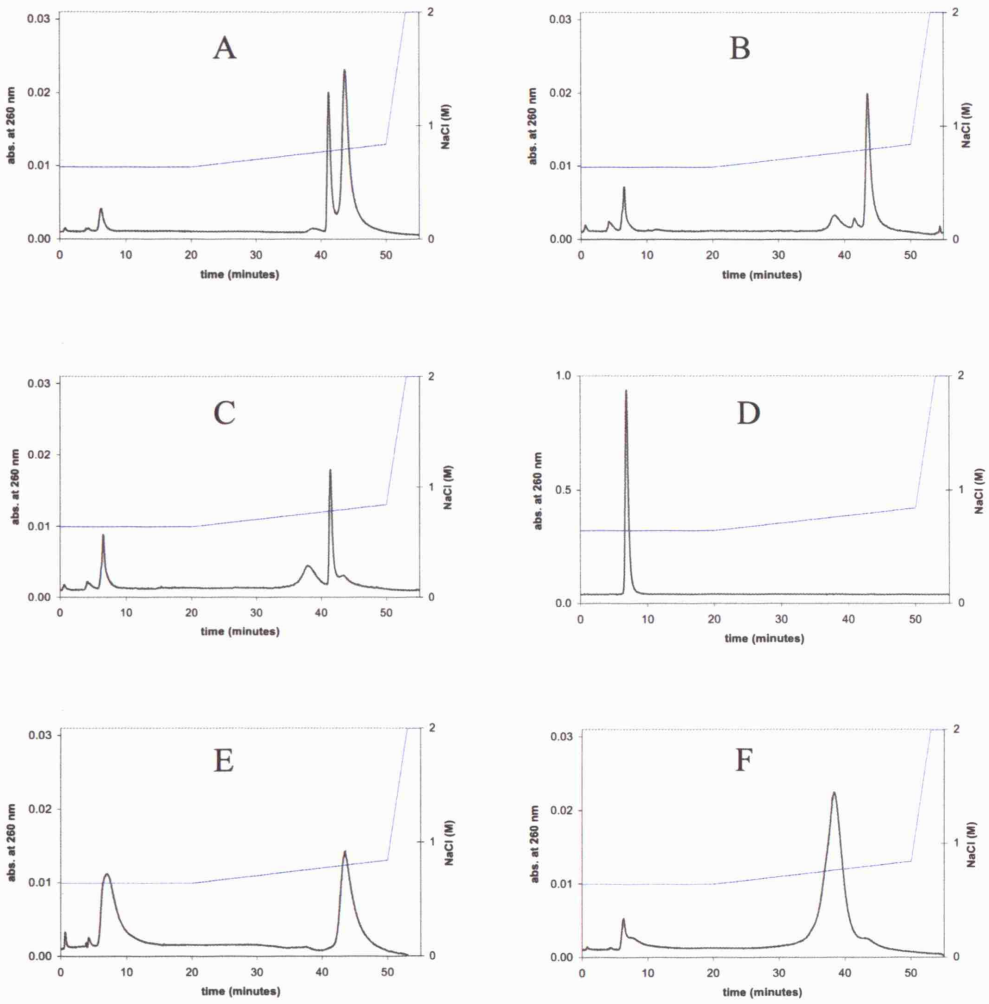

Figure 3.2. Chromatograms for pure components in Q Sepharose HP analytical method. A: Qiagen-purified pSVß plasmid DNA (see Figure 3.1 Lane 3); B: high supercoiled-content psvß plasmid (see Figure 3.1 Lane 4); C: high-relaxed-content psvß plasmid (see Figure 3.1 Lane 5); D: *E. coli* rRNA (see Figure 3.1 Lane 6); E: chromosomal DNA sample (see Figure 3.1 Lane 7); F: single-stranded *E. coli* chromosomal DNA (see Figure 3.1 Lane 8).

elute at approximately 41.5 minutes (panel C) and the supercoiled form elutes at approximately 44 minutes (panel B). Also apparent are flow-through peaks at approximately 4.5 minutes and 6.5 minutes. As evidenced from panel D which shows the chromatogram for purified *E. coli* ribosomal RNA, the 6.5-minute peak in panels A, B and C is probably due to slight amounts of remaining RNA impurities in these samples.

Figure 3.2 panel E shows the chromatogram for purified double-stranded *E. coli* chromosomal DNA. Note that considerable impurity remains in this sample as evidenced by the 6.5-minute peak; based on the chromatogram for purified RNA (panel D) and the agarose gel of this sample (Figure 3.1 Lane 7) this peak is mainly due to RNA. Of important note in panel E is that the chromosomal DNA peak elutes at 44 minutes, the same elution time as for supercoiled plasmid DNA (panel B); therefore a mixture of these two forms would not be resolved without sample pre-treatment. Panel F shows the chromatogram for purified single-stranded *E. coli* chromosomal DNA. This nucleic acid form elutes at 38.5 minutes compared to 44 minutes for the double-stranded form. Based on this, the small peaks observed at 38.5 minutes in the purified pSVβ plasmid DNA chromatograms (panels A, B, and C) are due to single-stranded DNA.

Figure 3.3 demonstrates the potential for higher recovery of chromosomal DNA using capillary shear pre-treatment. Shearing of samples is believed to fragment large stretches of chromosomal DNA (if present), such that they are not physically trapped in the Q Sepharose HP media. Trials showed that greater than

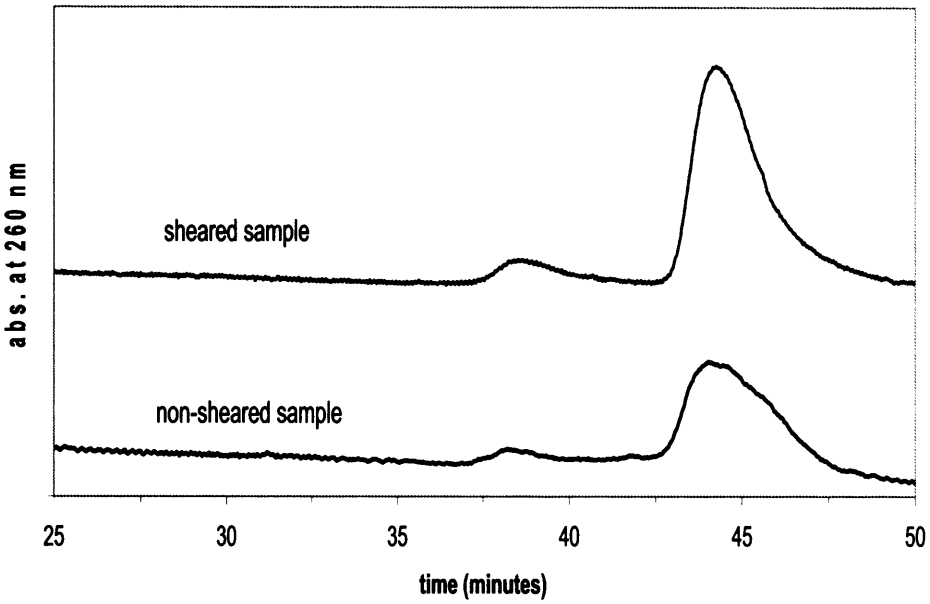

Figure 3.3 Effect of shear on recovery of chromosomal DNA in Q Sepharose HP analytical method. Bottom: chromatogram for non-sheared purified chromosomal DNA sample in TE buffer; Top: chromatogram for same sample following capillary shear pre-treatment.

two passes through a 2 cm length of 0.018 cm diameter PEEK capillary tubing was sufficient to maximise chromosomal DNA recovery in the analytical method, therefore 10 passes were typically used.

3.2.5 Standard curves

Standard curves were generated for each component of interest by plotting HPLC peak area against mass loaded to the method (based on absorbance at 260 nm). Separate curves were generated for RNA (6.5-minute peak), single-stranded DNA (38.5 minute peak), relaxed plasmid DNA (41.5-minute peak) and double-stranded DNA (44-minute peak). Standard curves are shown in Figure 3.4 and show good linear correlations over the mass range tested for each component (1.2 - 39 μg for RNA, 0.7 - 5.4 μg for single-stranded DNA, 0.4 - 3.1 μg for relaxed plasmid DNA, and 0.2 - 6.9 μg for double-stranded DNA). As might be expected, Figure 3.4 also shows that the standard curves for the less structured components (e.g. digested RNA) have greater slopes, indicative of lower extinction coefficients.

3.2.6 Development of chromosomal DNA denaturation step for analysis of supercoiled plasmid DNA

Based on the purified component runs, the method is capable of quantitating relaxed plasmid DNA but is unable to separate supercoiled plasmid from double-stranded chromosomal DNA without pre-treatment. To address this, studies were performed to determine if samples could be pre-treated to denature double-

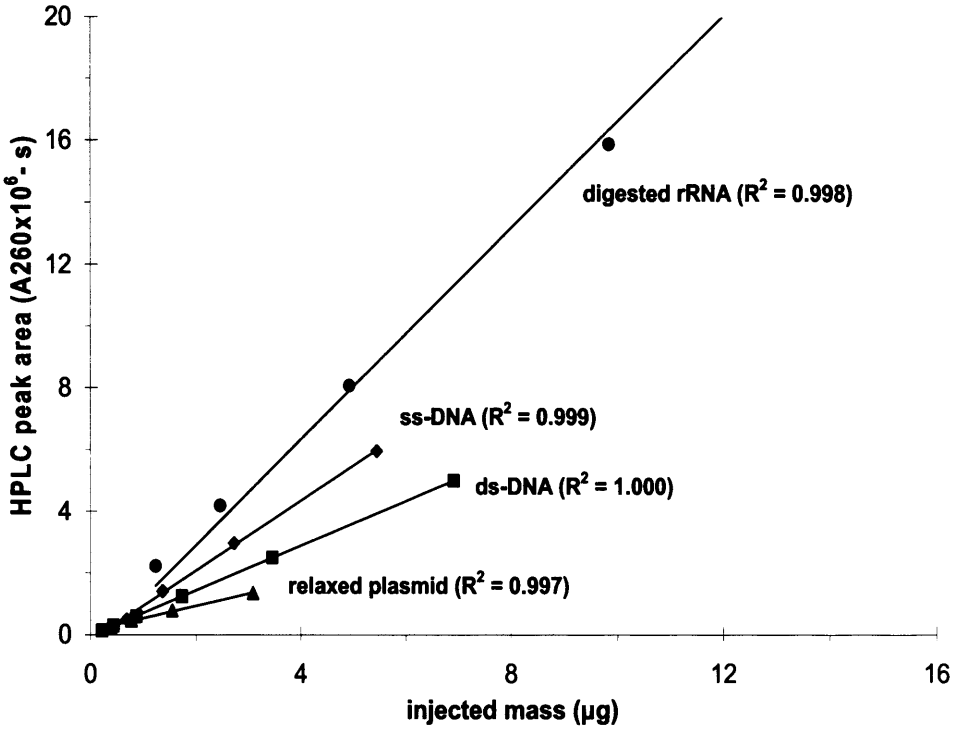

Figure 3.4 Standard curves for Q Sepharose HP analytical method, generated from purified components: RNA (6.5-minute elution peak with buffer injection peak subtracted, mass load range 1.2 - 39 µg based on A260 prior to RNase treatment, note only lower portion of this curve shown), single-stranded DNA (38.5-minute elution peak, mass load range 0.7 - 5.4 µg), double-stranded DNA (44-minute elution peak, mass load range 0.2 – 6.9 µg), and relaxed plasmid DNA (41.5-minute elution peak, load 0.4 – 3.1 µg).

stranded chromosomal DNA to single-stranded form in order to remove chromosomal DNA from the 44.0 minute elution peak *without affecting the elution of supercoiled plasmid.*

The first method attempted for this used ATP-Dependent Plasmid-Safe DNase, an enzyme which digests linear double-stranded DNA at slightly alkaline pH and, with lower efficiency, digests single-stranded DNA (both closed-circular and linear). This enzyme works by hydrolyzing these DNA forms to nucleotides, with magnesium and ATP serving as cofactors. The enzyme reportedly has no activity on supercoiled or relaxed double-stranded plasmid DNA. Samples of clarified lysate in TE buffer were treated per the kit instructions with increasing levels of added plasmid-safe DNase, then analyzed by agarose gel electrophoresis. As seen in Figure 3.5, chromosomal DNA denaturation increased with higher levels of plasmid-safe DNase, but even 15 DNase units/mL per nucleic acid A260 unit was left some residual undigested chromosomal DNA. High plasmid-safe DNase levels also resulted in some apparent degradation of supercoiled plasmid to relaxed form (not shown), therefore this method for chromosomal DNA denaturation was not pursued further.

The second method used heat to denature chromosomal DNA. It was thought that this may be possible based on previous work on bacterial cell lysis (Birnboim and Doly, 1979;Holmes and Quigley, 1981) and a method which converted non-supercoiled plasmid forms to single-stranded (Levy et al., 2000). These earlier studies suggest that for a mixture of chromosomal and plasmid

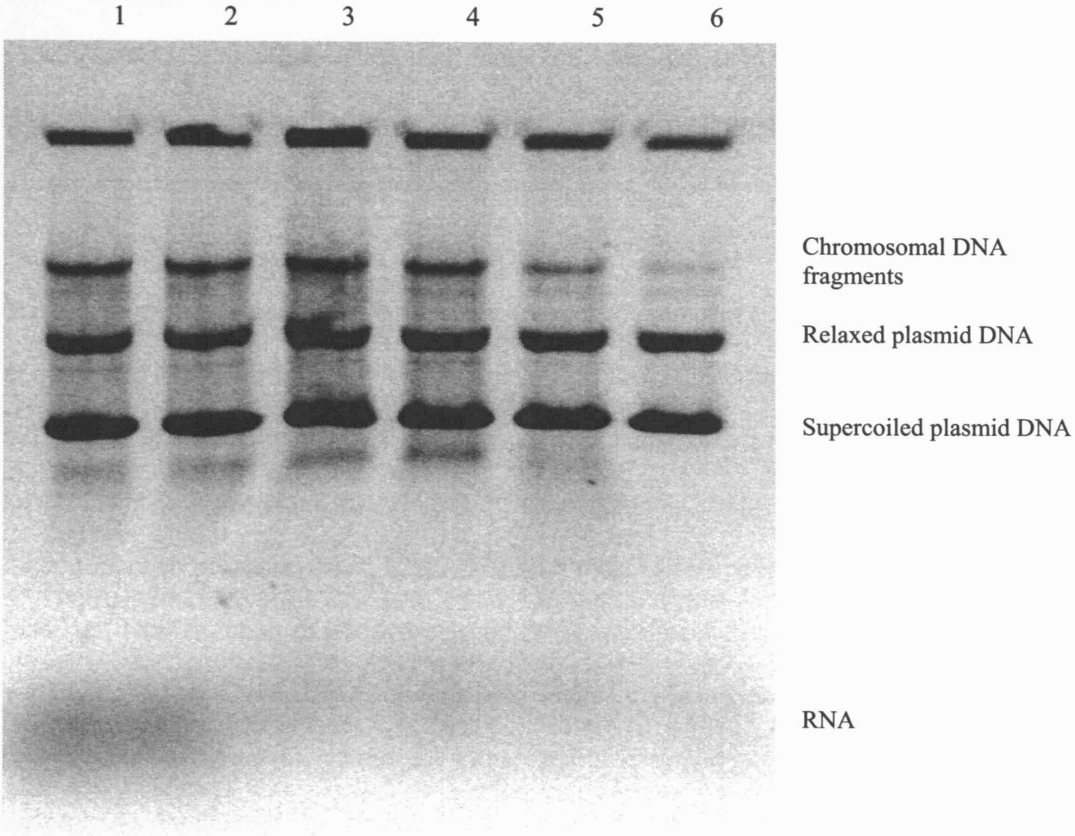

Figure 3.5 Effect of plasmid-safe (PS) DNase for double-stranded chromosomal DNA denaturation (0.8% agarose gel analysis). Lane 1: clarified lysate control in TE buffer; Lane 2: clarified lysate control in TE buffer incubated 1 hour at 37°C; Lane 3: clarified lysate control with reaction buffer added only but no DNase, incubated 1 hour at 37°C; Lane 4: clarified lysate with PS-DNase added at 1.0 units/mL per A260 unit, incubated 1 hour at 37°C; Lane 5: clarified lysate with PS-DNase added at 3.9 units/mL per A260 unit, incubated 1 hour at 37°C; Lane 6: clarified lysate with PS-DNase added at 15.4 units/mL per A260 unit, incubated 1 hour at 37°C (all samples diluted to same nucleic acid concentration with 10 mM Tris/ pH 8).

DNA, it is possible under controlled conditions to denature linear chromosomal DNA to single-stranded form without permanently denaturing supercoiled plasmid DNA. It is possible that both forms are converted to single-stranded while exposed to denaturing conditions, but that supercoiled plasmid renatures to its native form as long as each strand remains covalently closed circular.

To test this approach, purified *E. coli* chromosomal DNA samples were incubated at a range of temperatures for a 3 minute time period then chilled immediately in an ice bath for a minimum of 20 minutes before running each sample by the HPLC method. It was found that while 80 °C incubation reduced the 44.0 minute double-stranded peak somewhat, 85 °C or higher reduced this peak virtually to baseline. Next, samples of purified plasmid DNA were incubated at 85 °C for periods from 1 to 60 minutes, again with each sample chilled immediately upon removal from heating in an ice bath for a minimum of 20 minutes. Each of these samples was run in the HPLC method (see example in Figure 3.6) and some were also analyzed by agarose gel electrophoresis (Figure 3.7).

Densitometry analysis was performed on the supercoiled plasmid bands from the agarose gel for comparison to the 44.0 minute peak areas from the chromatograms. These data are shown in Figure 3.8, where HPLC peak areas and agarose gel band integrals are plotted versus incubation time, *with each normalised to its own 3-minute data point* for easier comparison.

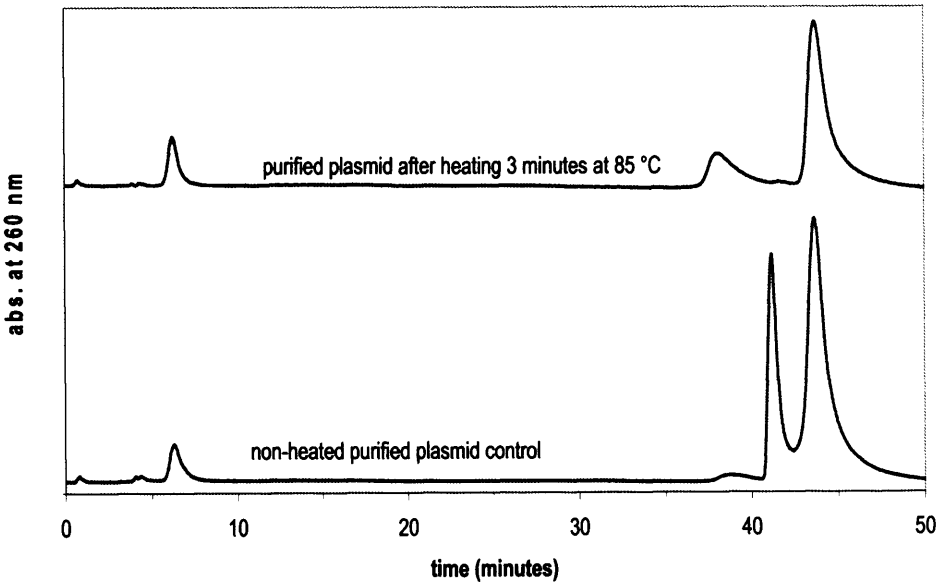

Figure 3.6. Example Q Sepharose HP chromatograms showing effects of controlled pre-heating at 85 °C on purified plasmid DNA. Bottom: non-heated purified plasmid DNA control sample in TE buffer; Top: same sample pre-treated by incubation for 3 minutes at 85°C, followed by incubation for 20 minutes in an ice bath. Peak at 6.5 minutes is residual digested RNA, peak at 38.5 minutes is residual single-stranded chromosomal DNA, peak at 41.5 minutes is relaxed plasmid DNA, and peak at 44 minutes is double-stranded DNA (primarily supercoiled plasmid).

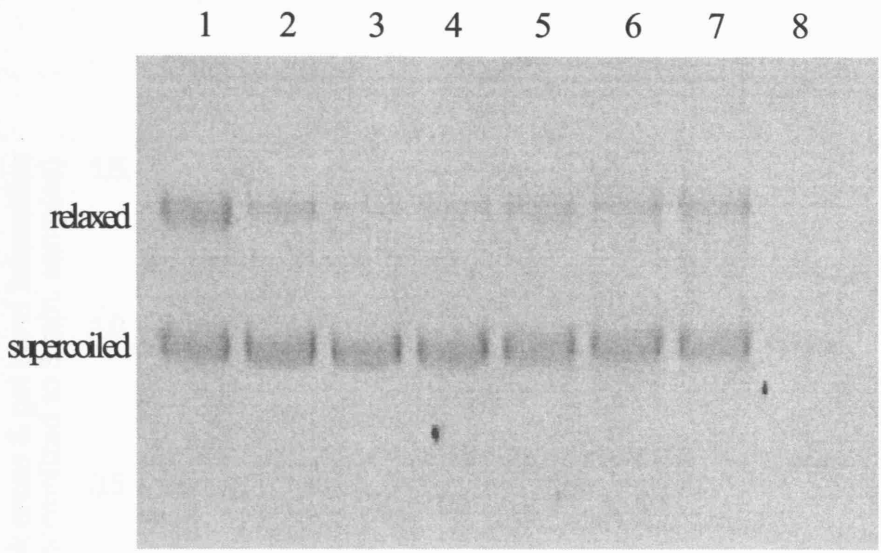

Figure 3.7. Effect of sample incubation time at 85 °C on relaxed and supercoiled plasmid DNA. 0.8% agarose gel of purified pSVβ plasmid DNA samples in TE buffer after incubation for varying lengths of time at 85 °C (each cooled in an ice bath for 20 minutes). Lane 1: non-heated control; Lanes 2-8 : 1, 2, 3, 5, 15, 30, 60 minutes incubation, respectively.

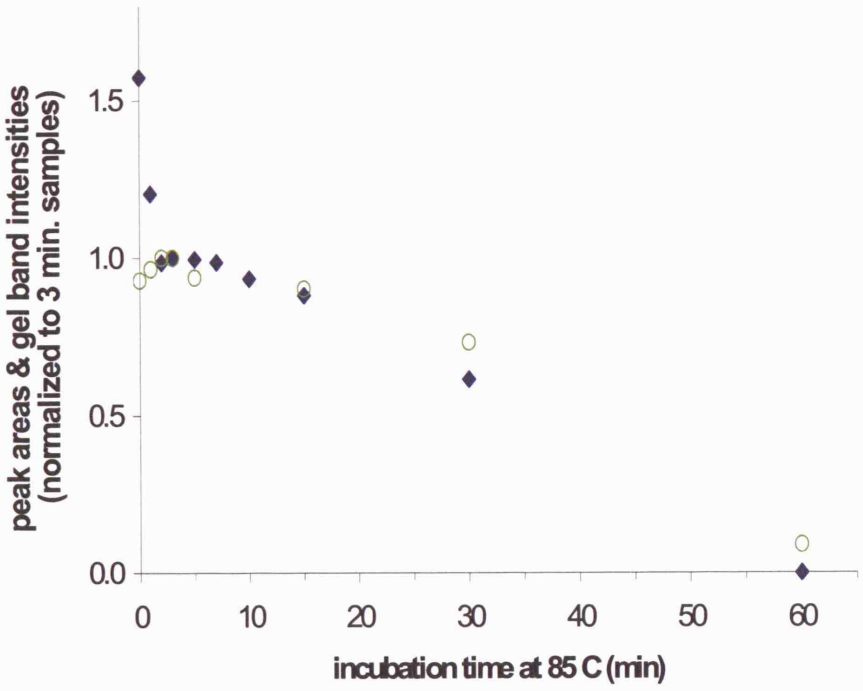

Figure 3.8. Method analysis for sample thermal pre-treatment for Q Sepharose HP method, showing 3-5 minutes incubation at 85 °C is sufficient for denaturing double-stranded chromosomal DNA while leaving supercoiled plasmid intact. Purified pSVβ plasmid DNA samples were incubated at 85°C for increasing lengths of time then cooled for 20 minutes in an ice bath. Each sample was analyzed by both Q Sepharose HP analytical HPLC and agarose gel electrophoresis. Plotted are double-stranded DNA peak areas from HPLC (solid diamonds) and supercoiled plasmid band densitometry integrals from agarose gel (open circles), each *normalised to its own 3-minute-incubation data point* (HPLC data calculated as sample peak area : 3-minute peak area, agarose gel data calculated as sample supercoiled band integral : 3-minute-supercoiled band integral).

As seen by the supercoiled bands in Figure 3.7 and plotted in Figure 3.8, supercoiled plasmid DNA remains intact until the 85 °C incubation time exceeds approximately 5 - 15 minutes. As mentioned previously, this may be because the circular strands of the plasmid remain covalently closed during this short heating period and re-anneal to their initial form upon cooling. For longer incubation times, some of the circular strands apparently become nicked such that they either separate and do not re-anneal upon cooling, or re-anneal in the relaxed form (this is supported by observing the increase in the relaxed plasmid band intensity between 5 and 30 minutes of heating, Figure 3.7 lanes 5-7).

Similarly the HPLC 44.0 minute peak areas show a plateau from approximately 2-7 minutes of 85 °C incubation followed by a decline for longer heating times due to supercoiled DNA degradation (Figure 3.8). However unlike the supercoiled bands from the agarose gel, *the HPLC peak areas also show a substantial decrease during the first two minutes of sample pre-incubation.* Since the agarose gel analysis has established that this decrease is not due to supercoiled plasmid degradation, this decrease must be due to conversion of other double-stranded DNA forms (e.g. chromosomal DNA) to single-stranded form. This reckoning is supported by the observation from Figure 3.6 that the decrease in the 44.0 minute double-stranded peak area is accompanied by an increase in the 38.0 minute single-stranded peak area.

Therefore, for samples containing a mixture of supercoiled plasmid and chromosomal DNA, pre-treating 150 μL samples by a 2-5 minute incubation at

85 °C followed by a 20 minute ice-bath incubation results in a 44.0 minute supercoiled-only peak in the HPLC method which can be quantified by peak area. Other double-stranded DNA forms can be quantified by subtracting the supercoiled plasmid quantity from the original total double-stranded DNA quantity. Further studies on heat denaturation are described in Section 5, where it was investigated in conjunction with divalent cation precipitation to enhance purification of supercoiled plasmid DNA.

3.2.7 Confirmation of method for samples containing varying proportions of supercoiled to relaxed plasmid form

A key feature of the HPLC method is its ability to distinguish and quantitate both relaxed and supercoiled forms of plasmid DNA. Given that these forms are chemically identical and elute in peaks with similar elution times (41.5 versus 44.0 minutes), studies were performed to confirm the resolution of these forms from mixture samples of varying ratios. A series of samples were prepared by combining portions of the high-supercoiled purified plasmid sample with portions of the high-relaxed purified plasmid sample to create samples that contained decreasing amounts of supercoiled plasmid and increasing amounts of relaxed plasmid. The combined samples were then analyzed by both agarose gel electrophoresis and the HPLC method. Separate HPLC runs were performed for supercoiled plasmid analysis after performing the chromosomal DNA denaturation pre-treatment described above. Figure 3.9 shows the agarose gel for this series and Figure 3.10 shows example chromatograms.

Regression analysis was used to check the correlation of relaxed and supercoiled chromatogram peak areas to the mixture ratio used. As shown in Figure 3.11, the HPLC peak areas for both the relaxed and supercoiled plasmid forms show good correlation to the mixture ratio used. This confirmed that the HPLC method is able to resolve both relaxed and supercoiled plasmid forms, regardless of their mass ratio in any given sample.

3.2.8 Effect of sample buffer

To check the utility and robustness of the HPLC method against different sample buffers that might be expected from different process streams, samples with varying cation concentrations were injected to the assay. Since the method relies on anion exchange, it was thought that high salt concentrations in samples could potentially interfere with the interaction between nucleic acids and the functional groups of the Q Sepharose HP stationary phase. It was found that monovalent cations up to 1.0 M did not interfere with the method, although divalent cations in excess of 0.25 M caused portions of single- and double-stranded DNA peaks to elute as part of the flow-through (not shown). This effect was mitigated either by dilution or by increasing concentration of monovalent cations (presumably due to competition among monovalent and divalent counterions for binding sites along the DNA surface).

Also it was observed that higher salt concentrations (ionic strengths greater than ~0.1) interfered with plasmid DNA during the chromosomal DNA denaturation

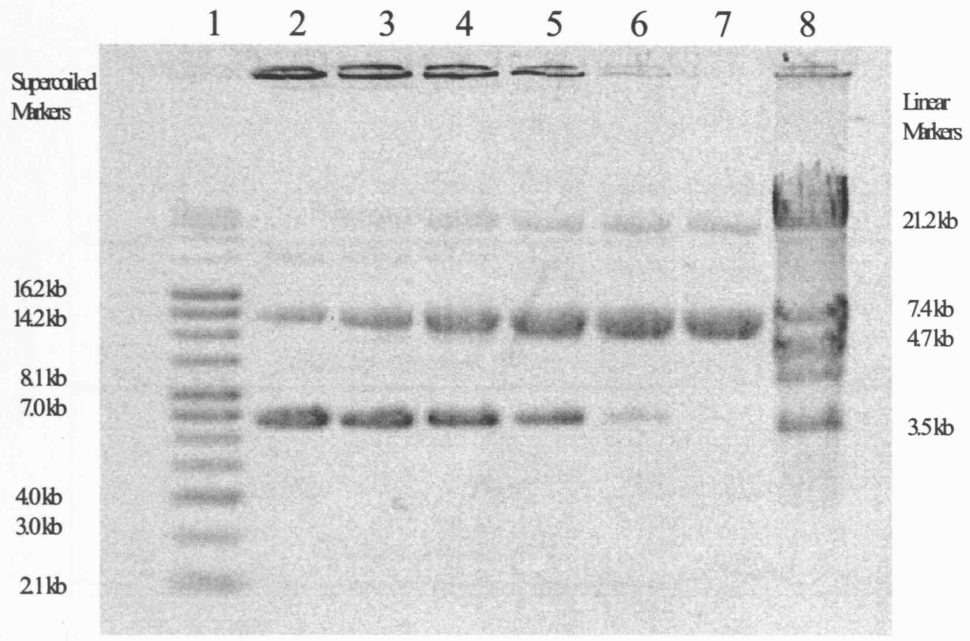

Figure 3.9. Samples for testing resolution of relaxed and supercoiled forms in the Q Sepharose HP analytical method (0.8% agarose gel). Combined samples were formed by mixing high-supercoiled-content and high-relaxed-content purified plasmid DNA samples in varying proportions. Lane 1: supercoiled ladder; Lane 2: 100% high-supercoiled sample; Lane 3: 75% high-supercoiled sample, 25% high-relaxed sample; Lane 4: 50% high-supercoiled sample, 50% high-relaxed sample; Lane 5: 25% high-supercoiled sample, 75% high-relaxed sample; Lane 6: 5% high-supercoiled sample, 95% high-relaxed sample; Lane 7: 100% high-relaxed sample; Lane 8: linear DNA ladder.

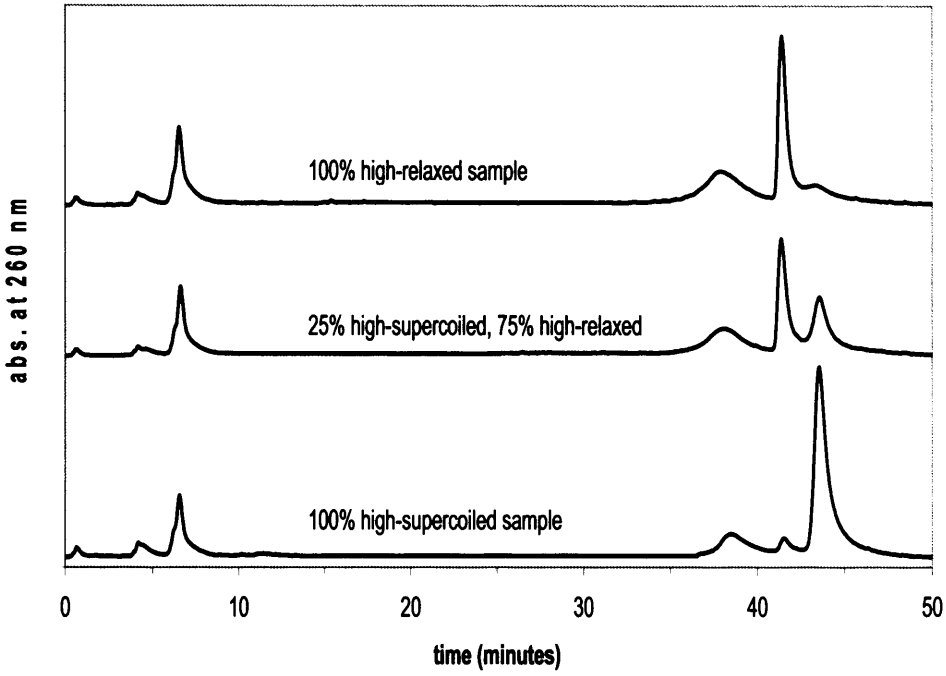

Figure 3.10. Q Sepharose HP chromatograms showing resolution of supercoiled and relaxed plasmid DNA forms, for samples containing varying supercoiled to relaxed ratios. Bottom: 100% high-supercoiled sample (Figure 3.9 Lane 2); Middle: 25% high-supercoiled sample, 75% high-relaxed sample (Figure 3.9 Lane 4); Top: 100% high-relaxed sample (Figure 3.9 Lane 7); samples shown were injected prior to heat-pre-treatment. Peak at 6.5 minutes is residual digested RNA, peak at 38.5 minutes is residual single-stranded chromosomal DNA, peak at 41.5 minutes is relaxed plasmid DNA, and peak at 44 minutes is double-stranded DNA (primarily supercoiled plasmid).

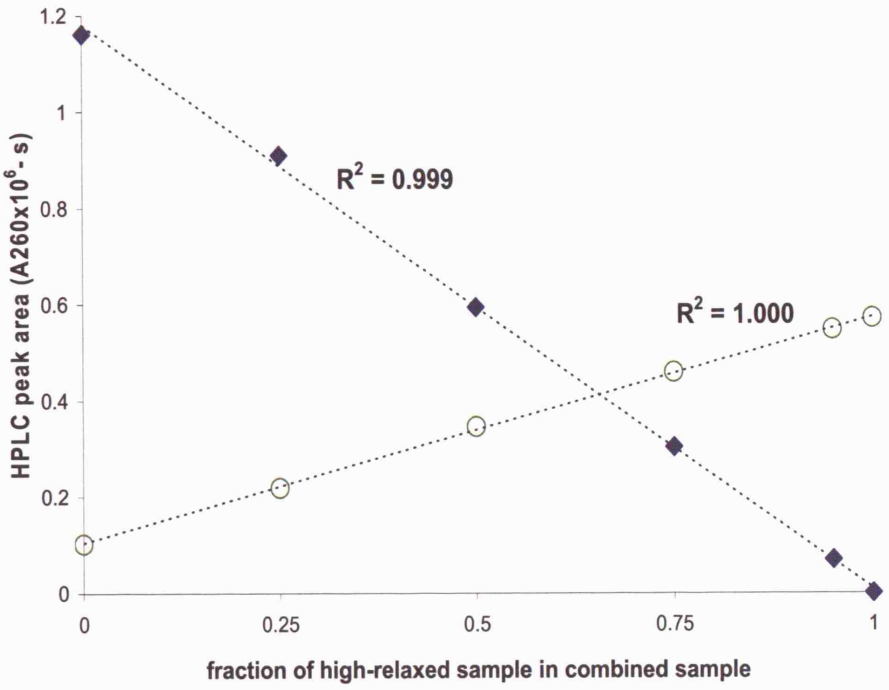

Figure 3.11 Correlation of supercoiled and relaxed plasmid HPLC peak areas to mixture ratio used, for combined samples with varying proportions of supercoiled to relaxed plasmid. Samples were formed by combining high-supercoiled-content and high-relaxed-content pSVβ plasmid DNA samples in varying ratios, indicated on horizontal axis by fraction of high-relaxed sample included in the combined sample. Relaxed plasmid peak areas (open circles, 41.5-minute elution) were determined from injections of non-heated samples; supercoiled peak areas (solid diamonds, 44-minute elution) were determined from separate runs of heat-pre-treated samples.

pre-treatment step. Plasmid peaks after pre-treatment were reduced significantly and did not appear to shift to the flow-through or other peaks, suggesting perhaps that heating in the presence of high salt resulted in aggregation or precipitation of supercoiled plasmid. This could be overcome by dilution or by performing a buffer exchange through alcohol precipitation / resuspension into TE buffer.

3.2.9 Application of HPLC method to process stream sample

To demonstrate the utility of the method, a process stream sample of clarified lysate containing a mixture of nucleic acids was analyzed. Figure 3.12 shows chromatograms for this sample before and after the chromosomal DNA denaturation pre-treatment. Concentrations of the nucleic acid components were calculated based on peak areas, dilution factors, and the standard curves.

3.2.10 Discussion

The HLPC method presented here should serve as an effective analytical tool for monitoring different nucleic acids in complex streams not only from precipitation experiments, but from purification process samples in general. The high correlation coefficients of the standard curves show that the assay provides accurate results over a wide concentration range and also suggest a high degree of reproducibility. However a few possible limitations should be pointed out. First, although the method should be applicable generally for quantifying nucleic acids in most typical process streams, the method has only been extensively

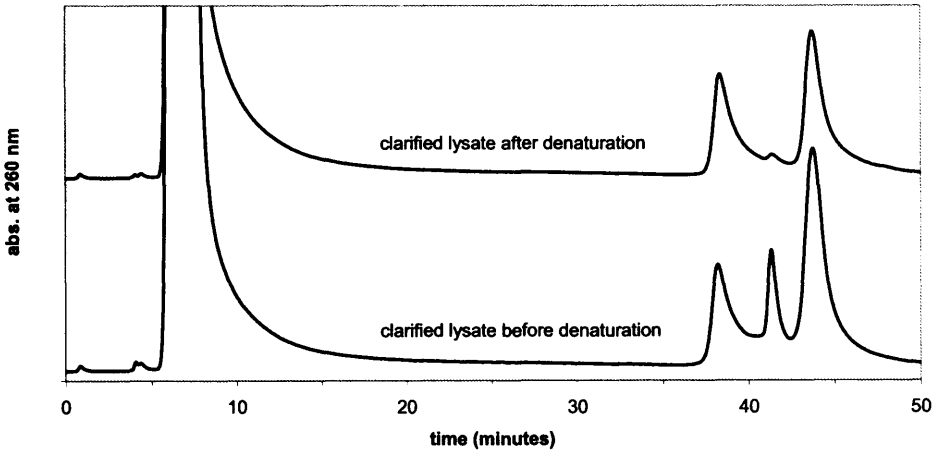

Nucleic Acid Component	Concentration (µg/mL)	Fraction of Total
RNA	2690	91.5%
single-stranded DNA	56	1.9%
double-stranded chromosomal DNA	44	1.5%
relaxed plasmid	59	2.0%
supercoiled plasmid	92	3.1%

Figure 3.12 Example of sample analysis using developed Q Sepharose HP analytical method. Shown are chromatograms for clarified lysate sample in TE buffer (see agarose gel Figure 3.1 lane 2) before and after heat denaturation (bottom and top chromatograms respectively). Peak at 6.5 minutes is digested RNA, peak at 38.5 minutes is single-stranded chromosomal DNA, peak at 41.5 minutes is relaxed plasmid DNA, and peak at 44 minutes is double-stranded DNA. From bottom chromatogram, concentrations were determined for RNA, single-stranded DNA, relaxed plasmid DNA, and total double-stranded DNA based on peak areas and standard curves; from top chromatogram, supercoiled plasmid DNA concentration was determined from the 44-minute peak area after sample heat-pre-treatment (3 minutes incubation at 85°C); double-stranded chromosomal DNA concentration was determined based on the difference in 44-minute peak areas for runs before and after sample pre-treatment (assumed no linear plasmid DNA based on the agarose gel analysis).

studied with streams sourced from the *E. coli* DH5α strain containing the pSVβ plasmid. Initial studies with a 20 kb plasmid (pQR150) showed similar results with the exception of decreased resolution of the relaxed form, suggesting that the method would likely be adaptable to other plasmids (e.g. possibly by using a shallower gradient in the case of pQR150).

A second consideration is that for this method, RNase-treated RNA elutes as part of the flow-through, showing very little interaction with the Q Sepharose HP resin. Other possible flow-through component such as proteins or sample buffer components could potentially affect the A260 signal for this peak if present in high enough concentrations relative to RNA. For most samples during purification, this generally is not a concern because RNA concentrations overwhelm contributions from other components. For quantitation of high-M_r RNA in samples with significant relative fractions of other flow-through impurities, an additional run without RNase-treatment could be used; undigested high-M_r RNA does not elute as part of the flow-through therefore the area difference between the two flow-through peaks would represent high-M_r RNA. Finally, it should be noted for the chromosomal DNA denaturation step, that although the decrease in the 44.0 minute double-stranded peak is normally accompanied by an increase in the 38.5 minute single-stranded DNA peak, this increase is normally less than would be expected for a full mass balance. This may be due to the denaturation step forming some large chromosomal DNA aggregates that do not elute until the column is regenerated with sodium hydroxide. For this reason, double-stranded chromosomal DNA should be

calculated based on the decrease in the 44.0 minute peak rather than the increase in the 38.0 minute peak.

In this method single-stranded DNA and relaxed plasmid DNA were shown to elute prior to double-stranded DNA in an increasing sodium chloride gradient; this is consistent with findings from Prazeres et al. (Prazeres et al., 1998) when Q Sepharose Fast Flow media (90 μm particle size) was used for plasmid purification at the preparative scale. The fact that relaxed plasmid elutes as a separate peak from supercoiled plasmid in both of these methods suggests that the interaction between DNA and the stationary phase is due to factors other than just anion-exchange, since the net charge of relaxed and supercoiled forms are presumably the same.

3.3 POROS-20 PI HPLC assay

This method was developed using a weak anion-exchange resin to provide an alternative assay for quantifying nucleic acid content from multi-component process streams. The POROS PI resin contains polyethyleneimine functional groups bound to polystyrene-divinylbenzene base particles. All samples were pre-treated with RNase just as in the Q Sepharose method. An alternative denaturing pre-treatment using a pH shift to approximately pH 12.5 (followed by returning to pH 8) instead of heating/cooling was also developed in conjunction with this method. Example chromatograms using this method are shown in Figure 3.13.

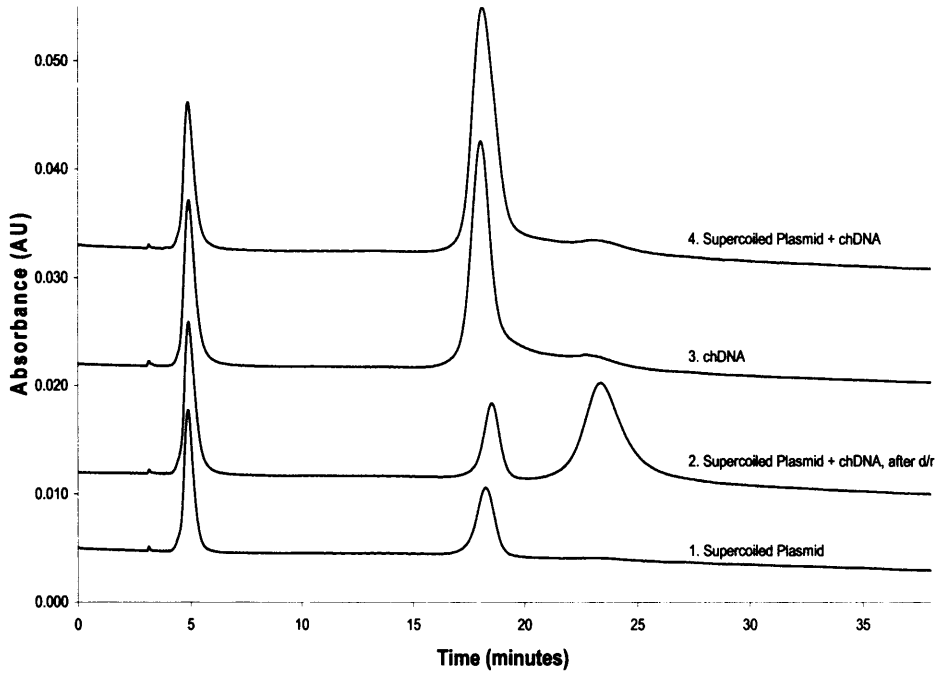

Figure 3.13 Example chromatograms for purified components from Poros-PI HPLC method. In this method, residual digested RNA elutes at 5 minutes, double-stranded DNA elutes at 18 minutes, and single-stranded DNA elutes at 23 minutes. Chromatograms from top to bottom, 4) supercoiled plasmid DNA combined with chromosomal DNA; 3) chromosomal DNA only; 2) supercoiled plasmid with chromosomal DNA after pH denaturing pre-treatment; 1) supercoiled plasmid DNA only.

3.4 Comparison of Q Sepharose HP and Poros PI assays

Both of these HPLC methods developed are effective in quantifying RNA, single-stranded DNA, total double-stranded DNA, and supercoiled plasmid DNA from multi-component process stream samples. A key difference between the two assays is the additional capability with the Q Sepharose HP method to resolve and quantitate relaxed forms of plasmid DNA.

It is interesting that although single-stranded DNA eluted prior to double-stranded DNA using the Q Sepharose HP strong-anion-exchange media (previous section), the elution order of these two forms was reversed when POROS weak-anion-exchange resin was used, and this held whether the single-stranded form was chromosomal as shown in previous sections or plasmid-derived (Prazeres et al., 1998). The Q Sepharose HP media in these studies contained quaternary amine functional groups bound to crosslinked agarose particles, while the POROS PI media contained polyethyleneimine functional groups bound to polystyrene-divinylbenzene particles. Prazeres et al. suggested that this reverse elution behaviour was due to either increased electrostatic interactions or increased hydrophobic interactions between single-stranded DNA portions and the POROS PI resin (Prazeres et al., 1998). Our studies lend further support to the hypothesis that the reverse elution behaviour is due to greater hydrophobic interactions between exposed bases of single-stranded DNA and the POROS PI polystyrene-divinylbenzene base matrix (hydrophobic) compared to the Q Sepharose HP agarose base matrix (hydrophilic). This reckoning is also supported by studies which showed single-stranded forms had greater retention

times during hydrophobic interaction chromatography (Diogo et al., 1999;Diogo et al., 2000).

3.5 Summary

Analytical techniques were developed to quantitate the different forms of nucleic acids found in typical purification process streams. The Q Sepharose HP assay is a high resolution strong anion-exchange assay with separation of nucleic acid forms based upon differential interaction with quaternary amine functional groups. The Poros PI assay is a weak anion exchange assay with separation based upon interaction with polyethyleneimine functional groups. Both methods provide the capability to quantify RNA, single-stranded DNA, total double-stranded DNA, and supercoiled plasmid DNA from multi-component process stream samples. A unique aspect of the Q Sepharose HP assay is the additional capability to resolve and quantitate relaxed forms of plasmid DNA. Because of this capability, the Q Sepharose HP method was used for analyses of multi-component process streams in this project. The development of this assay was important for the project because it provided the capability to obtain precipitation data on real multi-component process streams, to supplement data from single-component solubility studies.

4 PRELIMINARY INVESTIGATION OF NUCLEIC ACID PRECIPITATION PARAMETERS

4.1 Introduction

These initial studies were performed to investigate a broad range of precipitation parameters, to determine which parameters to pursue for more detailed study of plasmid DNA purification. Many of these experiments were single-component solubility experiments, with some follow-up experiments on multi-component clarified lysate stream using the HPLC analytical technique described in Section 3. The precipitation parameters investigated included cation valency and concentration (from dissolved salts), pH, initial nucleic acid concentration, addition of non-ionic polymer, and addition of organic anti-solvent.

4.2 Single-component solubilities in monovalent cation salts

Single-component experiments were performed using monovalent cation salts as precipitating agents to characterise solubility behaviour of the separate purified nucleic acid components (plasmid DNA, chromosomal dsDNA, chromosomal ssDNA, and rRNA). Figure 4.1 through Figure 4.4 show the results of these solubility experiments with sodium chloride, lithium chloride, and ammonium sulphate.

Note that in these experiments the initial nucleic acid concentrations were all between 50 and 100 μg/mL, although each component had a slightly different

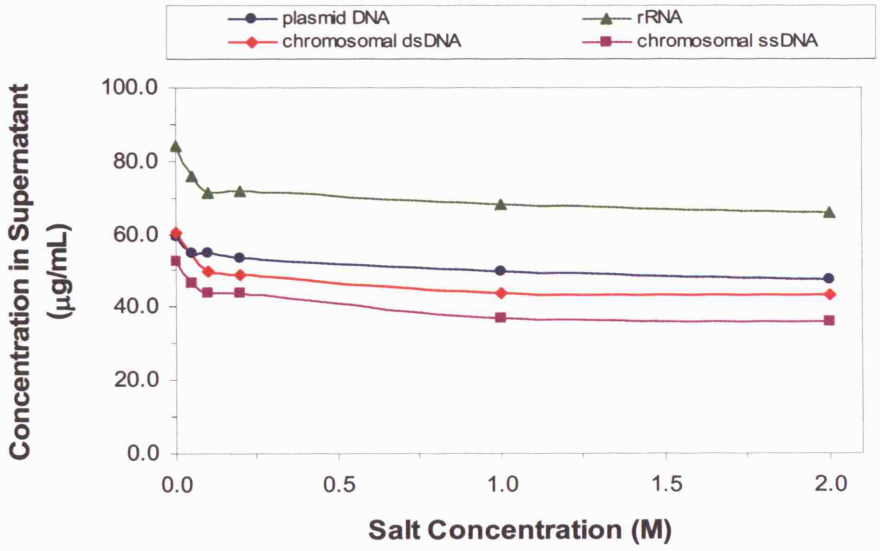

Figure 4.1 Solubilities of different purified nucleic acid forms in **sodium chloride** solution at pH 8, plotted as nucleic acid concentration in the supernatant versus salt concentration. Nucleic acid concentrations in supernatant samples were determined based on A260 measurements from separate samples; initial concentrations were 50-100 µg/mL for each component. Estimated average error for each measurement is ± 5%.

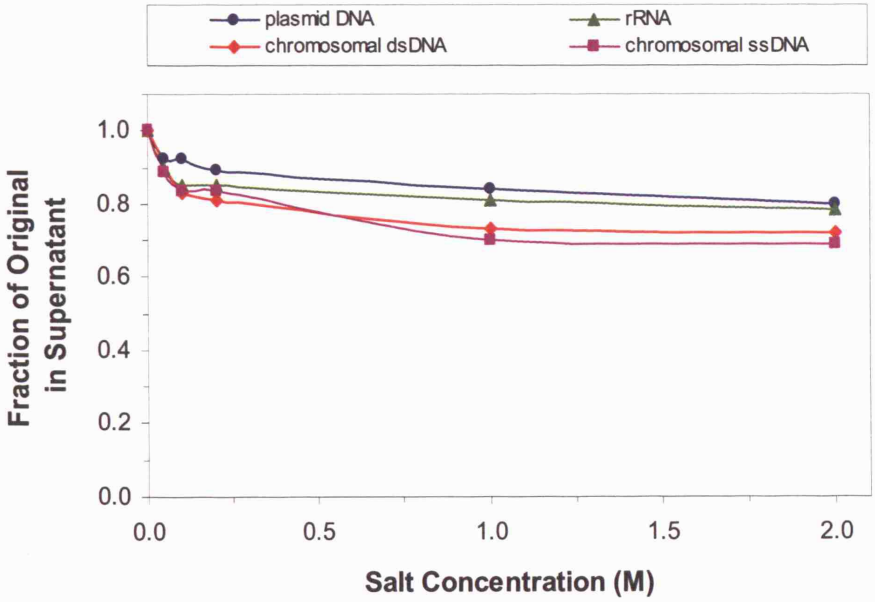

Figure 4.2 Solubilities of different purified nucleic acid forms in **sodium chloride** solution at pH 8, plotted as fraction of initial nucleic acid concentration in the supernatant versus salt concentration. Nucleic acid concentrations in supernatant samples were determined based on A260 measurements from separate samples; initial concentrations were 50-100 μg/mL for each component. Estimated average error for each measurement is ± 5%.

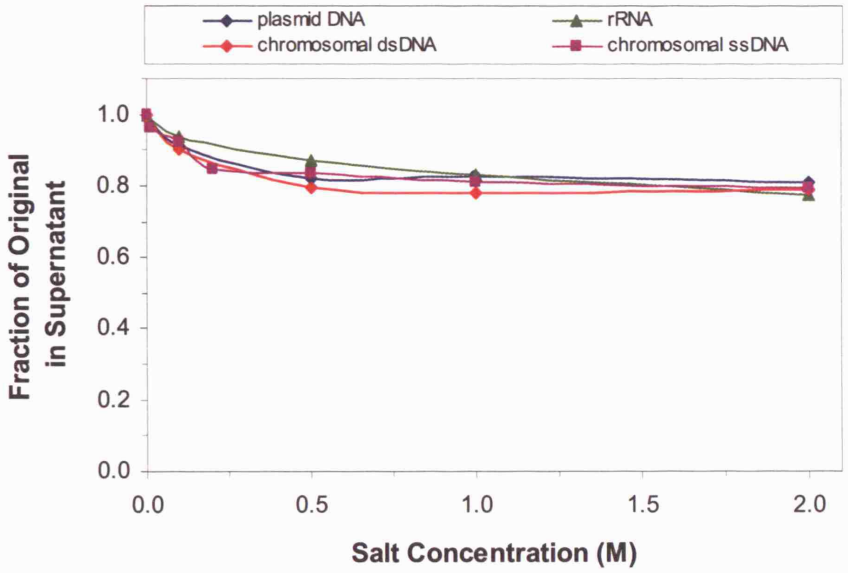

Figure 4.3 Solubilities of different purified nucleic acid forms in **lithium chloride** solution at pH 8. Nucleic acid concentrations in supernatant samples were determined based on A260 measurements from separate samples; initial concentrations were 50-100 μg/mL for each component. Estimated average error for each measurement is ± 5%.

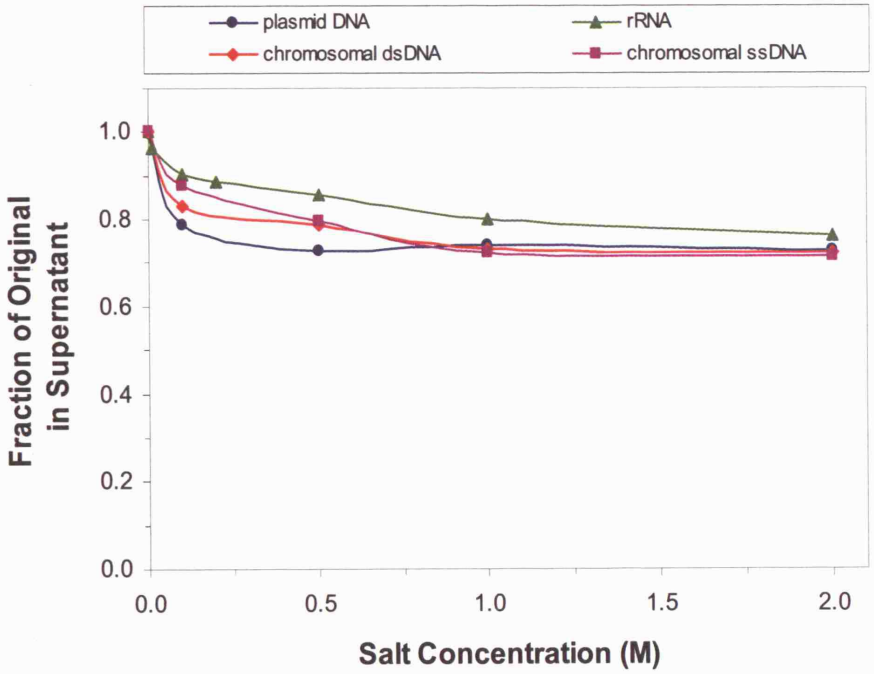

Figure 4.4 Solubilities of different purified nucleic acid forms in **ammonium sulphate** solution at pH 8. Nucleic acid concentrations in supernatant samples were determined based on A260 measurements from separate samples; initial concentrations were 50-100 μg/mL for each component. Estimated average error for each measurement is ± 5%.

initial concentration. Figure 4.1 shows single-component supernatant concentrations versus sodium chloride concentration. Figure 4.2 is the same plot with supernatant concentrations for each component normalised to its initial concentration (i.e. the fraction of initial concentration is plotted versus salt concentration). Generally it was found that nucleic acid concentration in the supernatant was proportional to initial concentration, i.e. the fraction precipitated was insensitive to initial concentration. This behaviour is consistent with the counterion condensation theory model (Manning, 1978), which suggests that as long cations are in excess of nucleic acid phosphate groups, the fraction of phosphates neutralised will be equivalent regardless of the nucleic acid concentration. Therefore solubility results in this thesis are presented in the normalised format shown in Figure 4.2. The effect of initial nucleic acid concentration is also discussed further in Section 4.6.

These results showed plasmid DNA, chromosomal DNA (primarily double-stranded), denatured chromosomal DNA (single-stranded), and ribosomal RNA to all be relatively soluble in solutions with monovalent cation salts. Even when salt levels were 2 M, all of these components showed approximately 70-80% of initial concentrations in the supernatant, compared to control supernatants with no salt added.

For purified double-stranded plasmid and chromosomal DNA, it was somewhat unexpected that solubilities were apparently less than 100% in monovalent cation solutions, since according to Wilson and Bloomfield's extension of Manning's counterion condensation theory (Manning, 1978;Wilson and Bloomfield, 1979),

monovalent cations should not provide sufficient charge neutralisation for collapse or aggregation of dsDNA molecules in aqueous solution. A number of possible reasons could help explain this observed behaviour. One possibility is the presence of soluble aggregates in the initial purified samples, which aggregated further to larger size upon introduction of the salt solution and were removed during centrifugation. Another possibility is the presence of small fractions of impurities (for example large single-stranded DNA, RNA, or even proteins) which precipitated in the presence of monovalent cation salts, possibly entraining dsDNA molecules. It is clear from agarose gel analysis of the purified components (Figure 3.1) that slight amounts of impurities were present in these samples. Similarly if primarily dsDNA molecules contained some single-stranded regions this too could conceivably result in some degree of precipitation by monovalent cations. Another possibility is that monovalent cations may have caused dsDNA molecules to adapt a more compact (although not collapsed) form, resulting in lower absorbance readings while remaining soluble. Of course a combination of the factors above may have been responsible for the observed behaviour as well.

It should be noted that lithium chloride in aqueous solution has been reported to be an effective precipitating agent for high molecular weight RNA (Barlow et al., 1963), however as seen in Figure 4.3 only partial precipitation of *E. coli* RNA by lithium chloride could be obtained with repeated attempts in the experiments here (for example only 23% of initial RNA concentration was precipitated in 2.0 M lithium chloride); perhaps these different observed behaviours could be due to specific differences in RNA structure used in the different experiments.

These experiments showed that all the nucleic acid forms studied were relatively soluble in the presence of monovalent cation salts, with little differences in solubility between the different forms. Therefore monovalent cation salts alone did not appear promising for separation of different nucleic acid forms by precipitation, and were not pursued further in this project.

4.3 Studies on divalent cation salts as precipitating agents

Single- and multi-component experiments were performed using divalent cation salts as precipitating agents to characterise solubility behaviour of the separate purified nucleic acid components.

4.3.1 Single-component solubilities in divalent cation salts

Figure 4.5 and Figure 4.6 shows the results of the single-component precipitation experiments with calcium chloride and magnesium chloride respectively. The solubility profiles shown in Figure 4.5 and Figure 4.6 show that divalent cations were highly effective at precipitating single-stranded DNA and rRNA, but that double-stranded DNA (plasmid or chromosomal) remains relatively soluble even at divalent cation concentrations as high as 0.5 M. Note the slight drop in solubility observed may have been due to remaining impurities in the dsDNA samples as explained in the previous section. These results led to the preliminary

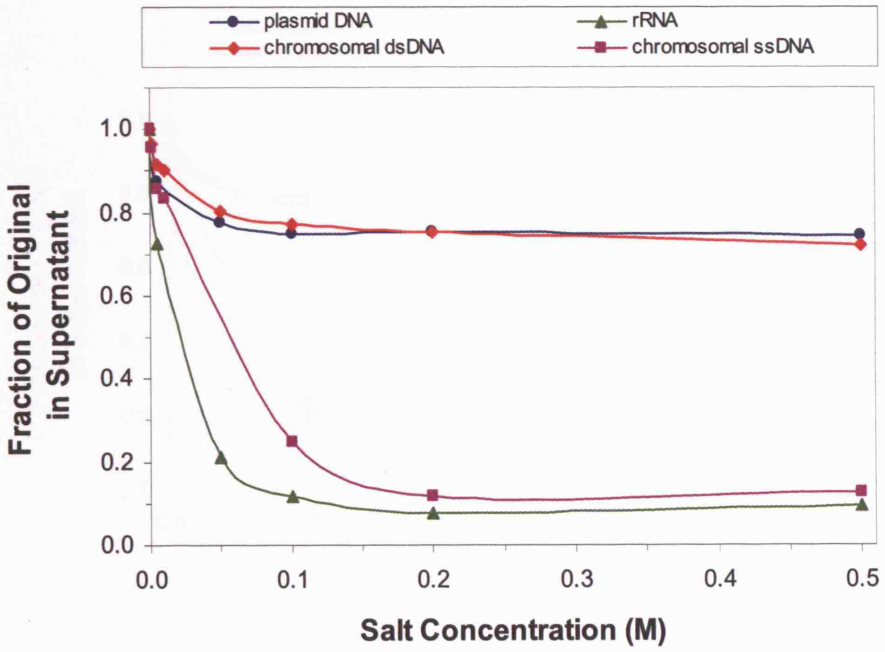

Figure 4.5 Solubilities of different purified nucleic acid form in **calcium chloride** solution at pH 8. Nucleic acid concentrations in supernatant samples were determined based on A260 measurements from separate samples; initial concentrations were 50-100 μg/mL for each component. Estimated average error for each measurement is ± 5%.

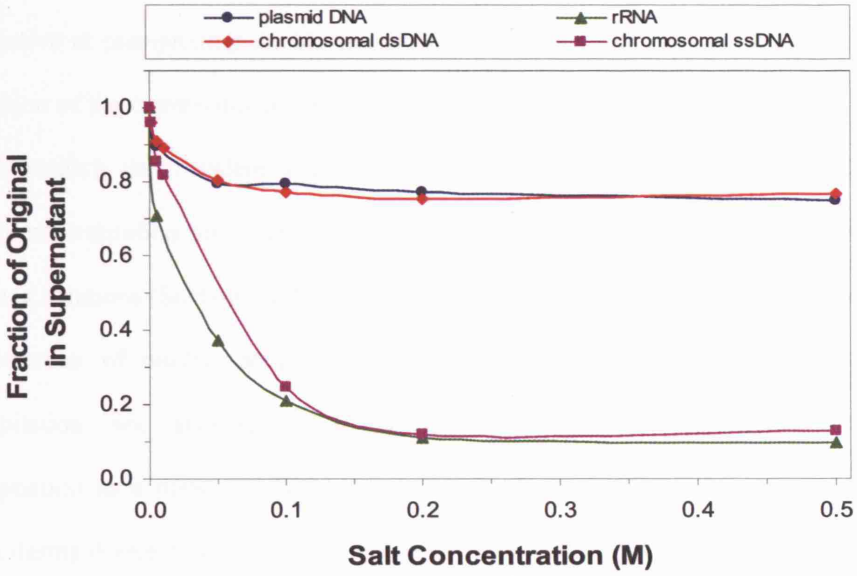

Figure 4.6 Solubilities of different purified nucleic acid forms in **magnesium chloride** solution at pH 8. Nucleic acid concentrations in supernatant samples were determined based on A260 measurements from separate samples; initial concentrations were 50-100 μg/mL for each component. Estimated average error for each measurement is ± 5%.

conclusion that higher degrees of single-strandedness result in lower nucleic acid solubility in divalent cation solutions. The fact that divalent cations were ineffective at precipitating double-stranded forms of DNA is also supported by extension of the counterion-condensation theory (Wilson and Bloomfield, 1979), which predicts that trivalent or higher cations are needed to provide sufficient charge neutralisation for collapse (or precipitation) of double-stranded DNA in aqueous solutions (Section 1.7.1). These single-component results suggested that fractionation of nucleic acid forms may be possible using divalent cation precipitation, and also led to the investigation of denaturation prior to precipitation as a means to improve separation of chromosomal from plasmid DNA during divalent cation precipitation.

4.3.2 Calcium chloride precipitation of E. coli clarified lysate

The encouraging results from single-component solubility experiments led to further investigation of divalent cation precipitation for multi-component streams. Calcium chloride precipitation of clarified lysate in TE buffer was first investigated, and results from these experiments are shown in Figure 4.7, Figure 4.8, and Figure 4.9. The agarose gel in Figure 4.7 clearly shows that 0.2 M calcium chloride precipitation was effective in clearing a significant fraction of RNA and as well as some chromosomal DNA from clarified lysate with minimal loss of plasmid DNA. The Q Sepharose HP HPLC assay was used to quantify nucleic acid forms in the feed and supernatant streams; this showed 83% RNA clearance (Figure 4.8), 100% clearance of single-stranded DNA, 70% clearance of double-stranded chromosomal DNA, and 48% clearance of relaxed plasmid

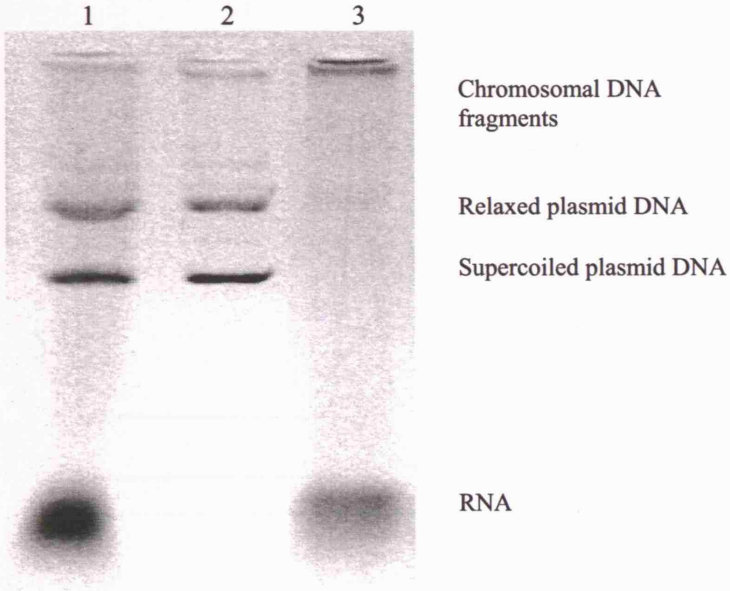

Figure 4.7 Effect of 0.2 M calcium chloride precipitation on clarified lysate (0.8% agarose gel). Lane 1: Clarified lysate in TE buffer (pH 8) prior to precipitation; Lane 2: Supernatant after precipitation/centrifugation; Lane 3: Resuspended pellet after precipitation/centrifugation.

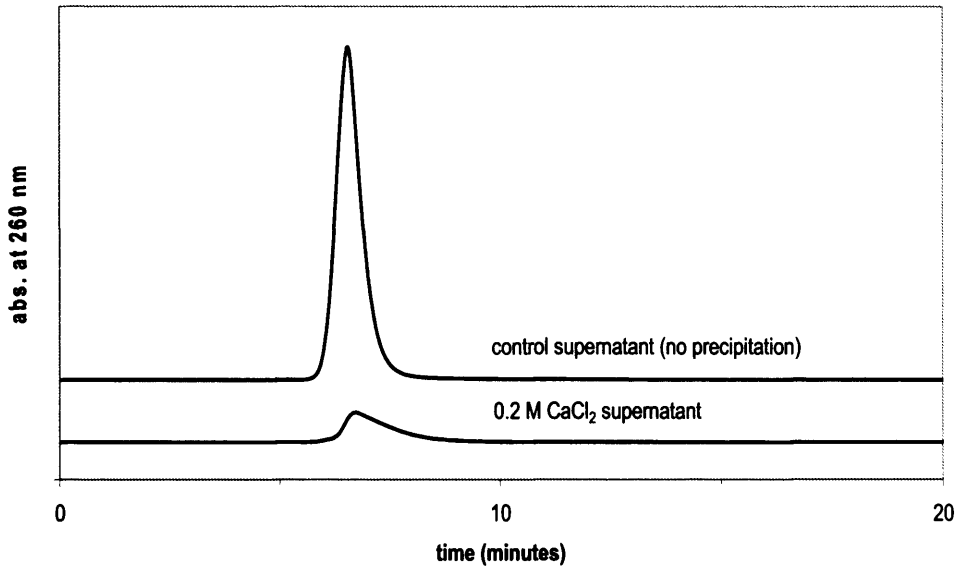

Component	Cl. Lysate Control Conc. (µg/mL)	0.2 M $CaCl_2$ Sup. Conc. (µg/mL)	0.2 M $CaCl_2$ Sup. Fraction of Orig.
RNA	2690	453	17%

Figure 4.8 Q Sepharose HP analytical chromatograms showing RNA peak to demonstrate effectiveness of calcium chloride precipitation. Top: clarified lysate control supernatant in TE buffer (no calcium chloride added, pH 8); Bottom: supernatant from clarified lysate following 0.2 M calcium chloride precipitation. Concentrations were determined from standard curves.

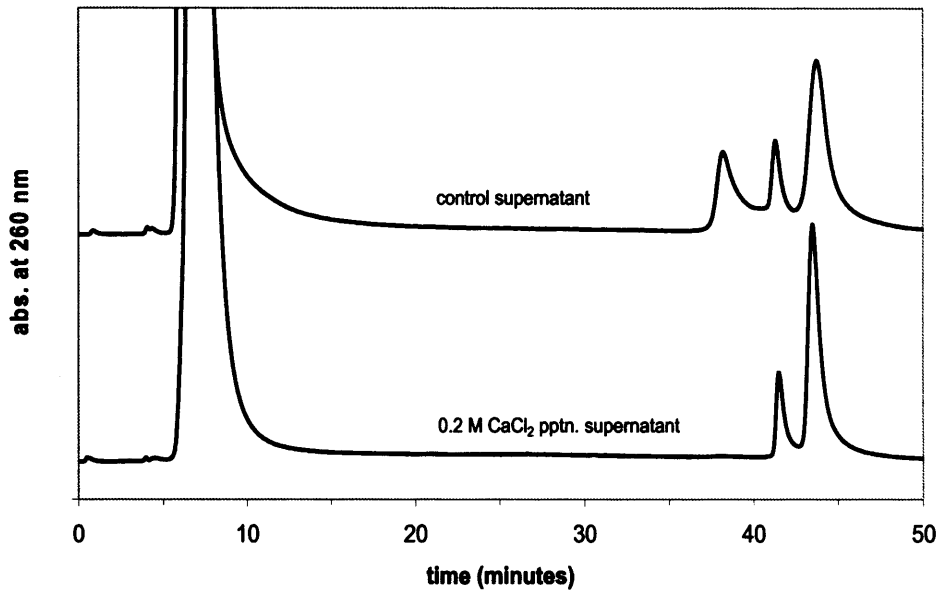

Component	Cl. Lysate Control Conc. (µg/mL)	0.2 M $CaCl_2$ Sup. Conc. (µg/mL)	0.2 M $CaCl_2$ Sup. Fraction of Orig.
single-stranded DNA	56	0	0%
ds-chromosomal DNA	44	13	30%
relaxed plasmid DNA	52	27	52%
supercoiled plasmid DNA	92	88	96%

Figure 4.9 Q Sepharose HP analytical chromatograms to demonstrate effectiveness of calcium chloride precipitation for DNA impurity clearance. Top: clarified lysate control supernatant in TE buffer (no calcium chloride added, pH 8); Bottom: supernatant from clarified lysate following 0.2 M calcium chloride precipitation. Peak at 6.5 minutes is digested RNA, peak at 38.5 minutes is single-stranded chromosomal DNA, peak at 41.5 minutes is relaxed plasmid DNA, and peak at 44 minutes is double-stranded DNA (primarily supercoiled plasmid). Component concentrations were determined from standard curves.

DNA with minimal supercoiled plasmid loss (Figure 4.9). From these results it was clear that divalent cation precipitation held promise for fractional precipitation purification of different nucleic acid forms. The fact that plasmid DNA remained in solution and did not precipitate was also encouraging from a recoverability/yield standpoint even though chromosomal dsDNA also remained in solution.

4.4 Single-component solubilities in trivalent polyamine

Single-component solubilities were tested for the trivalent polyamine spermidine^{3+}. Results are shown in Figure 4.10. As seen in Figure 4.10, plasmid DNA (double-stranded) was found to precipitate at a very low concentration of spermidine^{3+} (approximately 1 mM), consistent with previous findings for linear and circular DNA (Raspaud et al., 1998;Murphy et al., 1999). These findings are also consistent with the extension of the counterion condensation theory (Wilson and Bloomfield, 1979), which states that trivalent cations in aqueous solution should result in collapse or aggregation of dsDNA molecules (see Table 1.3). The results for rRNA are also consistent with previous findings (Murphy et al., 1999). The fact that dsDNA precipitates in the presence of spermidine^{3+} but RNA does not (opposite of the behaviour in divalent cation solutions) is very interesting. This has not been addressed theoretically in the literature; possible explanations include steric limitations to phosphate binding sites on RNA, RNA charge reversal, or insufficient ion-bridging due to the relatively smaller size of RNA compared to DNA. It also interesting that single-stranded DNA showed

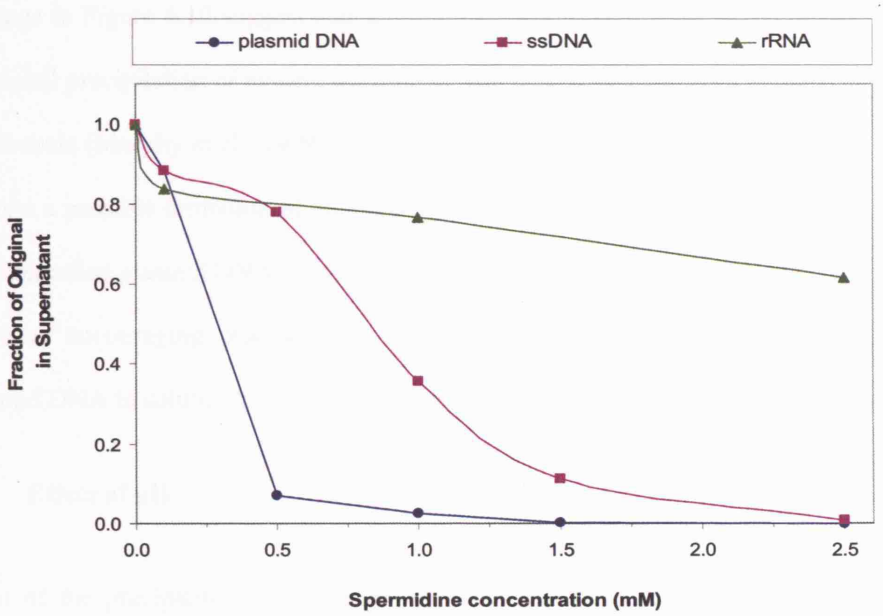

Figure 4.10 Solubilities of different purified nucleic acid forms in solution with the polyamine spermidine chloride at pH 8. Single-stranded DNA was formed by denaturing plasmid DNA (1.5 hrs at 95°C). Nucleic acid concentrations in supernatant samples were determined based on A260 measurements from separate samples; initial concentrations were 50-100 μg/mL for each component. Estimated average error for each measurement is ± 5%.

higher solubility in spermidine^{3+} solution than double-stranded DNA. The findings in Figure 4.10 suggest that spermidine^{3+} would be a good candidate for fractional precipitation of nucleic acid forms, and indeed this has been pursued at small-scale (Murphy et al., 1999). However if plasmid DNA were the species of interest a possible limitation of this strategy at large scale could be full recovery of supercoiled plasmid DNA from the precipitated pellet. Because of this and the previous encouraging results using divalent cation precipitation (which left plasmid DNA in solution), polyamine precipitation was not pursued further.

4.5 Effect of pH

Most of the precipitation experiments were carried out at pH 8, since nucleic acids are typically stable at pH 8 and most nucleic acid processing is carried out at this pH. A few follow-up experiments were performed at pH 6 to check if varying pH around neutral would exhibit different solubility behaviour. Plasmid DNA and rRNA single-component results are shown in Figure 4.11 for sodium chloride and Figure 4.12 for calcium chloride. Multi-component results using calcium chloride precipitation of clarified lysate are shown in Figure 4.13. For all of these experiments, very little difference in solubility behaviour was observed when carried out at pH 6 compared to pH 8. It appears that varying pH around neutral has little effect on nucleic acid solubility; since nucleic acids are highly charged molecules near neutral pH this finding was not surprising. The results in Figure 4.12 and Figure 4.13 showed that divalent cation precipitation on multi-component process streams would be robust with respect to variations in pH around neutral.

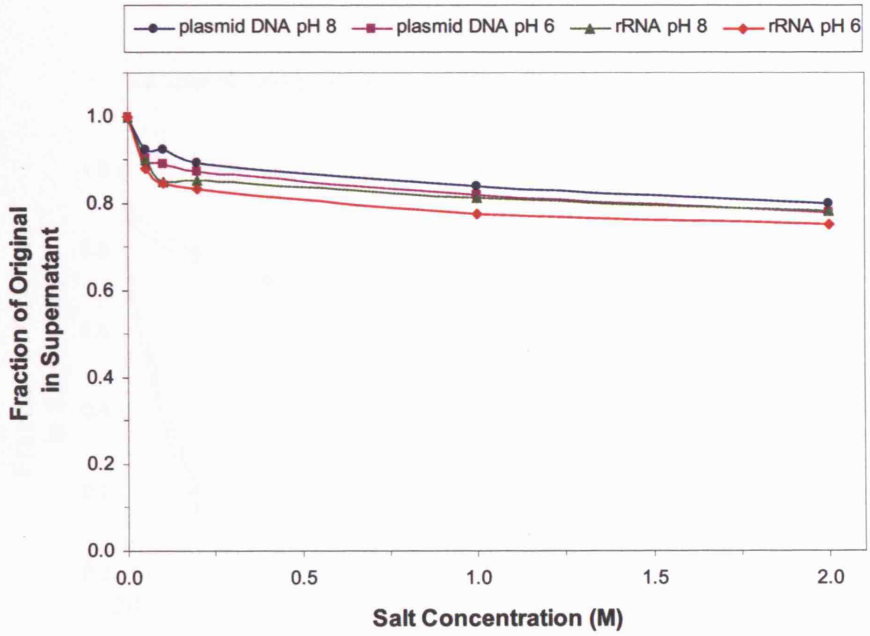

Figure 4.11 Solubilities of purified plasmid DNA and RNA in **sodium chloride solution at either pH 8 or pH 6**. Nucleic acid concentrations in supernatant samples were determined based on A260 measurements from separate samples; initial concentrations were 50-100 μg/mL for each component. Estimated average error for each measurement is ± 5%.

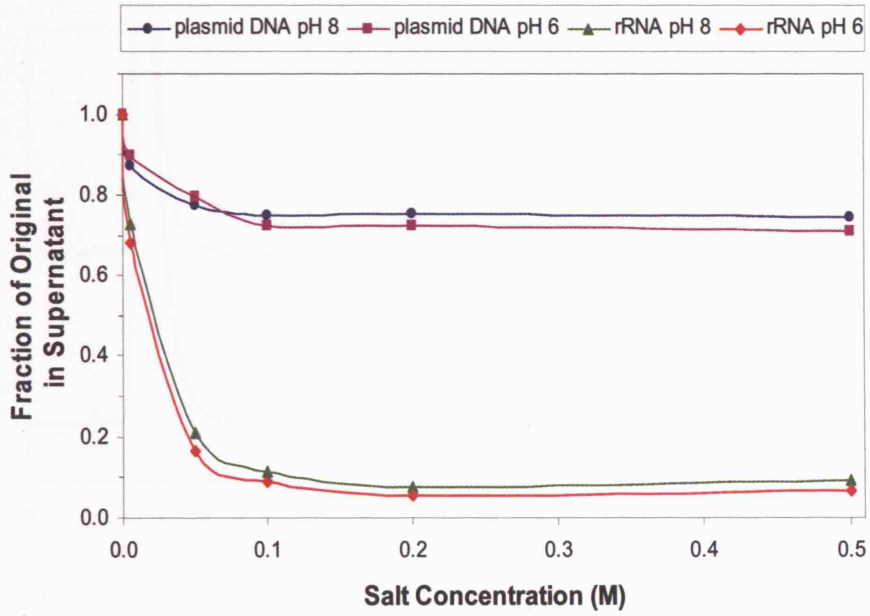

Figure 4.12 Solubilities of purified plasmid DNA and RNA in **calcium chloride solution at either pH 8 or pH 6**. Nucleic acid concentrations in supernatant samples were determined based on A260 measurements from separate samples; initial concentrations were 50-100 μg/mL for each component. Estimated average error for each measurement is ± 5%.

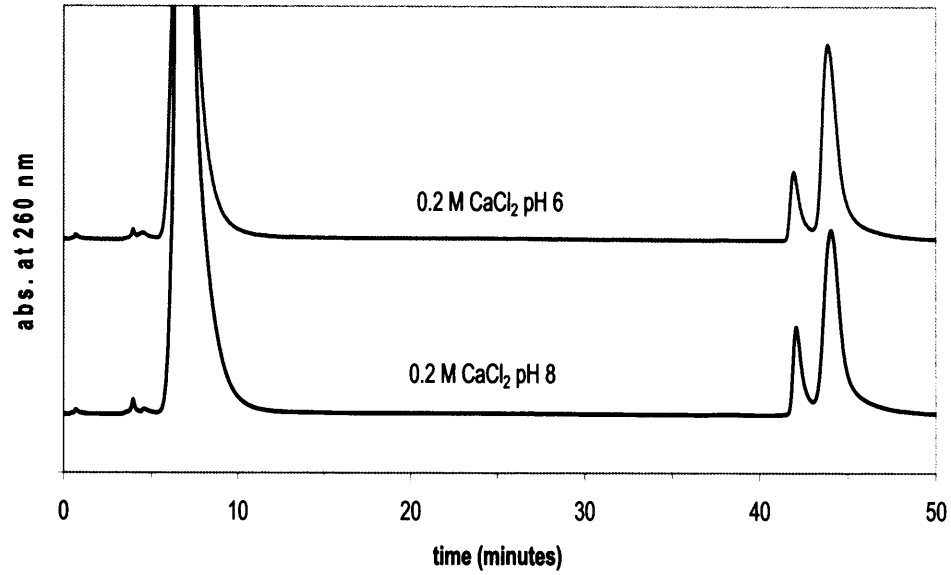

Component	Concentration (µg/mL) in pH 6 supernatant	Concentration (µg/mL) in pH 8 supernatant
RNA	303	290
single-stranded DNA	0.0	0.0
relaxed plasmid DNA	18.0	22.3
double-stranded DNA (incl sc-plasmid)	68.1	68.8

Figure 4.13 Comparison of Q Sepharose HP analytical chromatograms for supernatants from 0.2 M calcium chloride precipitations performed at pH 6 and pH 8. Peak at 6.5 minutes is digested RNA, peak at 38.5 minutes is single-stranded chromosomal DNA, peak at 41.5 minutes is relaxed plasmid DNA, and peak at 44 minutes is double-stranded DNA (primarily supercoiled plasmid). Component concentrations were determined from standard curves.

4.6 Effect of initial nucleic acid concentration

Single-component solubility experiments were carried out at 50 - 100 μg/mL initial nucleic acid concentration for all purified components. For plasmid DNA and chromosomal DNA, these concentrations were in the typical range for these components in clarified lysate process streams. However for RNA these concentrations were lower than the typical concentrations in clarified lysate (~2000 μg/mL) due to material limitations. To confirm that the single-component results for rRNA were representative of cases with higher initial concentrations, rRNA data from 0.2 M calcium chloride precipitation from Figure 4.5 (single-component solubility) were compared to Figure 4.8 (clarified lysate purification). In Figure 4.5, initial rRNA concentration was 50 μg/mL and the concentration in the supernatant was 4.5 μg/mL, for 91% clearance. In Figure 4.8, initial RNA concentration was 2690 μg/mL and the concentration in the supernatant was 453 μg/mL, for 83% clearance. Although the initial RNA concentrations and final supernatant concentrations in these two experiments were significantly different, the *fractions* remaining in the supernatants following divalent cation precipitation were roughly equal. As indicated in Table 1.2, in addition to rRNA clarified lysate also contains a small fraction of transfer RNA, which is more soluble than rRNA in calcium chloride solution, and could account for the slight difference in clearance levels in the two experiments. Therefore this comparison suggests that the single-component solubility results in salt solutions are representative in terms of fraction remaining in the supernatant.

This type of behaviour where concentration remaining in the supernatant is approximately proportional to initial concentration has also been observed for some types of proteins (Shih et al., 1992), and is consistent with the presence of a small sub-population of slightly different RNA molecules that are more soluble than the majority of RNA molecules in the presence of divalent cations. This relative insensitivity of solubility to initial nucleic acid concentration is also completely consistent with the counterion condensation theory model (Flock et al., 1996).

4.7 Effect of non-ionic polymer

Polyethylene glycol (PEG) was also investigated to determine if supplementing monovalent or divalent cation precipitation with a non-ionic polymer could help to fractionate nucleic acid forms. As discussed in Sections 1.6 and 0, addition of a non-ionic polymer such as PEG to a solution of biomolecules creates a steric exclusion force that can lead to aggregation or precipitation. The first experiment tested increasing levels of PEG-4000 in 0.75 M sodium chloride precipitation of clarified lysate. Results from this experiment, shown in Figure 4.14, showed that in 0.75 M sodium chloride, supercoiled plasmid DNA started to precipitate between 6.0% and 6.5% weight/volume PEG-4000 (lanes 2 and 4 respectively), and was fully in the precipitate phase by 8% weight/volume PEG-4000 (lane 10). Lanes 1 and 2 of Figure 4.14 show that using 0.75 M NaCl with 6.0% PEG-4000, some fractionation of RNA and chromosomal DNA from supercoiled plasmid DNA was obtained, however fractionation of these forms was not as complete as that obtained from divalent cation precipitation (Figure 4.7).

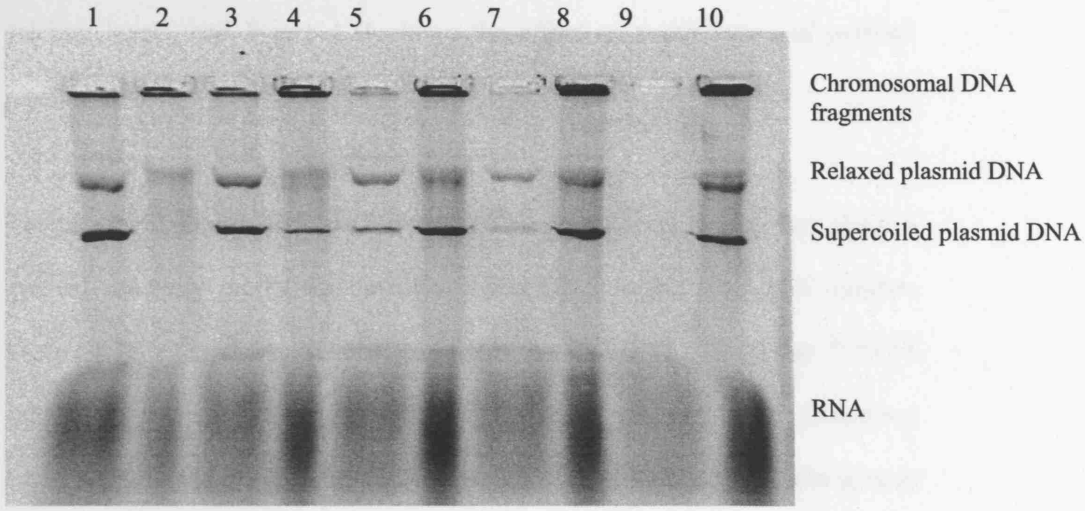

Figure 4.14 Effect of non-ionic polymer on monovalent cation precipitation of nucleic acids from clarified lysate solution. This 0.8% agarose gel shows effect of adding PEG-4000 at various levels to clarified lysate in 0.75 M NaCl buffer pH 8. Lanes 1/2: 6.0% weight/volume PEG-4000 supernatant/pellet; Lanes 3/4: 6.5% wt./vol. PEG-4000 supernatant/pellet; Lanes 5/6: 7.0% wt/vol. PEG-4000 supernatant/pellet; Lanes 7/8: 7.5% wt./vol. PEG-4000 supernatant/pellet; Lanes 9/10: 8.0% wt./vol. PEG-4000 supernatant/pellet.

This work was followed by investigating the effect of non-ionic polymer addition to divalent cation precipitation. Figure 4.15 shows the effect of PEG-4000 on calcium chloride precipitation of purified chromosomal DNA at two different calcium levels, and Figure 4.16 shows the effect on precipitation of purified plasmid DNA.

The results of Figure 4.15 are Figure 4.16 are interesting, in that they show a gradual solubility profile for double-stranded DNA in the salt / PEG system; Figure 4.15 even shows different solubility profiles for 0.05 M and 0.20 M calcium in the presence of PEG-4000. This result was somewhat unexpected since, according to the counterion condensation theory, for a single cation species in solution with dsDNA, charge neutralisation should be nearly independent of the bulk cation concentration (as long as cations are in excess of phosphate groups), and various studies *without* added polymer have suggested that this is the case. Note that the precipitation experiments in this project included 10 mM Tris for buffering, so although the divalent calcium cation concentrations used would be expected to dominate electrostatic interactions, these experiments did not strictly contain only one cation species. Based on these results, in the presence of PEG, the solubility behaviour of dsDNA appears similar to that of proteins (Mahadevan and Hall, 1992a) where bulk salt concentration in addition to PEG concentration affects solubility; other researchers have observed similar behaviour for DNA in salt / polymer systems (Vasilevskaya et al., 1995), although the mechanism for this behaviour is still

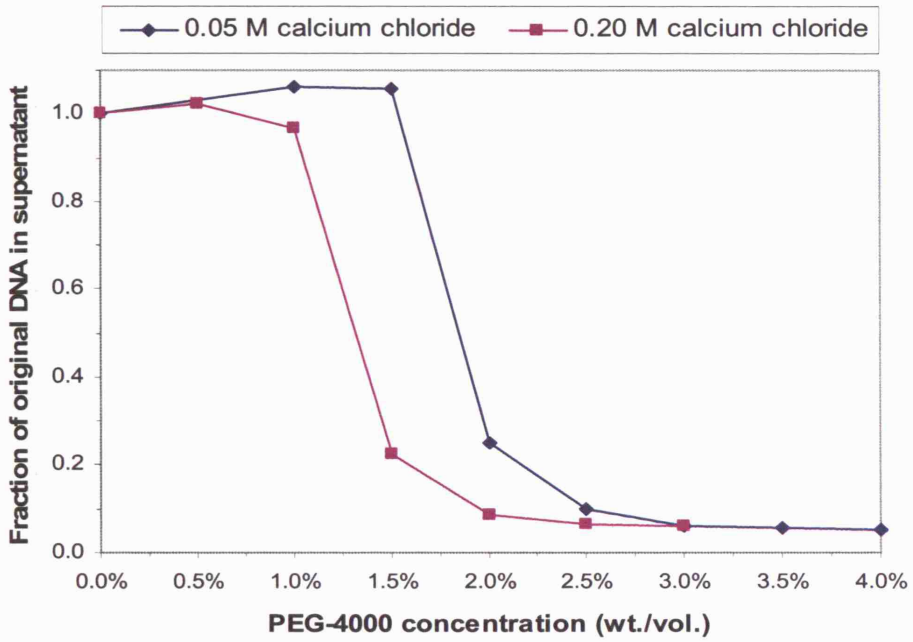

Figure 4.15 Effect of non-ionic polymer on divalent cation precipitation of double-stranded chromosomal DNA. PEG-4000 was added to varying levels in solutions of purified chromosomal DNA (from calf thymus) in either 0.05 M or 0.20 M calcium chloride solution pH 8. DNA concentrations in supernatant samples were determined from A260 measurements on separate samples. Initial DNA concentration was 200 μg/mL for all samples. Estimated average error for each measurement is ± 5%.

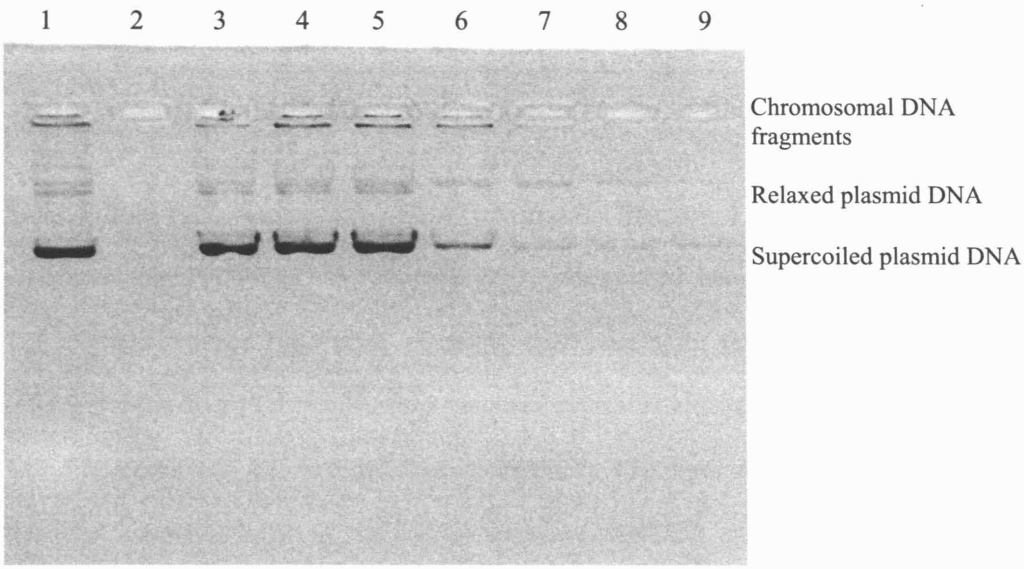

Figure 4.16 Analysis of selected supernatant samples from Figure 4.15, showing effect of non-ionic polymer on divalent cation precipitation of plasmid DNA. This 0.8% agarose gel shows effect of PEG-4000 / 0.20 M calcium chloride precipitation on supercoiled and relaxed plasmid DNA forms from purified solution in TE buffer. Lane 1: purified plasmid DNA in TE buffer; Lane 3: 0% wt./vol. PEG-4000 supernatant; Lane 4: 1.0% wt./vol. PEG-4000 supernatant; Lane 5: 2.0% wt./vol. PEG-4000 supernatant; Lane 6: 2.2% wt./vol. PEG-4000 supernatant ; Lane 7 : 2.4% wt./vol. PEG-4000 supernatant ; Lane 8 : 2.6% wt./vol. PEG-4000 supernatant ; Lane 9 : 2.8% wt./vol. PEG-4000 supernatant.

somewhat unclear. The solubility profiles of chromosomal and plasmid dsDNA in 0.2 M calcium chloride and varying PEG-4000 concentration are compared in Figure 4.17.

From Figure 4.17 chromosomal DNA precipitated between 1.0% and 2.0% weight/volume PEG-4000, and plasmid DNA precipitated between 2.0% and 3.0% weight /volume PEG-4000. Possible explanations for the difference in solubility behaviour of these two forms include molecular structural differences, size differences, and different initial concentrations. The chromosomal DNA in this experiment was larger in size and higher in concentration, and both of these factors have been found to be significant in fractional precipitation of proteins (Mahadevan and Hall, 1992b). Note that in both Figure 4.15 and Figure 4.17, at low concentrations of PEG-4000, A260 readings actually increased slightly compared to the no PEG samples; it is unclear why this occurred however it is believed that the slight increase observed was due to an assay artefact and not due to increased solubility at low PEG concentrations.

The results of Figure 4.17 suggest that 0.2 M divalent cation precipitation of clarified lysate could potentially be supplemented with approximately 2.0% weight/volume PEG-4000 to enhance separation of chromosomal DNA from plasmid DNA. Although this was an encouraging lead, denaturation plus divalent cation precipitation appeared more promising for separation of different nucleic acid forms including relaxed plasmid DNA from supercoiled plasmid DNA (see Section 5), therefore PEG precipitation was not pursued further.

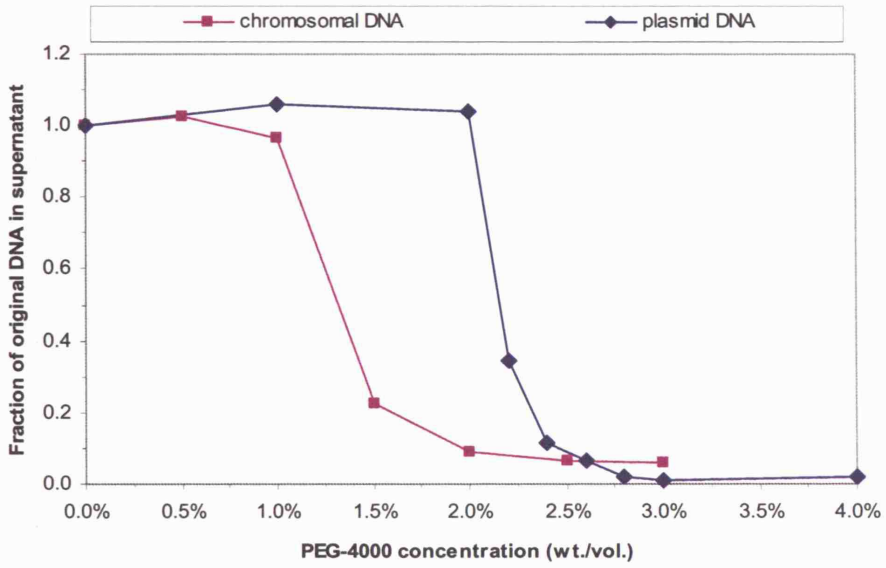

Figure 4.17 Effect of non-ionic polymer on divalent cation precipitation of chromosomal and plasmid DNA. PEG-4000 was added to varying levels in solutions of purified plasmid DNA in 0.20 M calcium chloride solution pH 8. DNA concentrations in supernatant samples were determined from A260 measurements on separate samples. Initial chromosomal DNA concentration was 200 μg/mL and initial plasmid DNA concentration was 25 μg/mL. Estimated average error for each measurement is ± 5%.

4.8 Effect of organic anti-solvents

Ethanol was investigated to determine if supplementing divalent cation precipitation with an organic anti-solvent could help to fractionate different nucleic acid forms. As discussed in Section 0, addition of an organic anti-solvent such as ethanol to an aqueous solution lowers the dielectric constant of the solution and thereby, according to counterion condensation theory, increases the fractional charge neutralisation of nucleic acid molecules. The first experiment tested increasing levels of ethanol in 0.2 M calcium chloride precipitation of clarified lysate. Supernatant results from this experiment are shown in Figure 4.18.

Figure 4.18 shows that plasmid DNA precipitated above a certain ethanol level between 7% and 9% volume/volume in 0.2 M calcium chloride. This is consistent with the idea of increased fractional charge neutralisation due to the presence of ethanol; note that without ethanol in solution plasmid DNA was soluble at or above 0.5 M calcium chloride (Figure 4.5). Further investigation using purified plasmid DNA showed a very sharp drop in solubility between 8% and 9% volume/volume ethanol (Figure 4.19 and Figure 4.20). Note that the data in Figure 4.19 shows a fair amount of variability at ethanol concentrations below 8%; the reasons for this variability are unclear however plasmid DNA most likely remained fully soluble at ethanol concentrations below 8%. Although the results with added ethanol were consistent with the counterion condensation

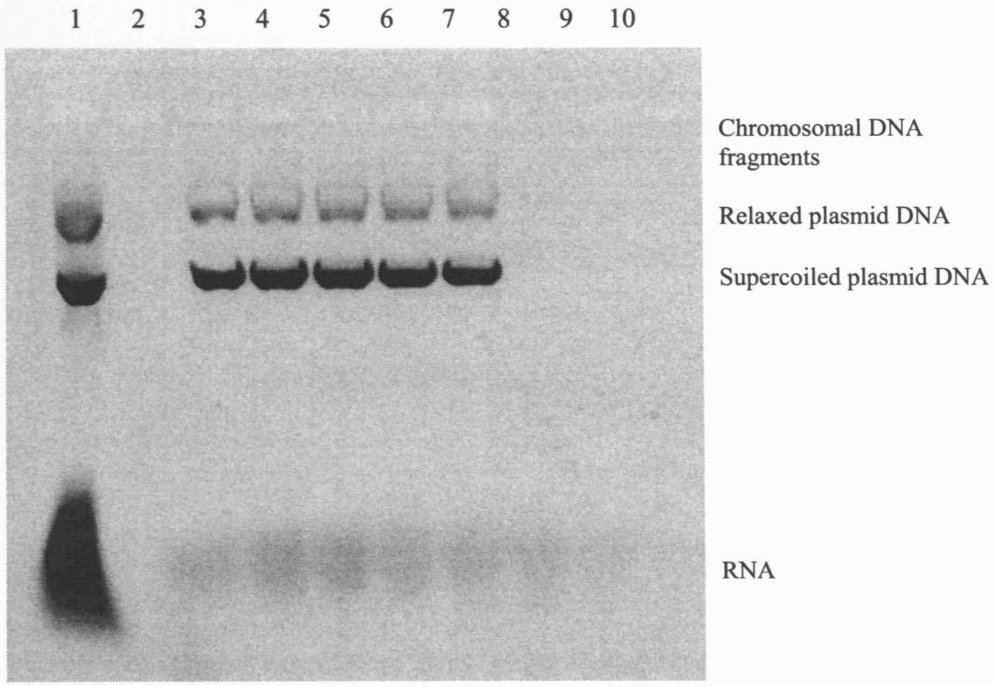

Figure 4.18 Effect of organic solvent on divalent cation precipitation of nucleic acids from clarified lysate solution. This 0.8% agarose gel shows supernatant samples from 0.2 M calcium chloride precipitation of clarified lysate in TE buffer (pH 8) with varying added ethanol concentrations. Lane 1: control with no added calcium chloride or ethanol; Lane 3: 0% ethanol; Lane 4: 1% vol./vol. added ethanol; Lane 5: 3% vol./vol. ethanol; Lane 6 : 5% vol./vol. ethanol ; Lane 7 : 7% vol./vol. ethanol; Lane 8: 9% vol./vol. ethanol ; Lane 9: 11% vol./vol. ethanol; Lane 10 : 13% vol./vol. ethanol.

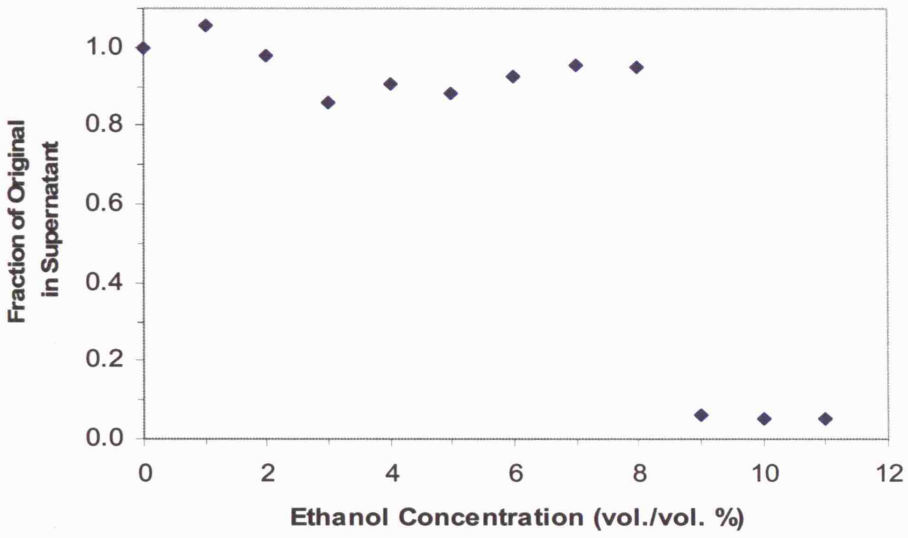

Figure 4.19 Further examination of the effect of organic solvent on divalent cation precipitation of plasmid DNA. Varying levels of ethanol were added to solutions of purified plasmid DNA in 0.2 M calcium chloride pH 8. Fractions of original plasmid concentration with no added ethanol (15 μg/mL based on supernatant from 200 mM calcium chloride addition only) are plotted versus percent ethanol added. Plasmid concentrations were determined based on A260 measurements of supernatants from separate samples. Estimated average error for each measurement is ± 10%. Also see Figure 4.20 for agarose gel from some of these supernatant samples.

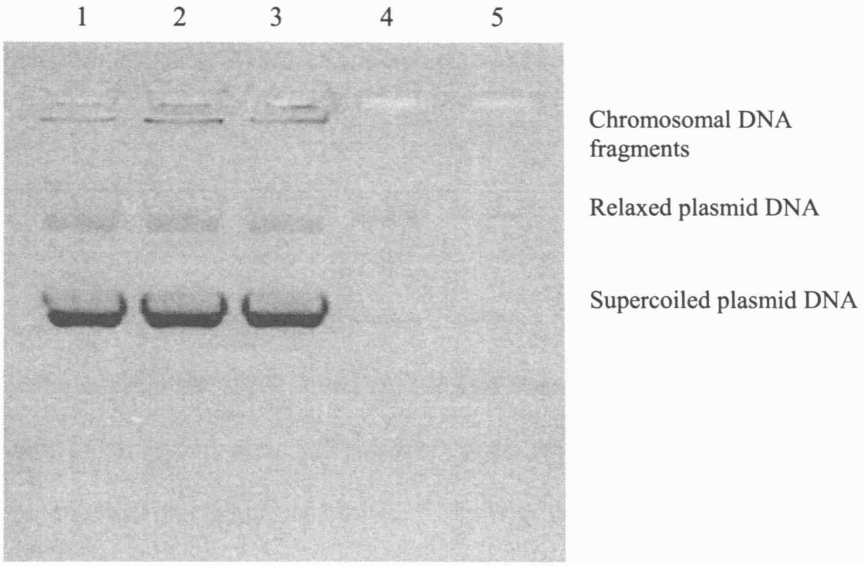

Figure 4.20 Further examination of the effect of organic solvent on divalent cation precipitation of plasmid DNA. This 0.8% agarose gel shows supernatant samples from 0.2 M calcium chloride precipitation of purified plasmid DNA in TE buffer (pH 8) with varying added ethanol concentrations. Lane 1: 6% vol./vol. ethanol; Lane 2: 7% vol./vol. ethanol; Lane 3: 8% vol./vol. ethanol; Lane 4 : 9% vol./vol. ethanol ; Lane 5 : 10% vol./vol. ethanol.

theory, unfortunately they did not show promise for improved fractionation of nucleic acids beyond the level provided by divalent cation precipitation alone, therefore inclusion of organic anti-solvents was not pursued further.

4.9 Summary

A number of precipitation parameters were investigated including cation valency, cation concentration, pH, initial nucleic acid concentration, and inclusion or non-ionic polymer or organic anti-solvents. From these studies, divalent cations and the trivalent polyamine spermidine^{3+} showed potential promise for fractional precipitation of different nucleic acid forms. Divalent cation precipitation seemed favourable to polyamine precipitation for plasmid DNA purification since plasmid remained in the supernatant phase during divalent cation precipitation while spermidine^{3+} was found to precipitate plasmid DNA. Results from experiments that included the non-ionic polymer PEG-4000 showed divalent cation precipitation of clarified lysate could potentially be supplemented with non-ionic polymer to enhance separation of chromosomal DNA from plasmid DNA. Comparison of RNA data from single-component and multi-component precipitation experiments suggested that single-component solubilities were representative in terms of fraction of initial nucleic acid concentration remaining in the supernatant. Given these preliminary precipitation results, divalent cation precipitation was pursued further as a purification technique for recovery of plasmid DNA.

5 DIVALENT CATION PRECIPITATION STUDIES FOR PLASMID DNA RECOVERY

5.1 Introduction

Given the promising preliminary results on the use of divalent cation precipitation as a potential purification technique (Section 4), more detailed studies were planned. These studies sought to understand better the sensitivities of this approach to process parameters such as initial contacting conditions and presence of monovalent cation salts, as well as to optimise the conditions of this step for plasmid DNA recovery, in terms of placement in the purification train and the type of divalent cation used. A denaturation step was also investigated for enhancing clearance of chromosomal dsDNA and relaxed plasmid DNA. Based on these studies a large-scale purification process scheme based on divalent cation precipitation is proposed for plasmid DNA recovery.

5.2 Kinetics of precipitation studies

A few experiments were performed to investigate whether separation of nucleic acid forms by precipitation would be sensitive to initial contacting conditions during addition of concentrated divalent cation salt solution. The first experiment monitored turbidity increase (as absorbance at 320 nm) over time (indicative of aggregation/ precipitation) after sub-surface bolus addition of concentrated divalent cation solution by micro-pipette to clarified lysate in a cuvette. Results of this experiment are shown in Figure 5.1. The long time

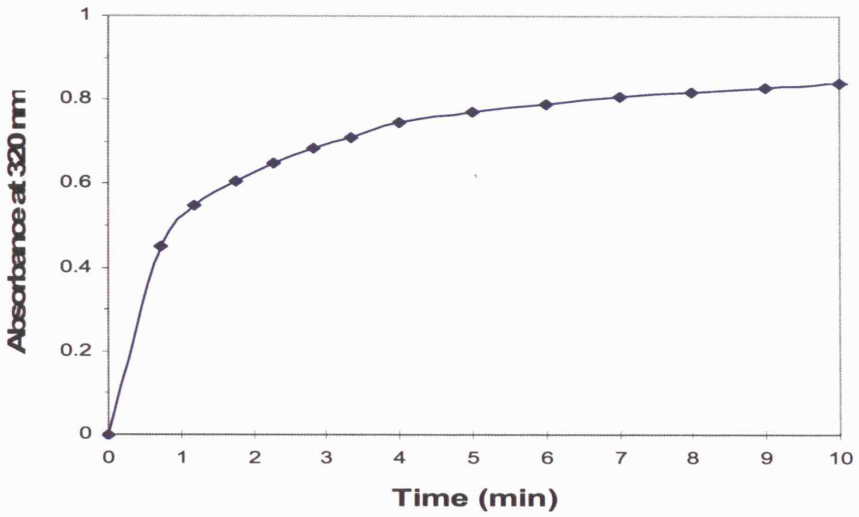

Figure 5.1 Kinetics of precipitation for nucleic acids in divalent cation solution. Turbidity was monitored by absorbance at 320 nm, after sub-surface bolus addition of 3 M calcium chloride stock to final concentration of 0.2 M in clarified lysate in TE buffer in a cuvette at time 0. Points represent single measurements; estimated average error for each measurement is ± 5%.

required to approach an absorbance asymptote (approximately 5 minutes) suggests that kinetics of precipitation for nucleic acids were relatively slow compared to typical examples from protein precipitation by salts (for examples see (Chan et al., 1986;Przybycien and Bailey, 1989;Iyer and Przybycien, 1995). This finding also suggested that solubilities would probably not be highly sensitive to initial contacting conditions. Results were further analyzed to approximate the order of the divalent cation precipitation reaction. If remaining soluble nucleic acid reactant concentration at any time is assumed to be proportional to unity minus absorbance at 320 nm (1 - A320), a plot of $(1\text{-}A320)^{-1}$ versus time can be used to investigate reaction order (see Appendix II for integrated rate laws). As shown in Figure 5.2, because this plot is nearly linear, it suggests roughly *second order kinetics* for the divalent cation precipitation reaction, consistent with Smoluchowksi theory (Section 1.6).

To investigate further the effect of initial contacting conditions on solubility, a reverse-order-of-addition experiment was performed to mimic both well-mixed and poorly-mixed initial contacting conditions for divalent cation precipitation of nucleic acids from clarified lysate. The results of this experiment are shown in Figure 5.3. These results show that the initial contacting conditions with the divalent cation precipitant had minimal impact on final solubilities when precipitation reactions are allowed to reach equilibrium; this outcome might be expected given the relatively slow kinetics of precipitation observed in Figure 5.1. Although precipitation and solubility experiments were generally performed under similar conditions in this project allowing several hours of contact time

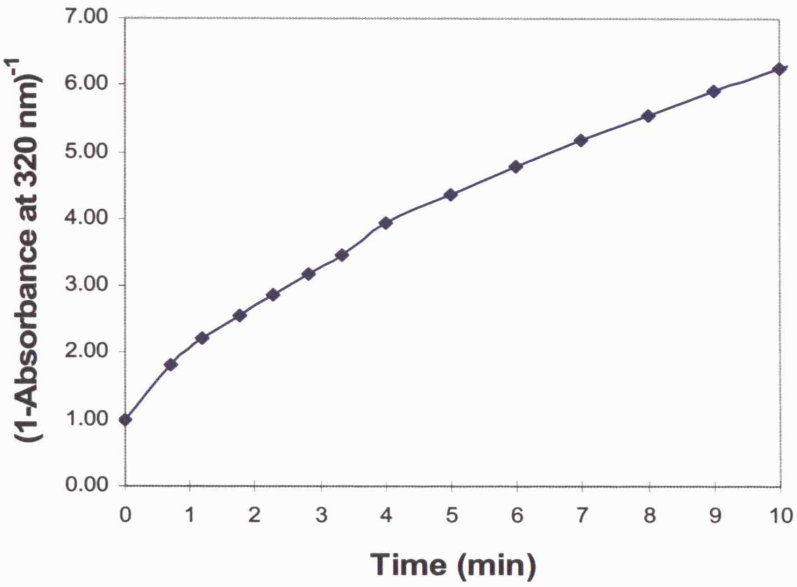

Figure 5.2 Investigation of reaction order for divalent cation precipitation of nucleic acids. Using data from Figure 5.1 for calcium chloride precipitation of clarified lysate, remaining soluble nucleic acid reactant concentration at any time was assumed to be proportional to 1-A320, and inverse of (1-A320) was plotted versus time. Near-linearity of the plot suggests approximate second order kinetics.

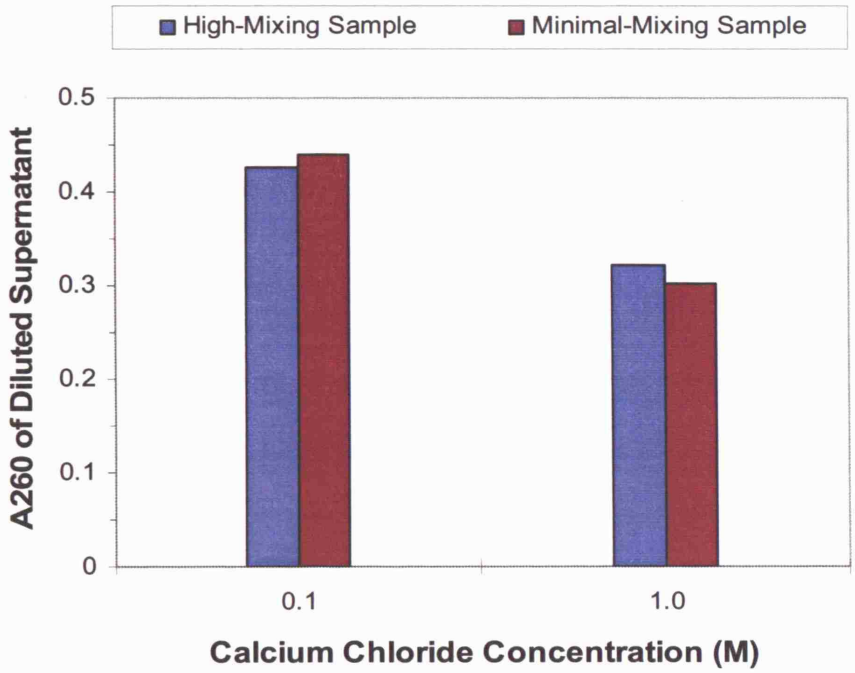

Figure 5.3 Effect of initial contacting conditions on nucleic acid solubility for divalent cation precipitation. Absorbance at 260 nm (A260) was measured for supernatant samples following calcium chloride precipitation of clarified lysate in TE buffer, using either 'high-mixing' or 'minimal-mixing' during introduction of the precipitating agent. For high-mixing samples, 3 M calcium chloride solution was added drop-wise to clarified lysate solution while vortexing to reach the target calcium chloride concentration. For minimal-mixing samples, clarified lysate solution was added drop-wise to pre-dispensed static 3 M calcium chloride solution with no mixing until 2 minutes after addition of final drop. Samples were agitated slowly using a shaker plate for 5 hours at room temperature before supernatant recovery via centrifugation. Supernatants were diluted 1:4 in TE buffer before measuring A260.

prior to precipitate removal, results from these kinetics studies showed that divalent cation precipitation reactions reached equilibrium within a few hours and that final nucleic acid solubilities were relatively insensitive to initial contacting conditions. This suggested that purification results following divalent cation precipitation would be robust in terms of initial contacting conditions.

5.3 Precipitation before/after neutralisation

Given the promising preliminary results for divalent cation precipitation of clarified lysate (Section 4.3.2), divalent cation precipitation further upstream was investigated in an effort to optimise further the placement of this precipitation step in the purification process train, as well as to gain a better understanding of precipitation mechanisms. Recall that during alkaline lysis sodium hydroxide is added to a concentration of 100 mM, which raises the pH to approximately 12.5. Potassium acetate is then added to a concentration of 1 M to neutralise the solution and precipitate cell debris and some chromosomal DNA, followed by clarification using filtration or centrifugation.

To investigate placement of a divalent cation precipitation step, an experiment was performed whereby concentrated calcium chloride solution was added in separate arms following either sodium hydroxide addition, neutralisation, or clarification. An additional arm with no calcium chloride addition was run as a control. Each arm was taken through clarification by centrifugation (the post-clarification addition arm used a second centrifugation to clear precipitates), and clarified lysate samples were run by the Q Sepharose HP assay to assess the

impact of divalent cation addition location on the nucleic acid profile; chromatograms from these studies are shown in Figure 5.4.

Comparing the chromatogram for 0.5 M calcium precipitation prior to neutralisation (bottom chromatogram) to the non-precipitated control (top chromatogram) in Figure 5.4 shows that virtually all the single-stranded DNA and most of the RNA was precipitated. However it also appears that the majority of double-stranded DNA was precipitated. This behaviour is consistent with the idea that the high pH environment during alkaline lysis temporarily converts plasmid DNA to single-stranded form while still remaining closed-circular. Since single-stranded DNA has been shown previously to have low solubility in the presence of divalent cations, it is likely that the converted plasmid DNA was precipitated along with chromosomal ssDNA when the calcium chloride was added.

The sample to which calcium chloride was added following rather than prior to neutralisation, but still prior to clarification, showed better plasmid DNA recovery. However compared to the control it appears some of the plasmid DNA was still not recovered in this sample. This could be due to calcium chloride being added in the presence of cell debris and potassium/SDS precipitate, which may have led to the entrainment of some soluble plasmid into the precipitate.

Precipitation of the clarified lysate sample showed good recovery of plasmid

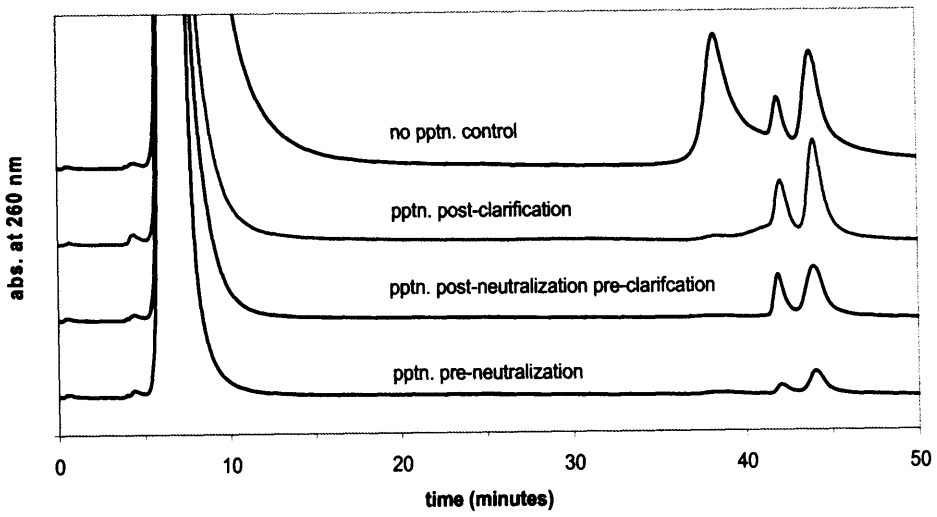

Component	Control Conc. (µg/mL)	Pptn. Post-Clar. Conc. (µg/mL)	Pptn. Post-Neutral. Conc. (µg/mL)	Pptn. Pre-Neutral. Conc. (µg/mL)
RNA	1966	692	669	539
single-stranded DNA	41	<3.4	<3.4	<3.4
relaxed plasmid DNA	18.4	16.4	6.3	1.5
double-stranded DNA (incl. sc-plasmid)	43	27	16	7.1

Figure 5.4 Effect of divalent cation precipitation before or after neutralisation / clarification following alkaline lysis. Shown are Q Sepharose HP analytical chromatograms on supernatant samples following clarification by centrifugation, from top to bottom: 1) No precipitation control (no calcium chloride added); 2) Precipitation following neutralisation and clarification by addition of 0.5 M calcium chloride; 3) Precipitation by addition of 0.5 M calcium chloride following neutralisation but prior to clarification; 4) Precipitation by addition of 0.5 M calcium chloride prior to neutralisation. Peak at 6.5 minutes is digested RNA, peak at 38.5 minutes is single-stranded chromosomal DNA, peak at 41.5 minutes is relaxed plasmid DNA, and peak at 44 minutes is double-stranded DNA. Component concentrations were determined from standard curves.

DNA and only slightly less clearance of RNA. Based on this experiment, the divalent cation precipitation step should be placed following both neutralisation and clarification steps for maximum recovery of plasmid DNA.

5.4 Effect of monovalent cations on divalent cation precipitation

Although the studies described in the preceding section showed divalent cation precipitation should be performed following neutralisation and clarification, and preliminary studies on clarified lysate had appeared promising (Section 4.3), it was unclear if a buffer exchange step was necessary following clarification to reduce the high monovalent salt concentration in clarified lysate prior to divalent cation precipitation. As mentioned previously, potassium acetate is added following alkaline lysis to a concentration of approximately 1 M to precipitate cell debris prior to clarification, therefore monovalent salt concentration is a key variable in the bioprocess sequence.

An initial experiment was performed to investigate this question. Calcium chloride stock solution was added to clarified lysate, which either had or had not been exchanged to TE buffer, to target a range of calcium chloride concentrations for precipitation. Effectiveness of precipitation was determined by measuring the absorbance at 260 nm of supernatant samples in comparison to control samples (lower A260 values in supernatant samples are indicative of more effective precipitation, i.e. greater nucleic acid impurity clearance). Results from this experiment are shown in Figure 5.5. These results suggest that

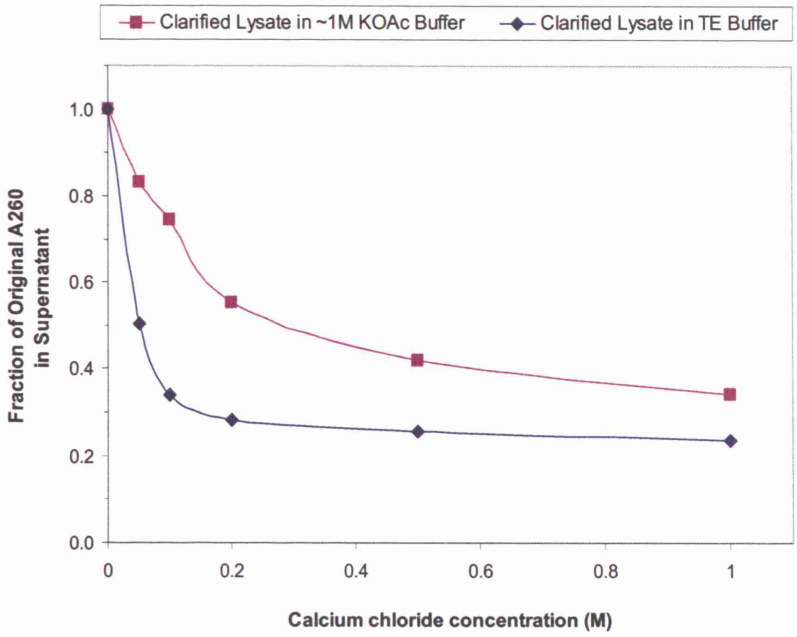

Figure 5.5 Effect of calcium chloride concentration on precipitation of *E. coli* clarified lysate, in either 1 M potassium acetate or TE buffer (pH 8) prior to precipitation. Samples were diluted 1:2 during precipitations therefore monovalent cation levels were 0.5 M potassium and 5 mM Tris during precipitation. Fractions were determined based on A260 measurements of supernatants from separate samples. Estimated average error for each measurement is ± 5%.

although calcium chloride precipitation is effective for impurity clearance from either type of clarified lysate solution, it appears to be more effective when clarified lysate has first been exchanged to a low salt buffer. Figure 5.5 also suggests that for clarified lysate in TE buffer, calcium chloride concentrations above 0.2 M provided little additional benefit for impurity clearance, consistent with single-component results (Figure 4.5).

This was tested further in an experiment using divalent cation precipitation of purified single-stranded DNA, with a constant divalent cation concentration and various levels of monovalent cation salts present during precipitation. Results from this experiment are shown in Figure 5.6; the figure clearly shows that divalent cations (in this case calcium ions) were less effective in precipitating ssDNA in the presence of higher concentrations of monovalent cations (in this case sodium ions). These findings are somewhat counterintuitive, because in this case DNA was more soluble in higher ionic strength solutions; typically for proteins increasing ionic strength reduces a protein's solubility (above the low ionic strength needed for salting-in). However note that according to the counterion condensation theory (Section 1.7.1) monovalent and divalent cations are thought to compete for binding sites on nucleic acid surfaces; therefore for a given concentration of divalent cations, higher concentrations of monovalent cations would result in greater association of monovalent cations and less association of divalent cations to the DNA surface, leading to less overall charge neutralisation and increased solubility. The results shown in Figure 5.5 and Figure 5.6 are consistent with the concept of different ion species competing for binding sites along the DNA surface under counterion condensation theory.

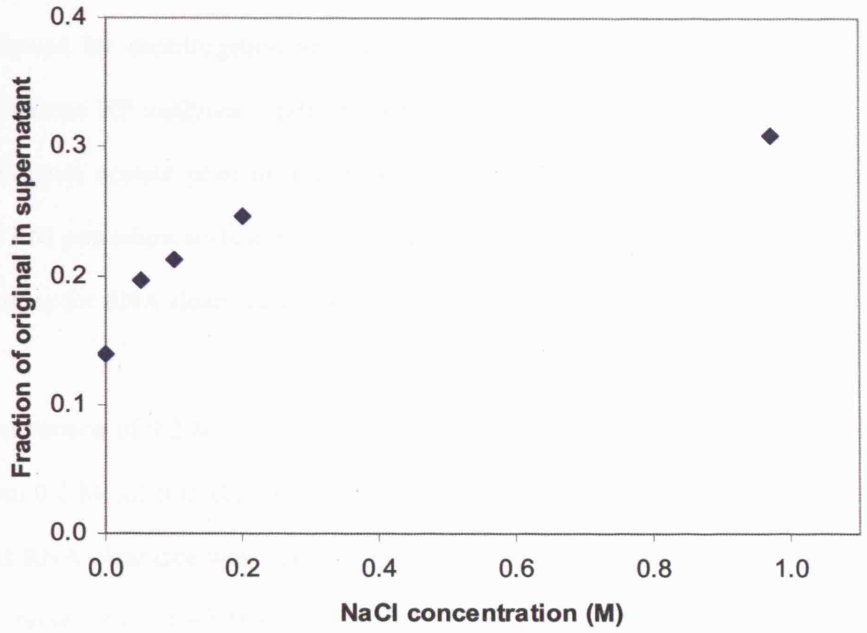

Figure 5.6 Effect of sodium chloride on divalent cation precipitation of single-stranded DNA. Plot shows solubilities of purified single-stranded DNA (from denatured plasmid) in 0.05 M calcium chloride solution with varying levels of added sodium chloride. Nucleic acid concentrations in supernatant samples were determined based on A260 measurements from separate samples; initial DNA concentration was 50 μg/mL for each sample. Estimated average error for each measurement is ± 5%.

These findings were further tested by performing a series of calcium chloride precipitations on clarified lysate solution which had not been buffer-exchanged, followed by centrifugation and analysis of supernatant samples using the Q Sepharose HP analytical method. The clarified lysate solution contained 1 M potassium acetate prior to introduction of calcium chloride and approximately 0.67 M potassium acetate during precipitation for all arms. Results showing the profiles for RNA clearance are shown in Figure 5.7.

Comparison of 0.2 M calcium chloride results shown in Figure 5.7 to the results from 0.2 M calcium chloride of clarified lysate in TE buffer (Figure 4.8) shows that RNA clearance was significantly less when precipitation was performed in the presence of ~0.67 M potassium (44% clearance versus 83% clearance in TE buffer). Also the solubility profile for RNA in the presence of potassium acetate shown in Figure 5.7 appears similar to the top profile shown in Figure 5.5, suggesting that the reduction in A260 in Figure 5.5 with increasing calcium chloride concentration was mainly due to precipitation of RNA. Figure 5.5 and Figure 5.7 further suggest that for cases where nucleic acids are in the presence of high concentrations of monovalent cation salts, 1-2 M of divalent cations may be necessary to maximise RNA clearance, compared to only 0.2 M of divalent cations when the monovalent cation concentration is low. However note that even when 1.0 M calcium chloride was used in the presence of ~0.67 M potassium, only 69% RNA clearance was achieved (Figure 5.7).

DNA results for 0.2 M calcium chloride precipitation in the presence of ~0.67 M

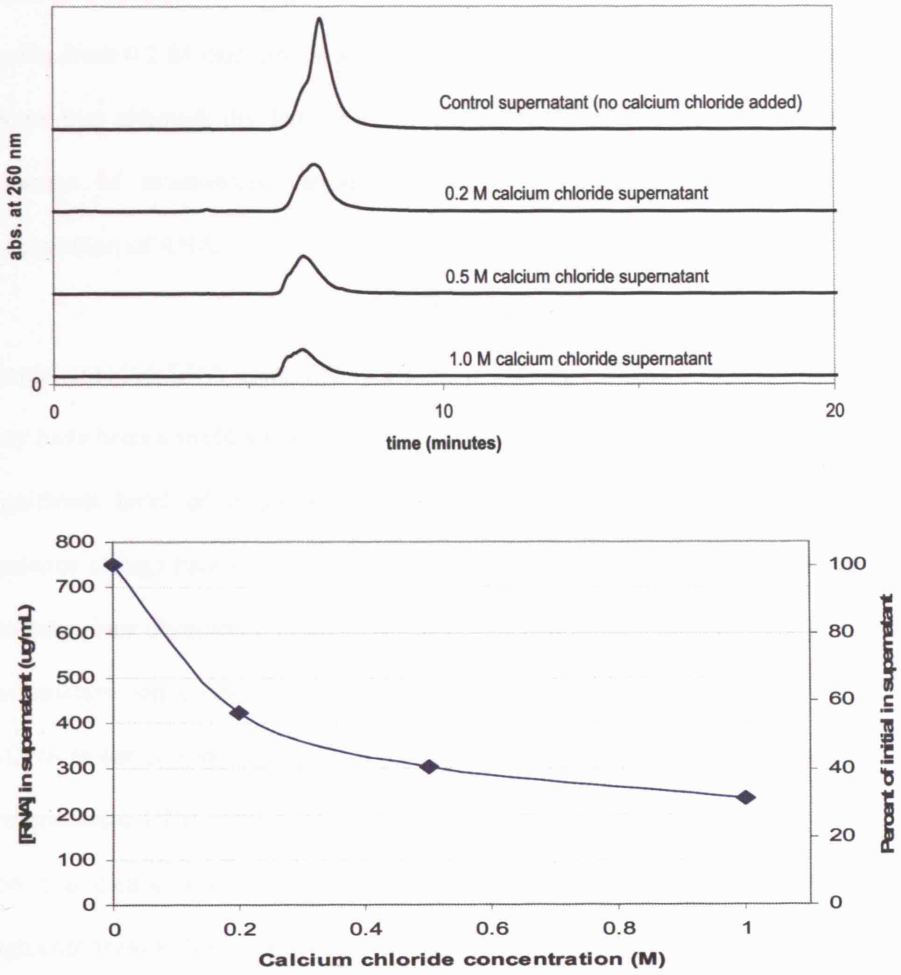

Figure 5.7 Calcium chloride precipitation of RNA from clarified lysate solution containing high monovalent salt concentration. Q Sepharose HP analytical chromatograms showing RNA peaks of supernatants from non-buffer-exchanged clarified lysate (all containing 1 M potassium acetate prior to precipitation or ~0.67 M potassium acetate during precipitation) following precipitation with calcium chloride. RNA concentrations were determined from standard curves.

potassium are shown in Figure 5.8. Comparing the results of Figure 5.8 to the results from 0.2 M calcium chloride of clarified lysate in TE buffer (Figure 4.9) shows that although divalent cation precipitation of DNA was affected by the presence of monovalent cations, it was not affected nearly as much as precipitation of RNA.

Single-stranded DNA clearance was similar although Figure 5.8 suggests there may have been a slight amount of single-stranded DNA that was not cleared. The significant level of single-stranded DNA clearance obtained (>76%) in the presence of high monovalent cation concentration was somewhat surprising given the behaviour observed for single-stranded DNA in Figure 5.6; however perhaps the calcium ion concentration at 0.2 M was just sufficient to still precipitate ssDNA in the presence of ~0.67 M potassium ions. Clearance of double-stranded chromosomal DNA appears roughly similar in both cases. However importantly note that clearance of relaxed plasmid DNA showed a substantial difference in high compared to low monovalent cation concentration; in low monovalent cation concentration 48% was cleared (Figure 4.9) compared to no clearance in the presence of high monovalent cation concentration (Figure 5.8).

Overall the results from these studies are consistent with the thinking that monovalent cations compete with divalent cations for binding sites along the nucleic acids' surfaces, and reduce the effectiveness of divalent cation precipitation for nucleic acids with single-stranded regions. To improve the

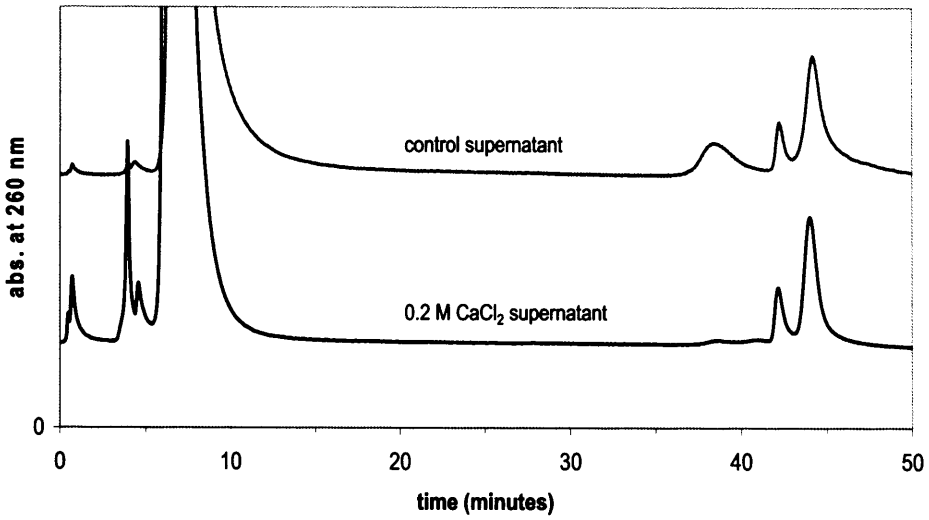

Component	Cl. Lysate Control Concentration (μg/mL)	0.2 M $CaCl_2$ Supernatant Conc. (μg/mL)	Fraction of Orig.
single-stranded DNA	14	<3.4	<24%
relaxed plasmid DNA	7.0	7.4	106%
double-stranded DNA (incl. sc-plasmid)	40	29	72%

Figure 5.8 Effect of high monovalent cation concentration on divalent cation precipitation for DNA impurity clearance from clarified lysate. Q Sepharose HP analytical chromatograms showing control and 0.2 M calcium chloride supernatants from non-buffer-exchanged clarified lysate (contained 1 M potassium acetate prior to precipitation, or 0.67 M potassium acetate during precipitation). Peak at 6.5 minutes is digested RNA, peak at 38.5 minutes is single-stranded chromosomal DNA, peak at 41.5 minutes is relaxed plasmid DNA, and peak at 44 minutes is double-stranded DNA. Component concentrations were determined from standard curves.

effectiveness of divalent cation precipitation of clarified lysate, especially for RNA and relaxed plasmid DNA, prior buffer-exchange to a low salt buffer such as TE buffer is recommended.

5.5 Investigation of other divalent cations for improved RNA clearance

Based on previous studies, calcium chloride precipitation of buffer-exchanged clarified lysate was effective in clearing most of the RNA in solution; however the concentration remaining in the supernatant (453 μg/mL) was still roughly 4-fold higher than the concentration of supercoiled plasmid (see Figure 4.8 and Figure 4.9). Therefore follow-up experiments were performed to determine if greater RNA clearance could be obtained with alternative divalent cation salts. Divalent cation stock solutions were prepared in different pH buffers (using 10 mM Tris background) to ensure solubility of the salt in concentrated stock solution. Results from an initial follow-up experiment are shown in Figure 5.9, and those from a confirmatory experiment are shown in Figure 5.10. These results showed divalent cation precipitation of clarified lysate by nickel sulphate and zinc acetate provided improved RNA clearance compared to calcium chloride precipitation by roughly a factor of two. Although it was somewhat unclear why these differences in RNA clearance were observed for different divalent cation salts (see further discussion in Section 6), nickel sulphate and zinc acetate were considered as attractive alternatives to calcium chloride as precipitating agents.

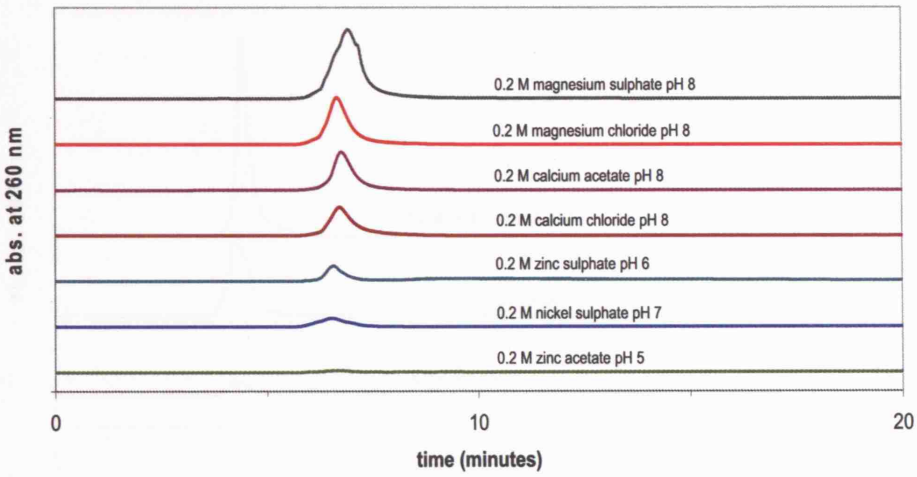

Sample	RNA Conc. (µg/mL)	Fraction of Orig.
No-pptn. Control (not shown)	1722	--
0.2 M magnesium sulphate pH 8	916	53%
0.2 M zinc sulphate pH 6	502	29%
0.2 M magnesium chloride pH 8	502	29%
0.2 M calcium acetate pH 8	386	22%
0.2 M calcium chloride pH 8	336	20%
0.2 M zinc acetate pH 5	135	8%
0.2 M nickel sulphate pH 7	130	8%

Figure 5.9 Investigation of different divalent cation salts for RNA precipitation from clarified lysate in TE buffer. Plot shows RNA peaks from Q Sepharose HP analytical chromatograms from supernatant samples following precipitation with the indicated divalent cation salts. Concentrations were determined from standard curves.

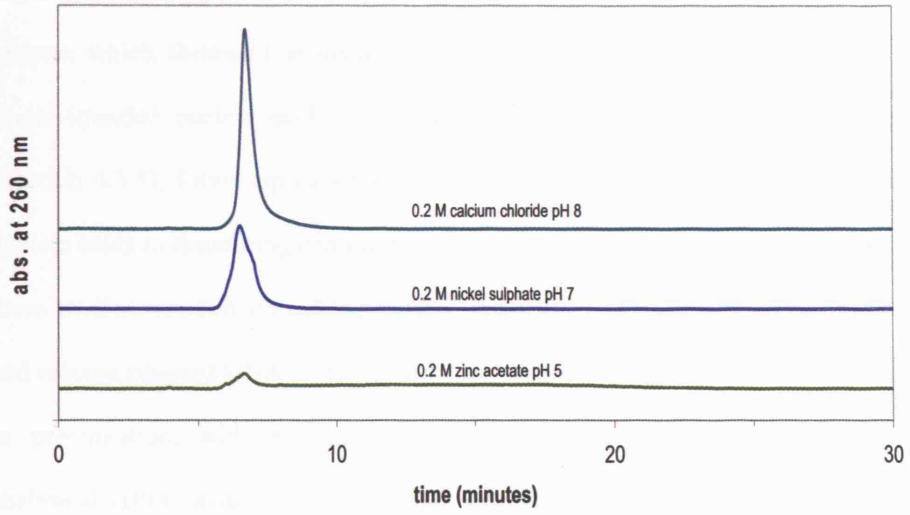

Sample	RNA Conc. (µg/mL)	Fraction of Orig.
No-pptn. Control	1722	--
0.2 M calcium chloride pH 8	290	17%
0.2 M nickel sulphate pH 7	176	10%
0.2 M zinc acetate pH 5	155	9%

Figure 5.10 Follow-up investigation of nickel sulphate and zinc acetate compared to calcium chloride for RNA precipitation from clarified lysate in TE buffer. Plot shows RNA peaks from Q Sepharose HP analytical chromatograms from supernatant samples following precipitation with the indicated salts. Concentrations were determined from standard curves.

5.6 Denaturation studies

Given the solubility results from purified single-component studies with divalent cations, which showed that divalent cations were effective for precipitation of single-stranded nucleic acid forms but ineffective for double-stranded forms (Section 4.3.1), follow-up experiments were pursued to investigate exposure of nucleic acids to denaturing conditions prior to precipitation. The thinking behind these studies was that if double-stranded 'impurity' forms such as chromosomal and relaxed plasmid DNA forms could be denatured to single-stranded form prior to precipitation, without denaturing supercoiled plasmid DNA (as in the analytical HPLC assay), divalent cation precipitation may be more effective in clearing these forms. If successful, the combination of these two steps would represent a novel method for plasmid DNA purification.

The first experiment to address this was a temperature melting study using purified chromosomal dsDNA, plasmid DNA and rRNA. As shown in Figure 5.11, an increase in relative absorbance is indicative of strand separation due to unstacking of the nitrogenous bases, leading to conversion to single-stranded form. From this study, chromosomal DNA showed the greatest increase in relative absorbance of the three forms, especially over 80 °C. This might be expected since chromosomal DNA fragments are linear while most plasmid DNA is closed circular. As mentioned previously, it was thought that both forms are converted to single-stranded while exposed to denaturing conditions, but that supercoiled plasmid likely renatures to its native form as long as each strand

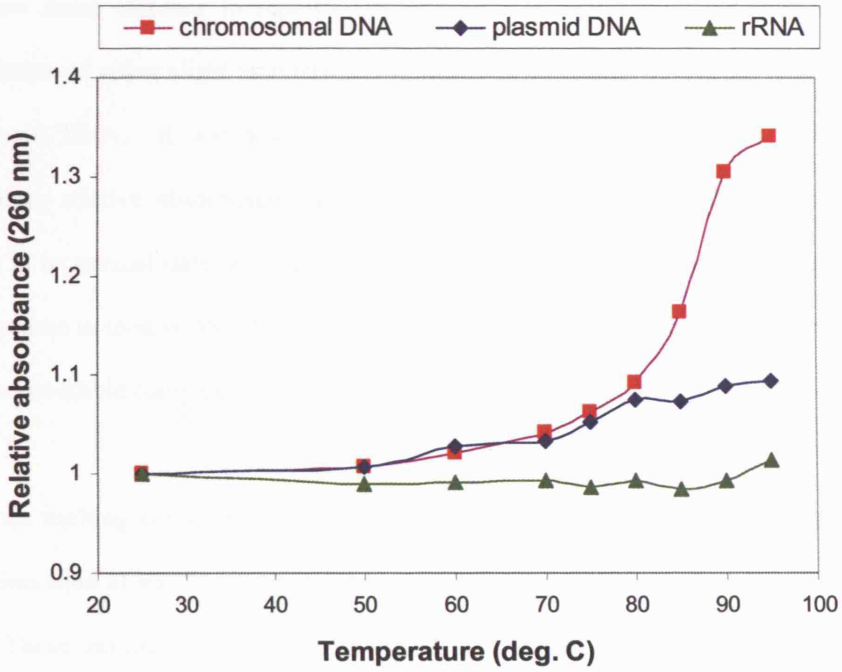

Figure 5.11 Melting experiment with different nucleic acid forms to investigate feasibility of temperature denaturation prior to precipitation. Samples of purified chromosomal dsDNA, plasmid DNA and ribosomal RNA from *E. coli* at 20 µg/mL in TE buffer were incubated at different temperatures for 10 minutes, followed by immediate cooling in ice bath for 10 minutes, followed by measurement of absorbance at 260 nm. Relative absorbance is the ratio of absorbance for a sample incubated at a given temperature to that for an unheated sample. Increase in relative absorbance is indicative of nucleic acid strand separation. Points represent single measurements from separate samples; estimated average error for each measurement is ± 5%.

remains covalently closed circular. It was interesting that purified plasmid DNA did show some increase in relative absorbance; this may have been due to denaturation of either slight amounts of impurities, or of nicked or relaxed forms of plasmid DNA. It was also interesting that purified rRNA showed little increase in relative absorbance; although this form has many single-stranded regions in its normal state prior to denaturation, the fact that rRNA showed such little increase in relative absorbance upon heating suggests this form may be more temperature-stable compared to the DNA forms.

Given the melting curve results, the next experiment investigated the effect of incubation time at 95 °C on denaturation of purified plasmid and chromosomal DNA. These results, shown in Figure 5.12 and Figure 5.13, indicated that incubation time is an important parameter in determining the denaturation profile. Both figures show no bands in the wells for heated samples, suggesting that heating was effective for breaking up nucleic acid aggregates. Both figures also show that for plasmid DNA, some reduction in the relaxed form can be obtained through temperature denaturation, and that an additional band was formed below the supercoiled band that became more prevalent with longer incubation times. These bands have been observed under certain conditions by other researchers, and have been characterised as denatured variants of plasmid DNA, containing significant stretches of single-stranded DNA (Sayers et al., 1996;Diogo et al., 1999). For chromosomal DNA, Figure 5.13 suggested that as little as 5 minutes of incubation at 90 °C was sufficient to denature chromosomal dsDNA to single-stranded form.

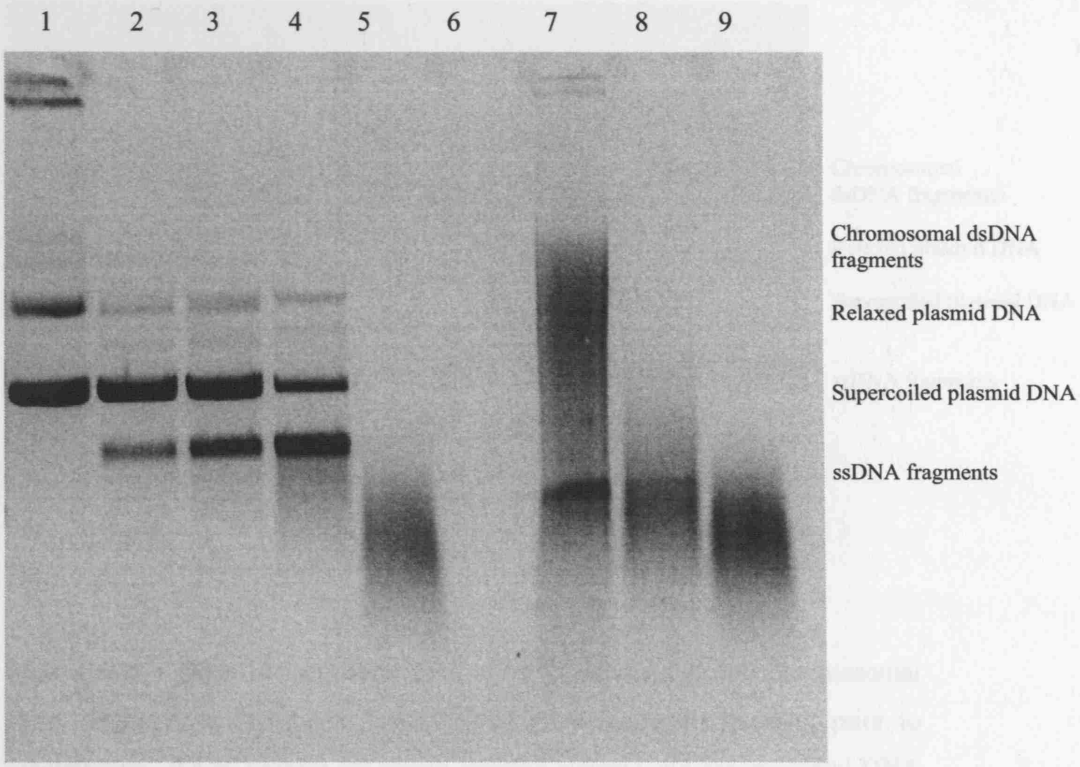

Figure 5.12 Effect of incubation time at 95°C on plasmid and chromosomal DNA structure, to investigate feasibility of temperature denaturation prior to precipitation. 0.8 % agarose gel shows purified plasmid and chromosomal DNA samples in TE buffer after incubation at 95°C for varying lengths of time, followed by immediate cooling in ice bath. Lane 1: unheated plasmid DNA control; Lane 2: plasmid DNA heated for 6 minutes; Lane 3: plasmid DNA heated for 10 minutes; Lane 4: plasmid DNA heated for 30 minutes; Lane 5: plasmid DNA heated for 90 minutes; Lane 7: unheated chromosomal DNA control; Lane 8: chromosomal DNA heated for 20 minutes; Lane 9: chromosomal DNA heated for 90 minutes.

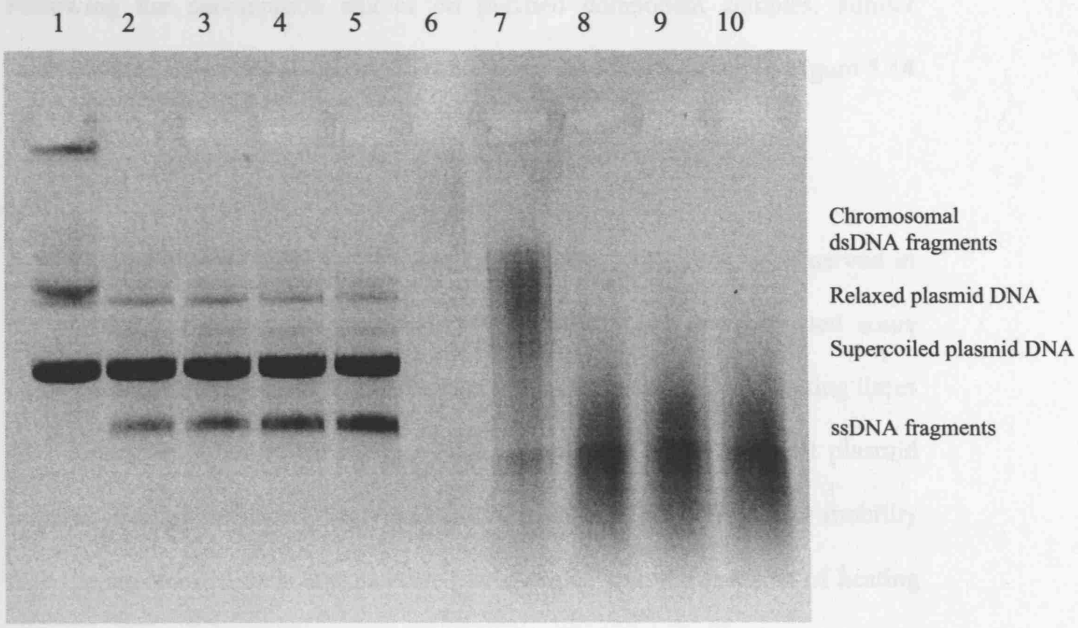

Figure 5.13 Effect of incubation time at 90°C on plasmid and chromosomal DNA structure, to investigate feasibility of temperature denaturation prior to precipitation. 0.8 % agarose gel shows purified plasmid and chromosomal DNA samples in TE buffer after incubation at 90°C for varying lengths of time, followed by immediate cooling in ice bath. Lane 1: unheated plasmid DNA control; Lane 2: plasmid DNA heated for 5 minutes; Lane 3: plasmid DNA heated for 10 minutes; Lane 4: plasmid DNA heated for 20 minutes; Lane 5: plasmid DNA heated for 30 minutes; Lane 7: unheated chromosomal DNA control; Lane 8: chromosomal DNA heated for 5 minutes; Lane 9: chromosomal DNA heated for 10 minutes; Lane 10: chromosomal DNA heated for 20 minutes.

Following the denaturation studies on purified component samples, similar studies were carried out on clarified lysate; these results are shown in Figure 5.14 and Figure 5.15.

A number of observations can be made from Figure 5.14. First, as observed in the purified component studies, heating appears to have disaggregated some chromosomal DNA, as seen by the absence of a band in the well for heating times of 1 minute or greater (lanes 3-8). Also as observed in the purified plasmid samples, heating produced plasmid DNA variants with slightly greater mobility than the supercoiled form that increased in intensity with the duration of heating (lanes 3-8). It also appears that the amount of relaxed form of plasmid was reduced from initial levels by heating, reaching a minimum level after 2-3 minutes of heating (lanes 4-5), and then increasing slightly after 3 minutes.

Because the initial reduction in relaxed DNA level coincided with the initial appearance of the denatured variant form, and since increases in relaxed DNA after 3 minutes could only be the result of degradation from the supercoiled form, the following degradation pathway upon heating is suggested:

supercoiled form $\rightarrow$ relaxed form $\rightarrow$ denatured variant form

$\downarrow$

(linear form)

This pathway is also plausible from a theoretical standpoint. It is well known

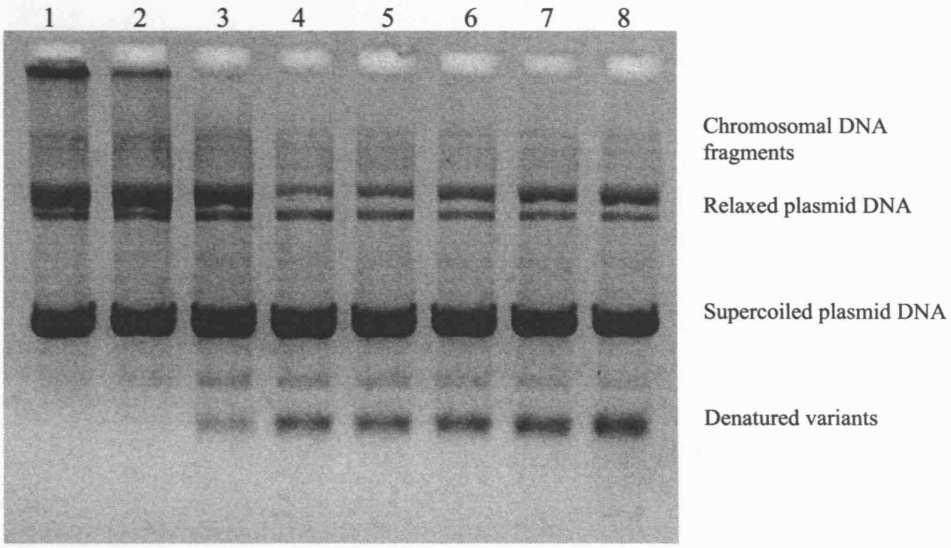

Figure 5.14 Effect of incubation time at 95°C on clarified lysate, to investigate feasibility of temperature denaturation prior to precipitation. 0.8% agarose gel shows clarified lysate samples in TE buffer after incubation at 95°C for varying lengths of time, followed by immediate cooling in ice bath. Lane 1: clarified lysate control (no heating); Lane 2: 0.5 minute heating; Lane 3: 1 minute heating; Lane 4: 2 minutes heating; Lane 5: 3 minutes heating; Lane 6: 4 minute heating s; Lane 7: 5 minutes heating; Lane 8: 6 minutes heating.

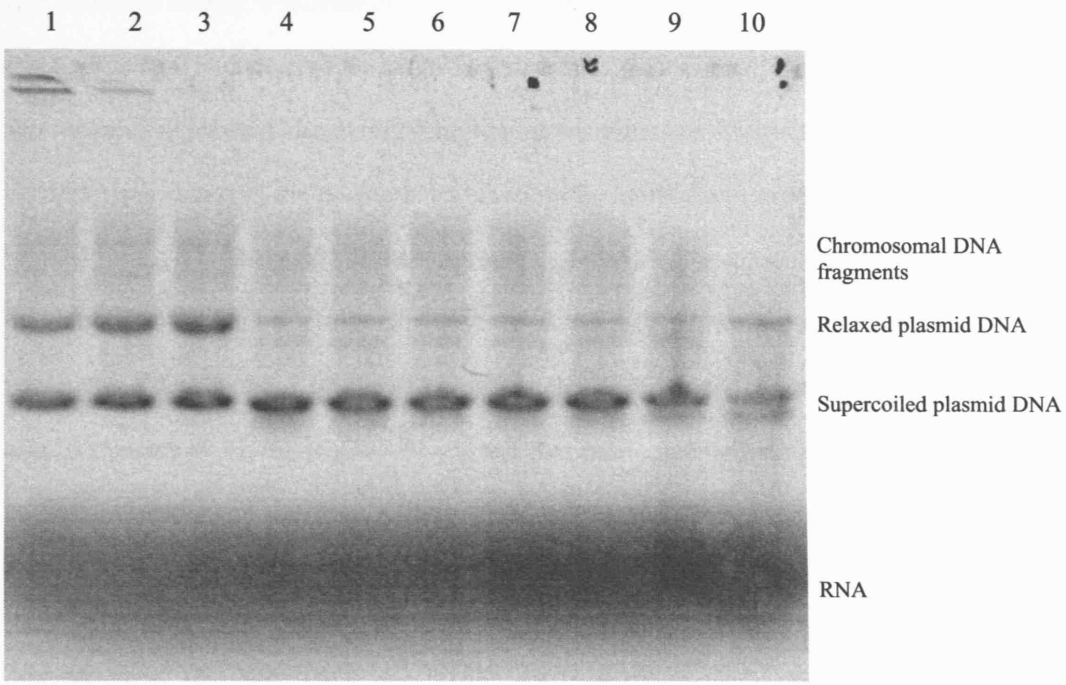

Figure 5.15 Effect of incubation time at 85°C on clarified lysate, to investigate feasibility of temperature denaturation prior to precipitation. 0.8% agarose gel shows clarified lysate samples in TE buffer after incubation at 85°C for varying lengths of time, followed by immediate cooling in ice bath. Lane 1: clarified lysate control (no heating); Lane 2: pre-heated for 0.5 minutes; Lane 3: pre-heated for 1 minute; Lane 4: pre-heated for 2 minutes; Lane 5: pre-heated for 3 minutes; Lane 6: pre-heated for 4 minutes; Lane 7: pre-heated for 5 minutes; Lane 8: pre-heated for 15 minutes; Lane 9: pre-heated for 30 minutes; Lane 10: pre-heated for 60 minutes.

that excessive heating will cause disruption of hydrogen bonds in double-stranded DNA, causing it to convert to the single-stranded form (Marmur and Doty, 1959). For supercoiled plasmid, denaturing conditions or enzymes are thought to first cut or 'nick' one strand of the double helix, causing the molecule to unwind to the relaxed form. It is likely that further exposure to denaturing conditions degrades the molecule further to create single-stranded forms. However under this reckoning, since Figure 5.14 shows an accumulation in relaxed plasmid levels after 3 minutes at 95 °C, this would suggest that once supercoiled degradation begins, the conversion rate from supercoiled to relaxed form may be greater than that for relaxed form to denatured variant form. Regardless it is clear from Figure 5.14 that an optimal duration of heating exists (approximately 2 minutes for 95 °C incubation) such that the double-stranded chromosomal and relaxed forms levels are converted to single-stranded forms with minimal effect on the supercoiled form.

A similar study was performed on clarified lysate using 85 °C incubation instead of 95 °C to determine if this may provide a wider optimal incubation time window. As seen in Figure 5.15, lanes 4 - 7 suggest that heating for 2-5 minutes at 85 °C provided similar conversion levels of double-stranded chromosomal and relaxed plasmid forms to single-stranded forms with minimal denaturation of supercoiled plasmid. These results in comparison to those in Figure 5.14 suggest that incubation at 85 °C may provide a wider optimal incubation window than incubation at 95 °C, which may be beneficial from a process robustness standpoint.

These studies showed that temperature could be used to denature chromosomal and relaxed plasmid DNA to single-stranded form without (permanently) denaturing supercoiled plasmid. Divalent cation precipitation studies were then performed on the heat-denatured materials. Although not studied here, it should be noted that a temporary pH shift (to approximately pH 12.5) followed by neutralisation could be developed as an alternative process option for denaturation of non-supercoiled DNA forms prior to precipitation.

5.7 Denaturation followed by divalent cation precipitation

With the understanding gained in both divalent cation precipitation and denaturation of different forms of nucleic acids, studies were performed to explore their synergistic effects for purification of supercoiled plasmid DNA.

In an initial experiment 0.5 M calcium chloride precipitation was performed on samples from the 95 °C incubation experiment on clarified lysate (Figure 5.14). Supernatant samples from these samples were run on an agarose gel and these results are shown in Figure 5.16.

Next 0.2 M calcium chloride precipitation was performed on samples from the 85°C incubation experiment on clarified lysate (Figure 5.15). Supernatant samples from these samples were run on another agarose gel and these results are shown in Figure 5.17.

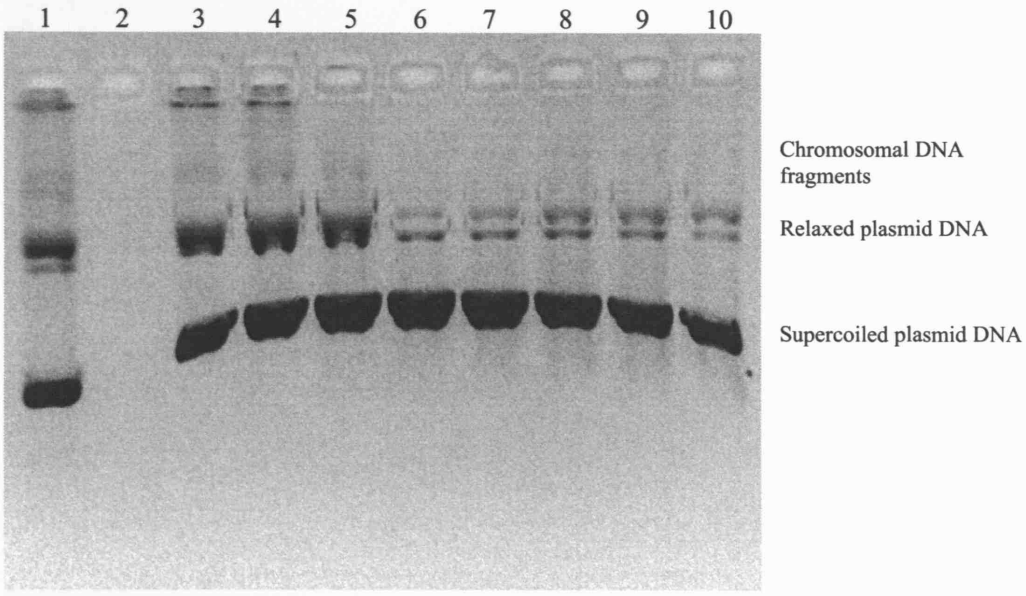

Figure 5.16 Effect of 95°C pre-heating time on divalent cation precipitation of clarified lysate samples. 0.8% agarose gel shows supernatants from 0.5 M calcium chloride precipitation of clarified lysate samples which had been pre-heated at 95°C for varying lengths of time followed by immediate cooling in ice bath (see Figure 5.14). Lane 1: clarified lysate control (no heating, no precipitation); Lane 3: non-heated control with precipitation; Lane 4: pre-heated for 0.5 minutes; Lane 5: pre-heated for 1 minute; Lane 6: pre-heated for 2 minutes; Lane 7: pre-heated for 3 minutes; Lane 8: pre-heated for 4 minutes; Lane 9: pre-heated for 5 minutes; Lane 10: pre-heated for 6 minutes. Note lower mobilities of supernatant samples are due to presence of calcium ions.

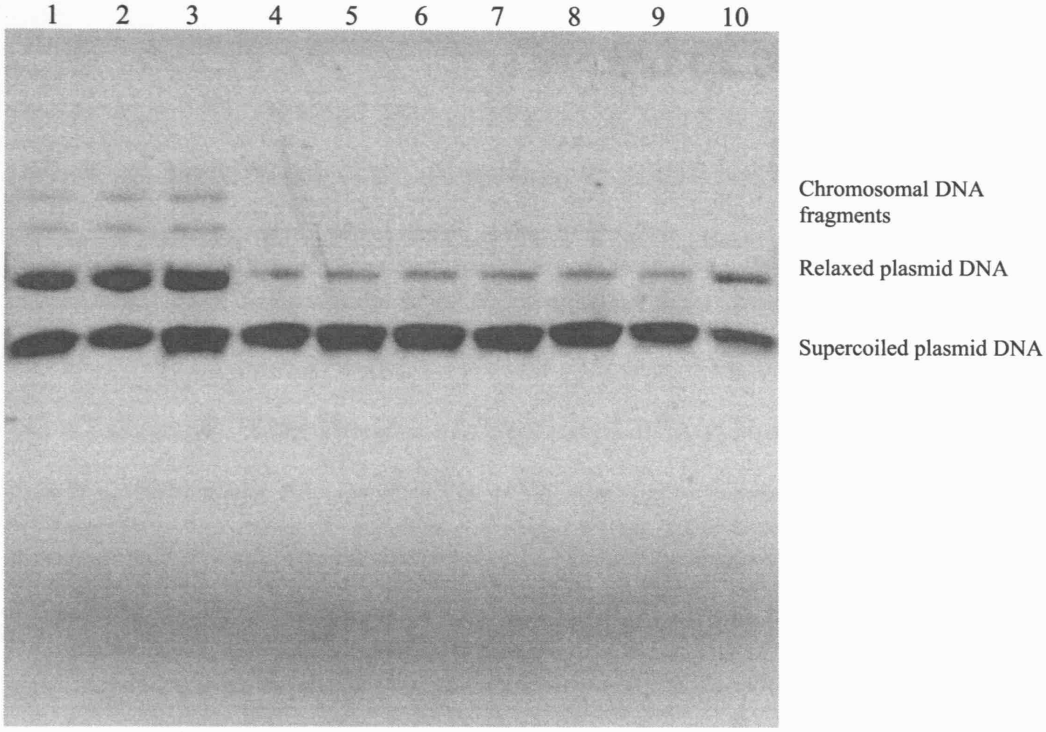

Figure 5.17 Effect of 85°C pre-heating time on divalent cation precipitation of clarified lysate samples. 0.8% agarose gel shows supernatants from 0.2 M calcium chloride precipitation of clarified lysate samples which had been pre-heated at 85°C for varying lengths of time followed by immediate cooling in ice bath (see Figure 5.15). Lane 1: clarified lysate control (no heating); Lane 2: 0.5 minute pre-heat; Lane 3: 1 minute; Lane 4: 2 minutes; Lane 5: 3 minutes; Lane 6: 4 minutes; Lane 7: 5 minutes; Lane 8: 15 minutes; Lane 9: 30 minutes; Lane 10: 60 minutes.

Comparing lane 1 in Figure 5.15 to lane 1 in Figure 5.17 shows that 0.2 M calcium chloride precipitation without pre-heating cleared some of the chromosomal DNA impurities while preserving full recovery of supercoiled plasmid. As suggested previously, chromosomal DNA clearance from samples that had not been denatured may have been due to some fragments or sections of chromosomal DNA being already in the single-stranded form. However, Figure 5.17 shows that samples that were pre-heated for 2 minutes or longer (lanes 4-10) had a significantly higher clearance of chromosomal DNA upon precipitation. This is consistent with the reasoning that pre-heating likely converted much of the aggregated or double-stranded chromosomal DNA to the single-stranded form prior to precipitation. Figure 5.17 also shows that pre-heating resulted in significantly reduced levels of relaxed DNA in precipitation supernatants, an expected result based on the results in Figure 5.15. Furthermore Figure 5.17 suggests little or no precipitation of the supercoiled form occurred. Finally, comparing Figure 5.17 to Figure 5.15, 0.2 M calcium chloride precipitation cleared any of the denatured form of plasmid that had formed upon heating. These results are consistent with the conclusion that divalent metal cations are effective precipitation agents for nucleic acid forms with single-stranded regions. Clearance of the denatured form by precipitation would be important from a process standpoint as a safeguard in case excessive denaturation occurred during the denaturation step. Figure 5.15 and Figure 5.17 show that pre-heating clarified lysate for 2-5 minutes at 85 °C prior to calcium chloride precipitation results in maximal chromosomal DNA and relaxed plasmid clearance with minimal supercoiled plasmid loss. To confirm these findings and also assess RNA clearance, the three-minute pre-heated/precipitated sample was run by the Q

Sepharose HP chromatographic assay; the clarified lysate and unheated precipitated samples were also run for comparison. These results are shown in Figure 5.18 and Figure 5.19.

Comparing the clarified lysate chromatogram to that from the non-denatured supernatant sample shows that 0.2 M calcium chloride alone provided RNA clearance of 83%, single-stranded DNA clearance of 100%, and double-stranded chromosomal DNA clearance 70%. Inclusion of the 2-minute pre-heating step did not provide any benefit to RNA clearance but did show an additional 26% clearance of double-stranded chromosomal DNA, and an additional 47% clearance of relaxed plasmid DNA. The chromatographic chromosomal DNA results in Figure 5.19 are consistent with the agarose gel in Figure 5.17.

Following the encouraging results using denaturation followed by calcium chloride precipitation, and recalling that nickel cation precipitation resulted in improved RNA clearance compared to calcium (Figure 5.9 and Figure 5.10), denaturation combined with nickel sulphate precipitation was tested. Supernatant samples from precipitations were assayed by the Q Sepharose HP assay. Figure 5.20 shows that as in the no denaturation case, nickel sulphate precipitation resulted in improved RNA clearance compared to calcium chloride precipitation when pre-denaturation (3 minutes at 85 °C) was used.

Also as expected, Figure 5.21 shows that nickel sulphate precipitation resulted in

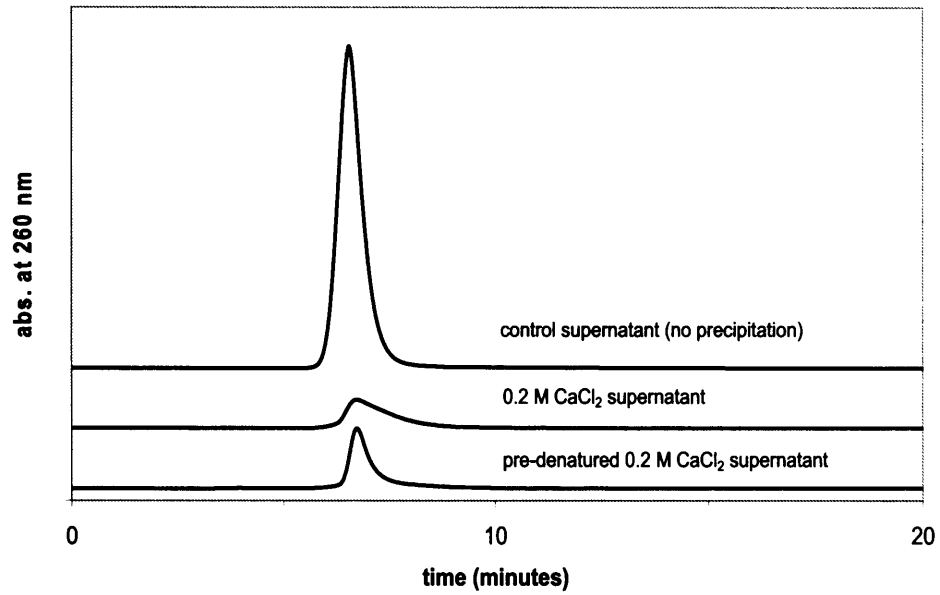

Component	Cl. Lysate Control Conc. (µg/mL)	0.2 M $CaCl_2$ Sup. Conc. (µg/mL)	0.2 M $CaCl_2$ Sup. Fraction of Orig.	Pre-Heated $CaCl_2$ Sup. Conc. (µg/mL)	Pre-Heated $CaCl_2$ Sup. Fraction of Orig.
RNA	2690	453	17%	584	22%

Figure 5.18 Q Sepharose HP analytical chromatograms showing effect of pre-denaturation on RNA clearance during divalent cation precipitation. Top: no denaturation/ no precipitation clarified lysate control supernatant; Middle: supernatant from non-denatured clarified lysate following 0.2 M calcium chloride precipitation; Bottom: supernatant from pre-denatured clarified lysate (heating 3 minutes at 85°C) followed by 0.2 M calcium chloride precipitation. RNA concentrations were determined from standard curves.

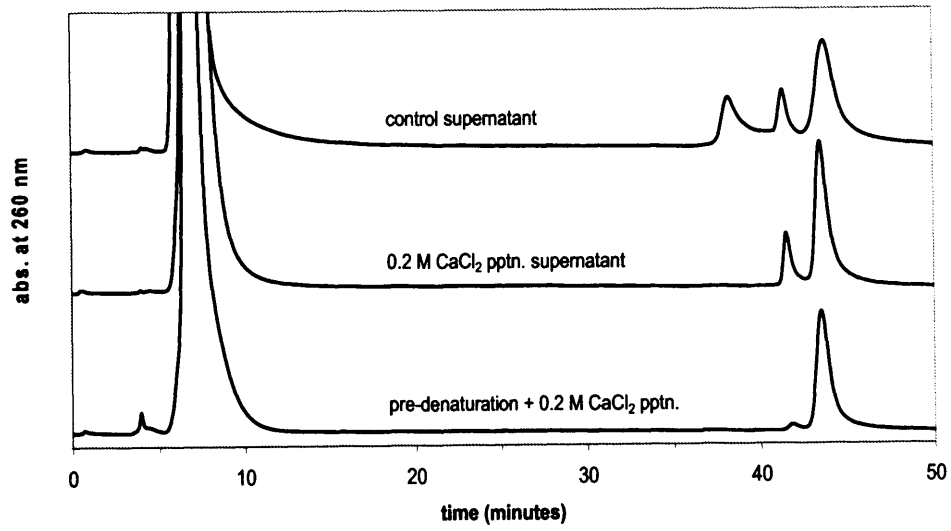

Component	CL Lysate Control Conc. (µg/mL)	0.2 M $CaCl_2$ Sup. Conc. (µg/mL)	0.2 M $CaCl_2$ Sup. Fraction of Orig.	Pre-Heated $CaCl_2$ Sup. Conc. (µg/mL)	Pre-Heated $CaCl_2$ Sup. Fraction of Orig.
single-stranded DNA	56	0	0%	0	0%
ds-chromosomal DNA	44	13	30%	1.8	4%
relaxed plasmid DNA	52	27	52%	2.7	5%
supercoiled plasmid DNA	92	88	96%	88	96%

Figure 5.19 Q Sepharose HP analytical chromatograms showing effectiveness of pre-denaturation on DNA impurity clearance during divalent cation precipitation. Top: no denaturation/ no precipitation clarified lysate control supernatant; Middle: supernatant from non-denatured clarified lysate following 0.2 M calcium chloride precipitation; Bottom: supernatant from pre-denatured clarified lysate (heating 3 minutes at 85°C) followed by 0.2 M calcium chloride precipitation. Peak at 6.5 minutes is digested RNA, peak at 38.5 minutes is single-stranded chromosomal DNA, peak at 41.5 minutes is relaxed plasmid DNA, and peak at 44 minutes is double-stranded DNA (primarily supercoiled plasmid). Component concentrations were determined from standard curves.

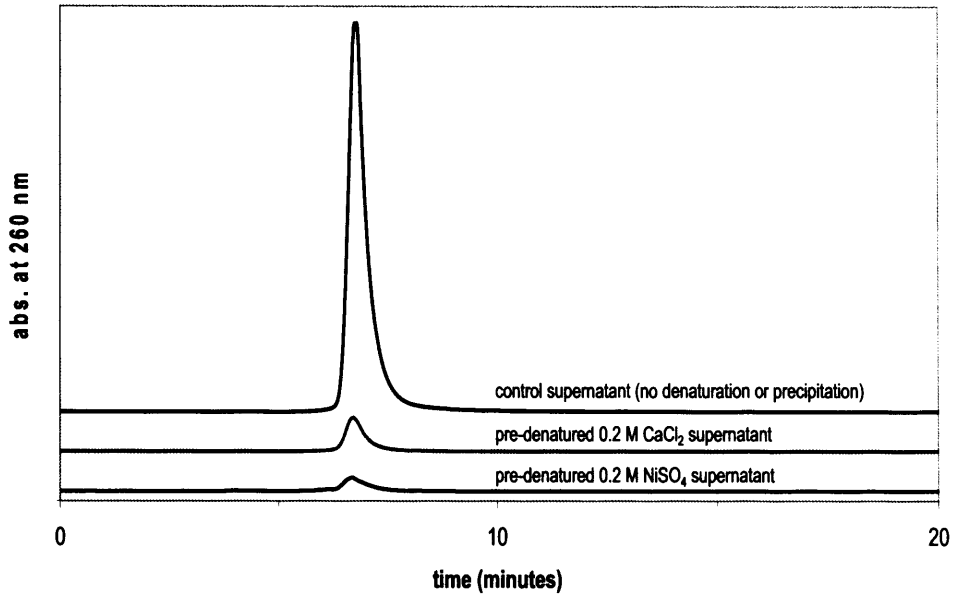

Component	CL Lysate Control Concentration (µg/mL)	0.2 M $CaCl_2$ Supernatant Conc. (µg/mL)	0.2 M $CaCl_2$ Supernatant Fraction of Orig.	0.2 M $NiSO_4$ Supernatant Conc. (µg/mL)	0.2 M $NiSO_4$ Supernatant Fraction of Orig.
RNA	2594	259	10%	137	5%

Figure 5.20 Effect of calcium and nickel cation precipitation for RNA clearance following pre-denaturation step. Shown are Q Sepharose HP chromatograms from supernatant samples starting from clarified lysate in TE buffer. Top: no denaturation/ no precipitation control supernatant; Middle: pre-denaturation (3 minutes at 85°C) + 0.2 M calcium chloride precipitation supernatant; Bottom: pre-denaturation (3 minutes at 85°C) + 0.2 M nickel sulphate supernatant. Component concentrations were determined from standard curves.

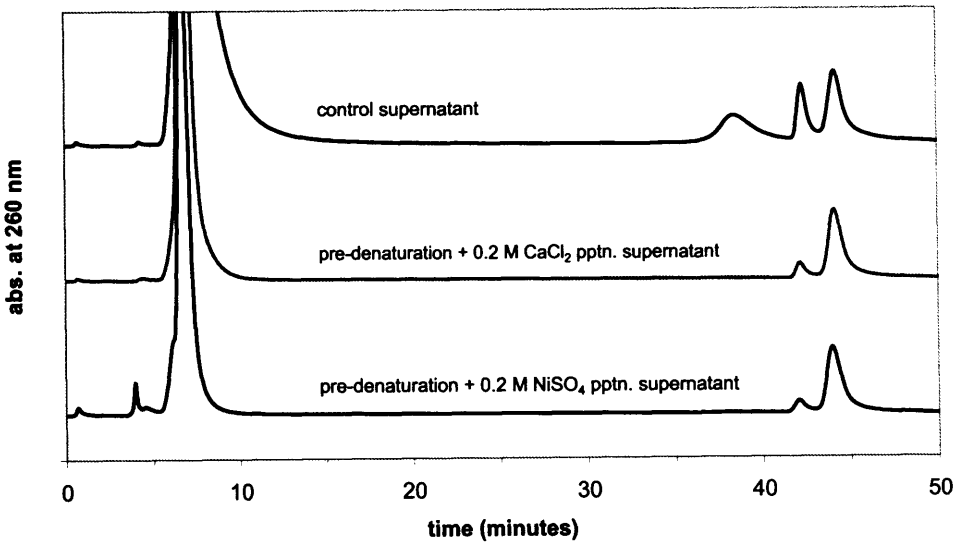

Component	Cl. Lysate Control Concentration (μg/mL)	0.2 M $CaCl_2$ Supernatant Conc. (μg/mL)	0.2 M $CaCl_2$ Supernatant Fraction or Orig.	0.2 M $NiSO_4$ Supernatant Conc. (μg/mL)	0.2 M $NiSO_4$ Supernatant Fraction or Orig.
single-stranded DNA	37	0	0%	0	0%
ds-chromosomal DNA	10	1.0	10%	0.9	9%
relaxed plasmid DNA	33	6.5	20%	5.9	18%
supercoiled plasmid DNA	52	50	98%	50	98%

Figure 5.21 Effect of calcium and nickel cation precipitation for DNA impurity clearance following pre-denaturation step. Shown are Q Sepharose HP chromatograms from supernatant samples starting from clarified lysate in TE buffer. Top: no denaturation/ no precipitation control supernatant; Middle: pre-denaturation (3 minutes at 85°C) + 0.2 M calcium chloride precipitation supernatant; Bottom: pre-denaturation (3 minutes at 85°C) + 0.2 M nickel sulphate supernatant. Peak at 6.5 minutes is digested RNA, peak at 38.5 minutes is single-stranded chromosomal DNA, peak at 41.5 minutes is relaxed plasmid DNA, and peak at 44 minutes is double-stranded DNA (primarily supercoiled plasmid). Component concentrations were determined from standard curves.

equivalent clearance of chromosomal DNA (single- and double-stranded) and relaxed plasmid DNA, along with equivalent recovery of supercoiled plasmid DNA.

Comparing past results for clarified lysate, denaturation combined with nickel cation precipitation showed the best performance in terms of purification of supercoiled plasmid DNA from other nucleic acid forms. This is performed by rapid heating of clarified lysate to 85 °C with a dwell time of 3 minutes, followed by rapid cooling to approximately 5°C, followed by 0.2 M nickel sulphate precipitation, followed by removal of precipitates using centrifugation or filtration.

5.8 Effects on plasmid stability

Throughout the experimental studies a few analytical results from the Q Sepharose HPLC assay suggested that introduction of divalent cations to plasmid DNA can result in plasmid instability. An example of this is shown in Figure 5.22, which compares chromatograms for a clarified lysate supernatant sample following 0.2 M calcium chloride precipitation (bottom) to a control supernatant sample to which calcium chloride had not been added (top). Comparison of the relaxed and supercoiled plasmid DNA peaks (41.5 and 44 minute retention times respectively) suggest that in this experiment some of the supercoiled plasmid was converted to the relaxed form upon introduction of 0.2 M calcium chloride, an outcome consistent with strand nicking due nuclease activity (precipitation of

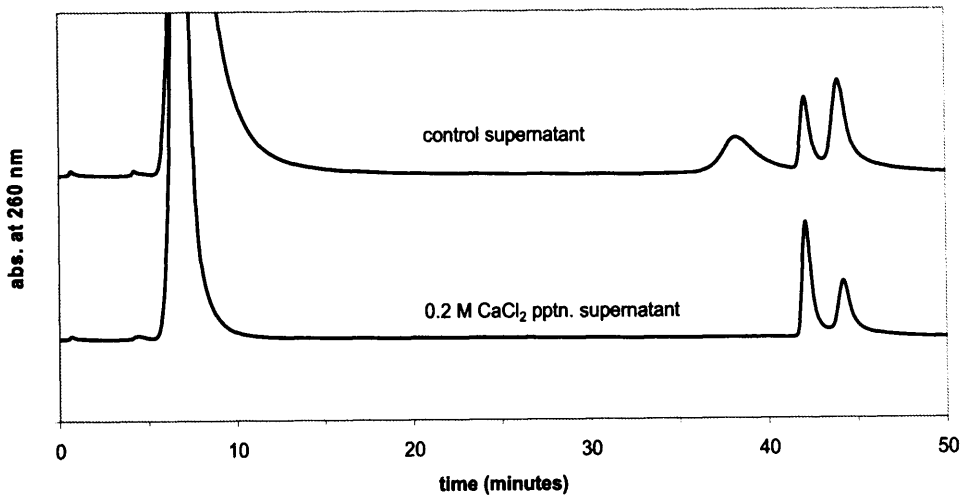

Component	Clarified Lyste Control Supernatant Conc. (µg/mL)	0.2 M $CaCl_2$ Precipitation Supernatant Conc. (µg/mL)
RNA	1853	266
single-stranded DNA	26	~0
relaxed plasmid DNA	23	37
double-stranded DNA (incl. sc-plasmid)	44	23

Figure 5.22 Example of instability of supercoiled plasmid DNA in the presence of divalent cations. Shown are Q Sepharose HP analytical chromatograms of supernatant samples. Top: clarified lysate control in TE buffer (no calcium chloride added); Bottom: following precipitation by addition of 0.2 M calcium chloride at room temperature. Peak at 6.5 minutes is digested RNA, peak at 38.5 minutes is single-stranded chromosomal DNA, peak at 41.5 minutes is relaxed plasmid DNA, and peak at 44 minutes is double-stranded DNA (primarily supercoiled plasmid). Component concentrations were determined from standard curves.

RNA and ssDNA occurred as expected). It is well known that divalent cations serve as cofactors for many enzymes, including *E. coli* endonucleases (Wilson and Murray, 1991). In this case it seems likely that the introduction of calcium chloride acted to increase the digestion kinetics for residual nucleases in the clarified lysate (with either calcium itself and/or another trace divalent cation introduced with the calcium serving as a cofactor). Other cases of supercoiled plasmid degradation similar to that shown in Figure 5.22 also occurred occasionally during precipitation experiments with divalent cations.

Temperature is known to be a major factor in enzyme kinetics, therefore based on the findings above, it is recommended to perform divalent cation precipitation at temperatures closer to 0°C to ensure minimal degradation of supercoiled plasmid. Also a study using the *E. coli* restriction endonucleases EcoR1 and EcoR5 showed that among several divalent cations studied, a consistent order of magnesium > zinc > nickel > calcium was obtained for increasing relative endonuclease activity (Vipond et al., 1995). Therefore if plasmid stability still appeared to be an issue during divalent cation precipitation even when performed at low temperatures, use of calcium over the other cations may be preferred (although this could result in slightly less RNA clearance as showed in Section 5.5).

5.9 Assessment of Scalability

At large-scale, divalent cation precipitation alone would probably not present significant engineering challenges. As suggested by the studies on kinetics of precipitation and contacting conditions (Section 5.2), differences in initial

mixing/contacting conditions appear to have little effect on nucleic acid solubilities. Also, precipitate particle sizes formed by divalent cation precipitation are generally large such that removal by filtration or centrifugation should not present problems. Thus divalent cation precipitation alone should be a fairly robust step.

However, a thermal denaturation step at 85 °C would need to be precisely controlled at large scale to avoid irreversible denaturation of supercoiled plasmid or nuclease activity due to extended incubation periods near 37 °C. This step could be carried out in batch mode in a jacketed process vessel with good mixing of the process stream to avoid local temperature gradients. An alternative option to performing thermal denaturation in batch mode would be flowing of the process stream through two heat exchangers in series; one heat exchanger for rapid heating followed by a second heat exchanger for rapid cooling, with the process flow rate and distance between the two heat exchangers adjusted to provide the desired dwell time. Alternatively, denaturation could be carried out in batch mode by a finely controlled change of the batch pH; however this could prove more challenging than thermal denaturation since local above-target pH regions near the base addition point could lead to irreversible supercoiled plasmid denaturation, and additional buffer or acid would need to be added for neutralisation.

5.10 Proposed large-scale purification process

Based on the studies of this project, a large-scale purification process scheme was conceived that incorporates thermal denaturation followed by divalent cation

precipitation into the process. A version of this process is shown in Figure 5.23. The version shown is a non-chromatographic process with a filtration focus for solids removal. This process scheme relies on precipitation and filtration for RNA clearance, to help ensure pathogens are not introduced through addition of mammalian-derived RNase. Note that centrifugation could be used in place of depth filtration for clarification following alkaline lysis, or in place of normal flow filtration following divalent cation precipitation. Depending on the plasmid size and impurity profile, the membrane steps could be optimised in terms of pore size, filtration area, and flow conditions. Nickel sulphate is indicated as the divalent cation salt for maximum RNA clearance. Following thermal denaturation at 85 °C, divalent cation precipitation at approximately 5 °C is recommended for supercoiled plasmid stability. Following addition of the divalent cation stock solution, one hour would allow the precipitation reaction to reach equilibrium, and slow mixing during this time is recommended to avoid size reduction of precipitate particles by shear. Based on results in this thesis, this non-chromatographic process would be expected to provide greater than 80% yield of supercoiled plasmid DNA, greater than 95% clearance of RNA and chromosomal DNA, greater than 80% clearance of relaxed plasmid DNA, and high clearance of protein and endotoxin impurities. Although this scheme would be expected to provide high yields of supercoiled plasmid DNA with very low impurity levels, if purity levels were not satisfactory (e.g. if endotoxin levels were higher than expected), a chromatographic step (e.g. hydrophobic interaction or size exclusion chromatography) could be inserted in place of the final polishing TFF buffer exchange for impurity reduction and buffer exchange.

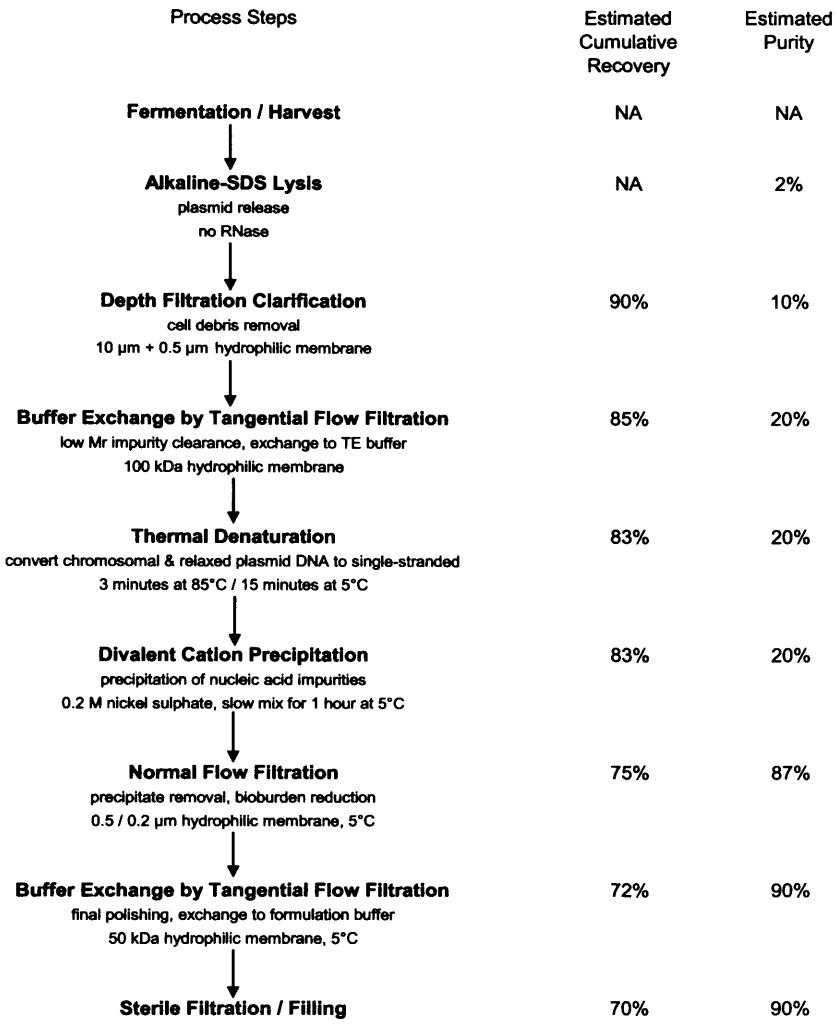

Figure 5.23 Process flow diagram for proposed non-chromatographic purification for recovery of supercoiled plasmid DNA. This process incorporates thermal denaturation and divalent cation precipitation steps investigated in this thesis. Recovery and purity of supercoiled plasmid DNA are estimated for each process step. The primary impurity component at end of this process is expected to be relaxed plasmid DNA.

5.11 Summary

The studies performed in this section focused on optimisation of the process parameters of divalent cation precipitation for recovery and purification of plasmid DNA. Kinetics studies suggested that divalent cation precipitation follows approximately second order kinetics and that initial contacting conditions had minimal impact on final solubility. It was found that optimal placement of a divalent cation precipitation step, in a process scheme starting from alkaline lysis of *E. coli* cells, would be following neutralisation, clarification, and low-salt-buffer exchange steps. Inclusion of a novel controlled denaturation step prior to divalent cation precipitation would enhance clearance of chromosomal dsDNA and relaxed plasmid DNA for recovery of supercoiled plasmid DNA. Nickel sulphate and zinc acetate divalent cation salts showed improved clearance of RNA compared to calcium chloride and other divalent cation salts. Results also showed that stability of plasmid DNA could be impacted by introduction of divalent cations and therefore precipitation with divalent cations should be carried out at temperatures near 0°C. Based on these studies, a non-chromatographic purification process using denaturation combined with nickel sulphate divalent cation precipitation was proposed.

6 PRECIPITATION MECHANISMS AND MODEL ASSESSMENT

6.1 Introduction

Part of the objectives of this project included investigation of mechanisms involved in precipitation of nucleic acids and evaluation of existing precipitation models, in order to gain a better understanding of the forces involved in these complex reactions. In this section various experiments and assessments were performed to investigate precipitation mechanisms, particularly those related to divalent cation precipitation, and two precipitation models were evaluated against the experimental results obtained in the project.

6.2 Effects of cation and anion types

As discovered during single-component solubility studies (Section 4), cation type has a significant impact on nucleic acid solubility. Monovalent cations were relatively ineffective for precipitation of any of the nucleic forms studied. Divalent cations were effective for precipitation of single-stranded nucleic acid forms (both DNA and RNA) but not double-stranded forms. These findings are consistent with counterion condensation theory.

For RNA precipitation, it was also found that some divalent cation salts were more effective than others; for the divalent cation salts tested in these studies, the order of effectiveness for precipitation was nickel sulphate ~ zinc acetate > calcium chloride ~ calcium acetate > magnesium chloride ~ zinc sulphate >

magnesium sulphate. The reasons for the differences in this series are somewhat unclear, however the cations with higher atomic weights (zinc and nickel) in this study were more effective for RNA precipitation. No trend was observed with ionic radius and precipitation effectiveness. Also note that differences were observed for a given cation with different anions (for example zinc acetate was much more effective than zinc sulphate, and magnesium chloride was more effective than magnesium sulphate); the apparent effectiveness of anions was in reverse order of the lyotropic series (i.e. chloride > acetate > sulphate). For protein precipitation effectiveness of anions is generally in the order of the lyotropic series. In contrast to divalent cation precipitation, trivalent cation polyamines were very effective for precipitation of dsDNA, partially effective for ssDNA, and relatively ineffective for RNA.

6.3 RNA resolubilisation in excess divalent cation concentration

It was observed in some divalent cation precipitation experiments that rRNA solubilities appeared slightly higher at 1.0 M cation concentration compared to 0.5 M. This phenomenon was explored further using calcium chloride precipitation of purified *E. coli* rRNA and testing solubility out to 2.5 M calcium as shown in Figure 6.1. Results clearly show that in calcium chloride solution, rRNA solubility first decreased then increased again for calcium concentrations higher than 1.0 M. As discussed in Section 1.6.3, adsorption of ions to particle surfaces can eventually lead to complete charge reversal and render the particle stable in solution again. The results in Figure 6.1 suggest that this likely occurred for rRNA in calcium chloride solution with minimal concentration of

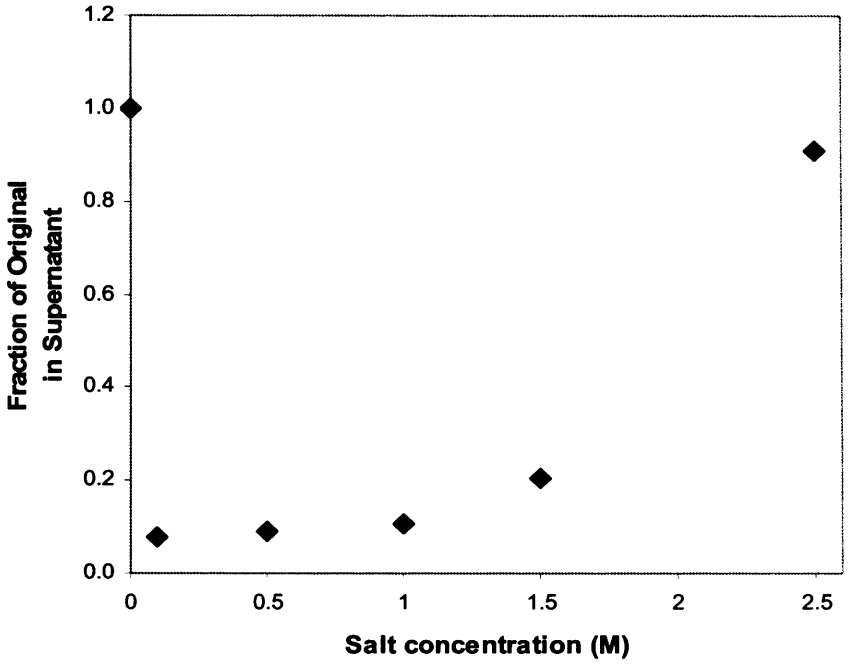

Figure 6.1 Resolubilisation of RNA at very high divalent cation concentrations. Plot shows solubilities of purified rRNA in solutions with varying calcium chloride concentrations at pH 8. Nucleic acid concentrations in supernatant samples were determined based on A260 measurements from separate samples; initial rRNA concentration was 100 μg/mL for each sample. Estimated average error for each measurement is ± 5%.

monovalent cations present; enough positively charged calcium ions would have bound to the negatively charged phosphate groups to reverse the net particle charge and resolubilise the particle. It should be noted that under counterion condensation theory, typically charge neutralisation is assumed to be the same as long as cations of a given valence are present in excess; however based on the Poisson-Boltzmann ion distribution model in cases such as this with bulk divalent cation concentrations in excess of 1.0 M, cation concentrations at the RNA particle surface would be significantly higher than for bulk cation concentrations in the range of 0.2 M (see Figure 1.4). These excess cations at the RNA surface may have been sufficient to reverse the effective particle charge to positive and thereby increase solubility. Also note that this phenomenon might also explain why RNA was found to be generally soluble in the presence of the trivalent polyamine spermidine^{3+} (Figure 4.10).

6.4 Importance of nucleic acid size

The effect of nucleic acid size was investigated by comparing divalent cation precipitation for two forms of purified *E. coli* RNA: ribosomal RNA (rRNA) and transfer RNA (tRNA). Recall from Table 1.2 that most rRNA molecules are significantly larger than tRNA (average rRNA size is approximately 1.5 kb compared to 0.08 kb for tRNA), and that rRNA makes up about 82% of the total RNA in an *E. coli* cell. Figure 6.2 shows the results of this study.

It is clear from Figure 6.2 that tRNA showed a much higher solubility in calcium chloride solution, and it is likely that this is because tRNA is a much smaller

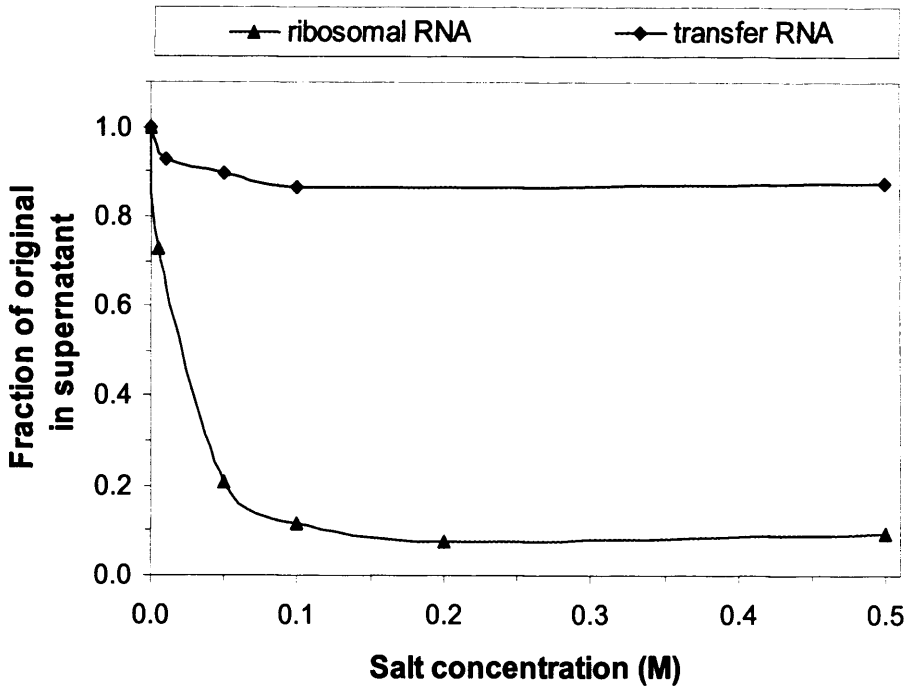

Figure 6.2 Solubilities of different size forms of *E. coli* RNA in divalent cation solution. Plot shows solubilities of transfer RNA (tRNA) and ribosomal RNA (rRNA) in solutions with varying calcium chloride concentrations at pH 8. Nucleic acid concentrations in supernatant samples were determined based on A260 measurements from separate samples; initial concentrations were 50-100 μg/mL for each component. Estimated average error for each measurement is ± 5%.

molecule compared to most rRNA molecules. Upon addition of calcium chloride tRNA molecules may have shown some aggregation due to perikinetic growth, however due to its small molecular size initial aggregate particles may not have reached the critical size necessary for further particle size growth due to orthokinetic aggregation.

Initial small aggregates would probably not be removed by centrifugation at 16,000 x g centrifugal force used in these experiments. Fortunately tRNA only makes up approximately 10% of the total RNA population with rRNA making up the bulk of the total RNA in clarified lysate.

The effect of nucleic acid size was further investigated by comparing divalent cation precipitation for purified rRNA to purified rRNA which had been pre-digested by RNase. Results of this experiment are shown in Figure 6.3. Just as in the previous experiment with tRNA, very little digested rRNA was precipitated, providing further support to the importance of nucleic acid size for divalent cation precipitation. Recall that previous precipitation experiments on clarified lysate have shown that most but not all RNA could be cleared by precipitation (for example see Figure 5.9). The experiments here suggest that the remaining RNA in the supernatants of previous experiments may well have been tRNA and smaller rRNA molecules. Also note that small RNA molecules would be expected to be cleared by the 100 kDa ultrafiltration step in the proposed process shown in Figure 5.23.

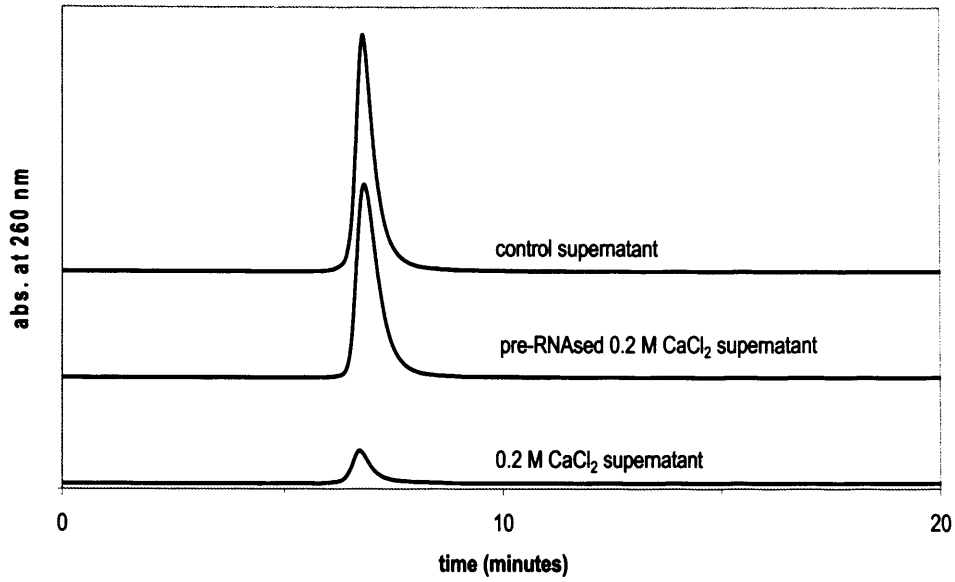

Sample	RNA Conc. (µg/mL)	Fraction of Orig.
Non-pptn. control supernatant	1718	--
Pre-RNased 0.2 M $CaCl_2$ pptn. supernatant	1628	95%
0.2 M $CaCl_2$ pptn. supernatant	287	17%

Figure 6.3 Impact of nucleic acid size on precipitation effectiveness. Q Sepharose HP analytical chromatograms showing RNA peaks of clarified lysate supernatant samples following precipitation. Top: non-precipitated clarified lysate control; middle: pre-treated with RNase prior to addition of 0.2 M calcium chloride to degrade RNA to small size prior to precipitation; bottom: precipitation with 0.2 M calcium chloride (not RNase pre-treated). RNA concentrations were determined from standard curves.

6.5 Hydrophobic interactions

The nitrogenous bases of nucleic acids (adenine, thymine, cytosine, guanine, uracil) are known to be hydrophilic on the edges (in the same plane as the aromatic ring(s)) but hydrophobic above and below their surfaces. In dsDNA or double-stranded stretches of RNA, hydrophobic interactions between the bases help determine the helical structure of these molecules, with the bases stacked in the interior and the hydrophilic ribose or deoxyribose sugar groups positioned on the exterior. ssDNA would be expected to have some degree of hydrophobic interaction between adjacent nitrogenous bases, but because these molecules are not stabilised by complementary base pairing, they have a more extended structure than dsDNA. Since both ssDNA and RNA have single-stranded regions with nitrogenous bases exposed to the solution environment, hydrophobic interactions between non-adjacent bases on the same or different molecule become more likely.

Recall that RNA was found to be generally soluble in the presence of monovalent cations but insoluble in the presence of divalent cations (for examples see Figure 4.2 and Figure 4.5). A possible explanation for this behaviour is that divalent cations provide sufficient charge neutralisation to allow these molecules to approach each other to very close proximity (~2 nm separation distance), such that van der Waals forces leads to aggregation and eventually precipitation. Indeed counterion condensation theory predicts that divalent cations will result in 90% charge neutralisation of double-stranded stretches of RNA (Table 1.4), but that monovalent cations will only result in 80% charge neutralisation. If RNA

solubility correlates with degree of charge neutralisation similarly to dsDNA, Wilson and Bloomfield's extension of the counterion condensation theory would suggest that 90% charge neutralisation is sufficient for condensation/ precipitation to occur. However, even if the threshold for RNA condensation were higher than the 89% neutralisation established for double-stranded DNA, divalent cations may still provide sufficient charge neutralisation for RNA molecules to approach each other to close enough proximity (less than ca. 80 nm separation distance) such that hydrophobic interactions would lead to aggregation/precipitation.

For ssDNA, counterion condensation theory predicts that divalent cations will only result in 72% charge neutralisation (see Table 1.5), much lower than the charge neutralisation for dsDNA and RNA, due to the more extended nature of ssDNA and lower axial charge density. Therefore to explain the behaviour of ssDNA aggregation/ precipitation in the presence of divalent cations (again see Figure 4.5 for example), it is hypothesised that divalent cations provide sufficient charge neutralisation to allow nucleotides to approach each other to close enough proximity such that intra- or inter-molecular hydrophobic interactions become important. These hydrophobic interactions would lead to aggregation of ssDNA and eventually to precipitation.

6.6 Steric exclusion forces

The effects of steric exclusion were evident in the PEG precipitation experiments (Section 4.7). In these experiments, the solubility behaviour of nucleic acids appeared similar to that of proteins in the presence of a neutral polymer.

Solubility was observed to decrease with increasing polymer concentration, increasing salt concentration, and increasing nucleic acid size. Also for a given polymer concentration, divalent cation salts were observed to be more effective than monovalent cation salts for decreasing nucleic acid solubility; and this difference was beyond what would be expected solely due to ionic strength differences. For example, in the presence of 3% PEG-4000, plasmid DNA was found to be soluble in 0.75 M sodium chloride (ionic strength 0.75 M) but insoluble in 0.2 M calcium chloride (ionic strength 0.6 M). The counterion condensation theory predicts charge neutralisation of 76% and 88% for dsDNA in solution with monovalent or divalent cations respectively (Table 1.3). Therefore, the steric exclusion precipitation mechanism for nucleic acids appears similar to that for proteins, but charge neutralisation as predicted by the counterion condensation theory may also be partially responsible for the behaviour observed.

6.7 Multi-component interactions

Somewhat surprisingly, few multi-component interactions were observed in this project. Generally results from single-component experiments were reproduced in experiments with multi-component streams such as clarified lysate. For example, Figure 4.5 shows in single-component experiments plasmid and chromosomal dsDNA to be generally soluble in 0.2 M calcium chloride solution, but ssDNA and RNA to generally insoluble. When 0.2 M calcium chloride was added to clarified lysate as shown in Figure 4.8 and Figure 4.9, the same solubility behaviour was observed. This finding suggests that plasmid DNA purification by divalent cation precipitation should not be highly sensitive to variations in other nucleic acid levels from batch to batch. Occasionally, recovery of dsDNA following divalent cation precipitation of clarified lysate was

slightly lower than might be expected (for example see Figure 5.8), however this behaviour was not significantly different from observations from single-component experiments and may not have been due to multi-component interactions. The only case where multi-component interactions were clearly suspected was for divalent cation precipitation following post-lysis neutralisation but prior to clarification (see Figure 5.4). In this case, dsDNA recovery (37%) was significantly lower than expected, and it seems likely that some of the dsDNA that was not recovered (especially larger chromosomal DNA fragments) was entrained into cellular debris and cleared during centrifugation.

6.8 Assessment of counterion condensation theory model

The following observations and findings from the experimental results were consistent with the counterion condensation theory model (Section 1.7.1):

1) *Solubility results for dsDNA in the presence of one cation counterion*, assuming charge neutralisation as outlined in Table 1.3. dsDNA (both chromosomal and plasmid) was found to be soluble in the presence of monovalent and divalent cations, but insoluble in the presence of trivalent cations (spermidine^{3+}). This behaviour was completely consistent with Wilson and Bloomfield's extension of the counterion-condensation theory that 89-90% threshold charge neutralisation is required for condensation of dsDNA.

2) *RNA solubility in the presence of one cation counterion*, assuming charge neutralisation as outlined in Table 1.4 and a condensation threshold value

between 81% and 89% charge neutralisation applies. This is consistent with the finding that rRNA was soluble in the presence of monovalent cations but largely insoluble with divalent cations. Resolubilisation in the presence of trivalent cations (spermidine^{3+}) was likely due to charge reversal (discussed further in item 7 below).

3) *ssDNA solubility in the presence of one cation counterion*, assuming charge neutralisation as outlined in Table 1.5 and that due to hydrophobic interactions, a threshold value between 45% and 71% charge neutralisation applies. This is consistent with the experimental findings that ssDNA was soluble in the presence of monovalent cations but largely insoluble with divalent cations. Given these findings, the predicted charge neutralisation of only 72% for ssDNA in the presence of a single divalent counterion species as shown in Table 1.5 is somewhat surprising. However recently other investigators have found evidence of excessive counterion condensation (beyond that predicted by counterion condensation theory alone) for ssDNA in high ionic strength solutions (Rant et al., 2003). Also note that the gradual solubility profile observed for ssDNA in the presence of trivalent cations (spermidine^{3+}) shown in Figure 4.10 cannot be readily explained or modelled by counterion condensation theory.

4) *Effect of dielectric constant.* It was observed that lowering the dielectric constant through addition of a sufficient volume fraction of organic solvent (ethanol) resulted in precipitation of dsDNA. This is consistent with the prediction of increased charge neutralisation due to lowering of dielectric constant put forth by the counterion condensation theory.

5) *Effect of added monovalent cation salt to a solution of nucleic acids and divalent cation salt.* It was observed that addition of a monovalent salt such as sodium chloride to a solution of nucleic acids and divalent cation salt increased the solubility of ssDNA and RNA. This finding was completely consistent with the concept of decreasing the degree of charge neutralisation of nucleic acids through addition of a lower valence cation, due to competition for nucleic acid binding sites, put forth by the counterion condensation theory.

6) *Insensitivity of soluble fraction remaining in the supernatant to initial nucleic acid concentration.* It was observed for RNA that solubility (in terms of fraction of remaining in the supernatant) in the presence of divalent cations was insensitive to initial nucleic acid concentration, and this is consistent with counterion condensation theory, providing counterions are present in excess.

7) *Resolubilisation of RNA at high counterion concentrations.* If the approximation of constant charge neutralisation for a cation with a given valence is not used, but instead counterion distribution is modelled by the Poisson-Boltzmann equation (Equation 1.3), this would predict greater charge neutralisation eventually leading to charge reversal (Raspaud et al., 1998). This could explain the observations of resolubilisation of RNA at high divalent cation concentrations or in the presence of trivalent polyamines in this project.

Overall, experimental results in this project were very consistent with the counterion condensation theory, therefore in most cases this approach should be used to model nucleic acid solubility.

6.9 Assessment of Cohn equation model

Although counterion condensation theory appears to be a reasonable model for nucleic acid solubility in most cases, certain aspects of the experimental results could not be readily explained by this approach. For the following aspects, the Cohn solubility model (Section 1.7.2) could be used to in place of or to supplement counterion condensation theory:

1) *Nucleic acid solubility in the presence of non-ionic polymer and monovalent or divalent cations.* Steric exclusion effects are not accounted for in counterion condensation theory. The Cohn equation has successfully been used to model steric exclusion effects due to added non-ionic polymer in protein / salt solutions (Foster et al., 1973). This same methodology could also likely be used to predict nucleic acid solubility. Based on the results in Section 4.7, indeed the same trends that are relevant for protein solubility appear to be relevant for nucleic acid solubility (larger nucleic acids, more concentrated nucleic acids, and increased charge neutralisation all showed decreased solubility in the presence of non-ionic polymers).

2) *ssDNA solubility in the presence of trivalent cations.* As mentioned above, the gradual solubility profile observed for ssDNA in the presence of trivalent

cations (spermidine^{3+}, Figure 4.10) is not readily explained by counterion condensation theory. Although the mechanism behind this solubility profile is unclear, this behaviour could be modelled using the Cohn equation.

3) *Certain aspects of RNA and ssDNA solubility in the presence of monovalent or divalent cation salts.* Although most observations of nucleic acid solubility in this project were consistent with counterion condensation theory, the solubility profiles for RNA and ssDNA in the presence of divalent cations were somewhat gradual (Figure 4.5 and Figure 4.6). As mentioned previously, hydrophobic interactions are likely involved with the solubility of these components, therefore the Cohn equation could probably be used in conjunction with counterion condensation theory to model solubility behaviour in these cases. For example, counterion condensation theory might be used for predicting the onset of precipitation for these components, with the actual solubility profile modelled by the Cohn equation.

6.10 Summary

A number of mechanisms involved in nucleic acid precipitation were investigated in this section. High bulk divalent cation concentrations in excess of 1.0 M were shown to resolubilise RNA; this behaviour was likely to be the result of high divalent cation concentrations at the RNA surface leading to net charge reversal. As demonstrated with RNA, nucleic acid size is an important factor for clearance by divalent cation precipitation; small nucleic acids or fragments may not form large enough aggregates for continued particle growth prior for clearance by centrifugation or filtration. It was hypothesised that hydrophobic interactions

play a significant role during divalent cation precipitation of single-stranded DNA and RNA. Solubilities of nucleic acids in multi-component streams were observed to be similar to solubilities in single-component experiments, suggesting that interactions between different forms of nucleic acids were minimal during the precipitation reaction. It was also observed that most precipitation results in this project were consistent with the counterion condensation theory model, however in a few cases the Cohn equation could be used to help describe the observed solubility behaviour.

7 CONCLUSIONS AND RECOMMENDATIONS

7.1 Conclusions

Two HPLC analytical methods were developed to allow quantitation of different nucleic acid forms from multi-component process streams, one based on Q Sepharose HP strong anion exchange media and the other based on Poros PI weak anion exchange media. Both methods provide the capability to quantify RNA, single-stranded DNA, total double-stranded DNA, and supercoiled plasmid DNA from multi-component process stream samples. A unique aspect of the Q Sepharose HP assay is the additional capability to resolve and quantitate relaxed forms of plasmid DNA. These methods are useful tools for tracking different nucleic acid forms throughout a purification process, and the Q Sepharose HP method proved invaluable in this project for monitoring precipitation results on real multi-component process streams.

Single-component precipitation studies showed that monovalent cation salts alone were relatively ineffective precipitating agents for any of the nucleic acid forms studied. Divalent cation salts were effective precipitating agents for nucleic acids containing single-stranded regions including RNA and chromosomal ssDNA, whereas the trivalent polyamine spermidine^{3+} was effective for precipitating dsDNA and ssDNA but not RNA. Results suggested these agents may be useful for separation of nucleic acid forms from process streams by fractional precipitation. Supplementing divalent cation precipitation with ethanol did not show promise for fractional precipitation beyond divalent cation precipitation

alone, however supplementing with the non-ionic polymer PEG-4000 suggested that this could enhance separation of chromosomal DNA from plasmid DNA. Varying pH around neutral had little effect on nucleic acid solubility in monovalent and divalent cation salt solutions, showing fractional precipitation would be relatively robust with respect to pH. Nucleic acid solubilities were relatively insensitive to initial nucleic acid concentration in terms of fraction of initial remaining in the supernatant.

Further studies on divalent cation precipitation showed precipitation kinetics to be approximately second order and relatively slow, such that this step is robust in terms of initial contacting conditions. Divalent cation precipitation was shown to be more effective in a buffer containing low concentrations of monovalent cations, due to monovalent and divalent cations competing for binding sites on the nucleic acid surfaces. For plasmid DNA recovery, the optimal position of a divalent cation precipitation step as part of a purification process was determined to be following alkaline lysis, neutralisation, clarification, and low-salt-buffer exchange steps. A novel controlled thermal denaturation step was shown to improve significantly the clearance of chromosomal dsDNA and relaxed plasmid DNA, when performed prior to divalent cation precipitation for recovery of purified supercoiled plasmid DNA. This step is believed to denature all double-stranded forms to single-stranded, with only supercoiled plasmid DNA renaturing to double-stranded form upon cooling due to it being covalently closed circular. The divalent cation salts nickel sulphate and zinc acetate showed improved clearance of RNA compared to calcium chloride during divalent cation precipitation. Results also showed that stability of plasmid DNA could be

compromised by the introduction of divalent cations, therefore precipitation with divalent cations should be carried out at temperatures near 0°C. Based on these studies, a non-chromatographic purification process without RNase was proposed; this process scheme uses denaturation combined with nickel sulphate divalent cation precipitation for recovery of highly purified plasmid DNA. Avoiding the use of chromatography would represent a significant cost savings compared to current large-scale plasmid DNA purification processes, and avoiding the use of RNase helps ensure that mammalian-derived pathogens are not introduced to the process stream.

Furthermore, very high bulk divalent cation concentrations in excess of 1.0 M were shown to resolubilise RNA; this behaviour was likely to be the result of high divalent cation concentrations at the RNA surface leading to net charge reversal. Nucleic acid size was shown to be an important factor for clearance by precipitation; small nucleic acids such as tRNA or fragments may not form large enough aggregates for continued particle growth prior to centrifugation or filtration, therefore process steps to clear these forms such as tangential flow filtration should be included as part of a purification process. It was hypothesised that hydrophobic interactions play a significant role during divalent cation precipitation of single-stranded DNA and RNA. Comparison of precipitation results from single-component and multi-component streams suggested that interactions between different forms of nucleic acids were minimal during the precipitation reaction, another positive aspect for process robustness. Finally, most precipitation results in this project were found to be consistent with

Manning's counterion condensation theory model; however in a few cases the Cohn equation would help describe the solubility behaviour observed.

7.2 Recommendations for future work

Following are a few thoughts on possible follow-up work from this project:

1) The process scheme shown in Figure 5.23 is based on careful consideration, however it has not been attempted with the order of process steps shown. Follow-up work could investigate this process scheme at small-scale in preparation for a larger scale trial. Particular issues will require an understanding of the impact of reactor design on the size and strength of precipitate particles, and their suitability for removal by filtration. Much of the foundation for this work has been laid previously for protein precipitation.

2) In Section 4.7, experiments with PEG-4000 in 0.2 M calcium chloride resulted in slightly different solubility profiles for purified chromosomal and plasmid DNA. These data suggested that this system might be useful for fractionation of these two forms. Follow-up experiments with purified components could be performed to confirm this result and investigate if this system could be used for fractionation of other nucleic acids forms as well. Sensitivities to PEG size, cation type, cation concentration, and nucleic acid concentration could be investigated with step optimisation in mind.

3) In Section 4.4, solubility experiments in the presence of the polyamine spermidine^{3+} showed dsDNA to be insoluble, RNA to be soluble, and ssDNA to be partially soluble. The dsDNA results were completely expected based on counterion condensation theory, however the ssDNA and RNA results could not be readily explained. Follow-up experiments could investigate the mechanism underlying these solubility behaviours. For example, it is unclear if RNA remained soluble due to charge reversal, or alternatively due to steric limitations that limited spermidine^{3+} binding, or some other mechanism. These results are also encouraging from a process standpoint, showing the potential for another option for fractionation of different nucleic acid forms.

4) Although numerous studies have been reported in the literature showing that dsDNA collapses or condenses at low nucleic acid concentration with sufficient charge neutralisation, similar studies have not been performed on ssDNA or RNA. A better understanding of the mechanisms involved could lead to improved ability to fractionate different nucleic acid forms.

5) Most experiments in this project used the same plasmid DNA size of 6.9 kb. Different plasmids could be investigated using the denaturation plus divalent cation precipitation approach, to investigate sensitivity to plasmid size.

REFERENCES

1. Arakawa,T. and S.N.Timasheff. 1985. Mechanism of poly(ethylene glycol) interaction with proteins. *Biochemistry* 24:6756-6762.

2. Arnott,S., D.W.Hukins, S.D.Dover, W.Fuller, and A.R.Hodgson. 1973. Structures of synthetic polynucleotides in the A-RNA and A'-RNA conformations: x-ray diffraction analyses of the molecular conformations of polyadenylic acid--polyuridylic acid and polyinosinic acid--polycytidylic acid. *J. Mol. Biol.* 81:107-122.

3. Arscott,P.G., A.Z.Li, and V.A.Bloomfield. 1990. Condensation of DNA by trivalent cations. 1. Effects of DNA length and topology on the size and shape of condensed particles. *Biopolymers* 30:619-630.

4. Atha,D.H. and K.C.Ingham. 1981. Mechanism of precipitation of proteins by polyethylene glycols. Analysis in terms of excluded volume. *J. Biol. Chem.* 256:12108-12117.

5. Atkinson,A. and G.W.Jack. 1973. Precipitation of nucleic acids with polyethyleneimine and the chromatography of nucleic acids and proteins on immobilised polyethyleneimine. *Biochim. Biophys. Acta* 308:41-52.

6. Barlow,J.J., A.P.Mathias, R.Williamson, and D.B.Gammack. 1963. A simple method for the quantitative isolation of undegraded high molecular weight ribonucleic acid. *Biochem. Biophys. Res. Commun.* 13:61-66.

7. Bhikhabhai, R. A process for the purification of plasmid DNA. WO99/16869. 1999. (patent)

8. Birnboim,H.C. and J.Doly. 1979. A rapid alkaline extraction procedure for screening recombinant plasmid DNA. *Nucleic Acids Res.* 7:1513-1523.

9. Bloomfield,V.A. 1991. Condensation of DNA by multivalent cations: considerations on mechanism. *Biopolymers* 31:1471-1481.

10. Bloomfield,V.A. 1997. DNA condensation by multivalent cations. *Biopolymers* 44:269-282.

11. Camp,T.R. 1953. Flocculation and flocculation basins. *Proc. ASCE* 79:1-18.

12. Carter,M.J. and I.D.Milton. 1993. An inexpensive and simple method for DNA purifications on silica particles. *Nucleic Acids Res.* 21:1044.

13. Chan,M.Y.Y., M.Hoare, and P.Dunnill. 1986. The kinetics of protein precipitation by different reagents. *Biotechnol. Bioeng.* 28:387-393.

14. Christenson.H.K., J.Fang, B.W.Ninham, and J.L.Parker. 1990. Effect of divalent electrolyte on the hydrophobic attraction. *J. Phys. Chem.* 94:8004-8006.

15. Cohen,S.N., A.C.Chang, H.W.Boyer, and R.B.Helling. 1973. Construction of biologically functional bacterial plasmids in vitro. *Proc. Natl. Acad. Sci. U. S. A* 70:3240-3244.

16. Cohn,E.J. and J.D.Ferry. 1943. *Proteins, Amino Acids, and Peptides (editors Cohn, E. J. and Edsall, J. T.)*586-622.

17. Colote,S., C.Ferraz, and J.P.Liautard. 1986. Analysis and purification of plasmid DNA by reversed-phase high-performance liquid chromatography. *Anal. Biochem.* 154:15-20.

18. Cordes,R.M., W.B.Sims, and C.E.Glatz. 1990. Precipitation of nucleic acids with poly(ethyleneimine). *Biotechnol. Prog.* 6:283-285.

19. Derjaguin,B.V. and L.V.Landau. 1941. Theory of the stability of strogly charged lyophobic sols and of the adhesion of strongly charged particles in solutions of electrolytes. *Acta Physicochim. URSS* 14:733-762.

20. Diamont, H. and Andelman, D. General criterion for controllable conformational transitions of single and double stranded DNA. 2005. (unpublished work)

21. Diogo,M.M., J.A.Queiroz, G.A.Monteiro, S.A.Martins, G.N.Ferreira, and D.M.Prazeres. 2000. Purification of a cystic fibrosis plasmid vector for gene therapy using hydrophobic interaction chromatography. *Biotechnol. Bioeng.* 68:576-583.

22. Diogo,M.M., J.A.Queiroz, G.A.Monteiro, and D.M.Prazeres. 1999. Separation and analysis of plasmid denatured forms using hydrophobic interaction chromatography. *Anal. Biochem.* 275:122-124.

23. Dixon,M. and E.C.Webb. 1961. Enzyme fractionation by salting-out: a theoretical note. *Adv. Protein Chem.* 16:197-219.

24. Dock-Bregeon,A.C., B.Chevrier, A.Podjarny, J.Johnson, J.S.de Bear, G.R.Gough, P.T.Gilham, and D.Moras. 1989. Crystallographic structure of an RNA helix: [U(UA)6A]2. *J. Mol. Biol.* 209:459-474.

25. Draper,D.E. 2004. A guide to ions and RNA structure. *RNA.* 10:335-343.

26. Eastman,E.M. and R.H.Durland. 1998. Manufacturing and quality control of plasmid-based gene expression systems. *Adv. Drug Deliv. Rev.* 30:33-48.

27. Elimelech,M., J.Gregory, X.Jia, and R.A.Williams. 1995. Particle Deposition and Aggregation. Butterworth-Heinemann, Oxford.

28. Ferreira,G.N.M., J.M.S.Cabral, and D.M.F.Prazeres. 1997. A comparison of gel filtration chromatographic supports for plasmid purification. *Biotechnology Techniques* 11:417-420.

29. Ferreira,G.N.M., J.M.S.Cabral, and D.M.F.Prazeres. 1998. Monitoring of process streams in the large-scale production and purification of plasmid DNA for gene therapy applications. *Pharm. Pharmacol. Commun.* 5:57-59.

30. Flock,S., R.Labarbe, and C.Houssier. 1995. Osmotic effectors and DNA structure: effect of glycine on precipitation of DNA by multivalent cations. *J. Biomol. Struct. Dyn.* 13:87-102.

31. Flock,S., R.Labarbe, and C.Houssier. 1996. Dielectric constant and ionic strength effects on DNA precipitation. *Biophys. J.* 70:1456-1465.

32. Foster,P.R., P.Dunnill, and M.D.Lilly. 1973. The precipitation of enzymes from cell extracts of saccharomyces cerevisiae by polyethylene glycol. *Biochim. Biophys. Acta* 317:505-516.

33. Franklin,R.E. and R.G.Gosling. 1953a. Evidence for 2-chain helix in crystalline structure of sodium deoxyribonucleate. *Nature* 172:156-157.

34. Franklin,R.E. and R.G.Gosling. 1953b. Molecular structure of nucleic acids. Molecular configuration in sodium thymonucleate. *Nature* 171:740-741.

35. Frigerio,N.A. and T.P.Hettinger. 1962. Protein solubility in solvent mixtures of low dielectric constant. *Biochim. Biophys. Acta* 59:228-230.

36. Fuchs,N. 1934. Uber die stabilitat und aufladung der aerosale. *Z. Physik. Chem.* 89:736-743.

37. Gao,X. and L.Huang. 1995. Cationic liposome-mediated gene transfer. *Gene Ther.* 2:710-722.

38. Gosule,L.C. and J.A.Schellman. 1976. Compact form of DNA induced by spermidine. *Nature* 259:333-335.

39. Hardy,W.B. 1900. A preliminary investigation of the conditions which determine the stability of irreversible hydrosols. *Proc. R. Soc. Lond.* 66:110-125.

40. Harries,D., S.May, and A.Ben-Shaul. 2003. Curvature and Charge Modulations in Lamellar DNA-Lipid Complexes. *J. Phys. Chem.* 107:3624-3630.

41. Hoffmeister,F. 1888. Zur Lehre von der Wirkung der Salze. *Arch. Exp. Pathol. Pharmakol* 24:247.

42. Holmes,D.S. and M.Quigley. 1981. A rapid boiling method for the preparation of bacterial plasmids. *Anal. Biochem.* 114:193-197.

43. Hoopes,B.C. and W.R.McClure. 1981. Studies on the selectivity of DNA precipitation by spermine. *Nucleic Acids Res.* 9:5493-5504.

44. Horn,N.A., J.A.Meek, G.Budahazi, and M.Marquet. 1995. Cancer gene therapy using plasmid DNA: purification of DNA for human clinical trials. *Hum. Gene Ther.* 6:565-573.

45. Imanaka,T. and S.Aiba. 1981. A perspective on the application of genetic engineering: stability of recombinant plasmid. *Ann. N. Y. Acad. Sci.* 369:1-14.

46. Israelachvili,J.N. 1992. Intermolecular and Surface Forces. Academic Press, San Diego.

47. Iyer,H.V. and T.M.Przybycien. 1995. Metal affinity protein precipitation: effects of mixing, protein concentration, and modifiers on protein fractionation. *Biotechnol. Bioeng.* 48:324-332.

48. Jolly,D. 1994. Viral vector systems for gene therapy. *Cancer Gene Ther.* 1:51-64.

49. Juckes,I.R. 1971. Fractionation of proteins and viruses with polyethylene glycol. *Biochim. Biophys. Acta* 229:535-546.

50. Labarca,C. and K.Paigen. 1980. A simple, rapid, and sensitive DNA assay procedure. *Anal. Biochem.* 102:344-352.

51. Lahijani,R., G.Hulley, G.Soriano, N.A.Horn, and M.Marquet. 1996. High-yield production of pBR322-derived plasmids intended for human gene therapy by employing a temperature-controllable point mutation. *Hum. Gene Ther.* 7:1971-1980.

52. Lander,R.J., M.A.Winters, F.J.Meacle, B.C.Buckland, and A.L.Lee. 2002. Fractional precipitation of plasmid DNA from lysate by CTAB. *Biotechnol. Bioeng.* 79:776-784.

53. Lee, A. L. and Sagar, S. Method for large scale plasmid purification. US06197553. 2001. (patent)

54. Lerman,L.S. 1971. A transition to a compact form of DNA in polymer solutions. *Proc. Natl. Acad. Sci. U. S. A* 68:1886-1890.

55. Levy,M.S., P.Loftian, R.O'Kennedy, M.Y.Lo-Yim, and P.Ayazi-Shamlou. 2000. Quantitation of supercoiled circular content in plasmid DNA solutions using a fluorescence-based method. *Nucleic Acids Research* 28:e57.

56. Lis,J.T. 1980. Fractionation of DNA fragments by polyethylene glycol induced precipitation. *Methods Enzymol.* 65:347-353.

57. Lis,J.T. and R.Schleif. 1975. Size fractionation of double-stranded DNA by precipitation with polyethylene glycol. *Nucleic Acids Res.* 02:383-389.

58. Livak,K.J., S.J.Flood, J.Marmaro, W.Giusti, and K.Deetz. 1995. Oligonucleotides with fluorescent dyes at opposite ends provide a quenched probe system useful for detecting PCR product and nucleic acid hybridization. *PCR Methods Appl.* 4:357-362.

59. London,F. 1937. The General Theory of Molecular Forces. *Trans. Faraday Soc.* 33:8-26.

60. Mahadevan,H. and C.K.Hall. 1992a. Experimental analysis of protein precipitation by polyethylene glycol and comparison with theory. *Fluid Phase Equilibria* 78:297-321.

61. Mahadevan,H. and C.K.Hall. 1992b. Theory of precipitation of protein mixtures by nonionic polymer. *AiChE Journal* 38:573-591.

62. Manning,G.S. 1969. Limiting laws and counterion condensation in polyelectrolyte solutions I. colligative properties. *J. Chem. Phys.* 51:924-933.

63. Manning,G.S. 1978. The molecular theory of polyelectrolyte solutions with applications to the electrostatic properties of polynucleotides. *Q. Rev. Biophys.* 11:179-246.

64. Marmur,J. and P.Doty. 1959. Heterogeneity in deoxyribonucleic acids 1.Dependence on composition of the configurational stability of deoyribonucleic acids. *Nature* 183:1427-1429.

65. Marquet,M., N.A.Horn, and J.A.Meek. 1995. Process development for the manufacture of plasmid DNA vectors for use in gene therapy. *BioPharm*26-37.

66. Melander,W. and C.Horvath. 1977. Salt effect on hydrophobic interactions in precipitation and chromatography of proteins: an interpretation of the lyotropic series. *Arch. Biochem. Biophys.* 183:200-215.

67. Middaugh,C.R., R.K.Evans, D.L.Montgomery, and D.R.Casimiro. 1998. Analysis of plasmid DNA from a pharmaceutical perspective. *J. Pharm. Sci.* 87:130-146.

68. Milburn,P., J.Bonnerjea, M.Hoare, and P.Dunnill. 1990. Selective flocculation of nucleic acids, lipids, and colloidal particles from a yeast cell homogenate by polyethyleneimine, and its scale-up. *Enzyme Microb. Technol.* 12:527-532.

69. Murphy,J.C., J.A.Wibbenmeyer, G.E.Fox, and R.C.Willson. 1999. Purification of plasmid DNA using selective precipitation by compaction agents. *Nat. Biotechnol.* 17:822-823.

70. Murthy,V.L. and G.D.Rose. 2000. Is counterion delocalization responsible for collapse in RNA folding? *Biochemistry* 39:14365-14370.

71. Oefner,P.J., S.P.Hunicke-Smith, L.Chiang, F.Dietrich, J.Mulligan, and R.W.Davis. 1996. Efficient random subcloning of DNA sheared in a recirculating point-sink flow system. *Nucleic Acids Res.* 24:3879-3886.

72. Ogston,A.G. 1962. Some thermodynamic relationships in ternary systems, with special reference to the properties of systems containing hyaluronic acid and protein. *Arch. Biochem. Biophys.* Suppl 1:39-51.

73. Olmsted,M.C. and P.J.Hagerman. 1994. Excess counterion accumulation around branched nucleic acids. *J. Mol. Biol.* 243:919-929.

74. Olvera de la Cruz,M.L., L.Belloni, M.Delsanti, J.P.Dalbiez, O.Spalla, and M.Drifford. 1995. Precipitation of highly charged polyelectrolyte solutions in the presence of multivalent cations. *J. Chem. Phys.* 103:5781-5791.

75. Paithankar,K.R. and K.S.Prasad. 1991. Precipitation of DNA by polyethylene glycol and ethanol. *Nucleic Acids Res.* 19:1346.

76. Parsegian,V.A., R.P.Rand, and D.C.Rau. 2000. Osmotic stress, crowding, preferential hydration, and binding: A comparison of perspectives. *Proc. Natl. Acad. Sci. U. S. A* 97:3987-3992.

77. Polosn,A., G.M.Potgieter, J.F.Largier, G.E.Mears, and F.J.Joubert. 1964. The fractionation of protein mixtures by linear polymers of high molecular weight. *Biochim. Biophys. Acta* 82:463-475.

78. Porschke,D., J.M.Burke, and N.G.Walter. 1999. Global structure and flexibility of hairpin ribozymes with extended terminal helices. *J. Mol. Biol.* 289:799-813.

79. Post,C.B. and B.H.Zimm. 1982. Theory of DNA condensation: collapse versus aggregation. *Biopolymers* 21:2123-2137.

80. Prazeres,D.M., G.N.Ferreira, G.A.Monteiro, C.L.Cooney, and J.M.Cabral. 1999. Large-scale production of pharmaceutical-grade

plasmid DNA for gene therapy: problems and bottlenecks. *Trends Biotechnol.* 17:169-174.

81. Prazeres,D.M., T.Schluep, and C.Cooney. 1998. Preparative purification of supercoiled plasmid DNA using anion-exchange chromatography. *J. Chromatogr. A* 806:31-45.

82. Przybycien,T.M. and J.E.Bailey. 1989. Aggregation kinetics in salt-induced protein precipitation. *AiChE Journal* 35:1779-1790.

83. Qiagen. Mega and Giga Protocol, Qiagen Plamid Purification Handbook, 17-18. 1998.

84. Rant,U., K.Arinaga, T.Fujiwara, S.Fujita, M.Tornow, N.Yokoyama, and G.Abstreiter. 2003. Excessive counterion condensation on immobilized ssDNA in solutions of high ionic strength. *Biophys. J.* 85:3858-3864.

85. Raspaud,E., d.l.C.Olvera, J.L.Sikorav, and F.Livolant. 1998. Precipitation of DNA by polyamines: a polyelectrolyte behaviour. *Biophys. J.* 74:381-393.

86. Record,M.T., Jr., C.P.Woodbury, and T.M.Lohman. 1976. Na+ effects on transition of DNA and polynucleotides of variable linear charge density. *Biopolymers* 15:893-915.

87. Rosenfeld,M.A., K.Yoshimura, B.C.Trapnell, K.Yoneyama, E.R.Rosenthal, W.Dalemans, M.Fukayama, J.Bargon, L.E.Stier, L.Stratford-Perricaudet, and . 1992. In vivo transfer of the human cystic fibrosis transmembrane conductance regulator gene to the airway epithelium. *Cell* 68:143-155.

88. Roy,K.B., T.Antony, A.Saxena, and H.B.Bohidar. 1999. Ethanol-induced condensation of calf thymus DNA studied by laser light scattering. *J. Phys. Chem. B* 103:5117-5121.

89. Rush,M.G. and R.C.Warner. 1970. Alkali denaturation of covalently closed circular duplex deoxyribonucleic acid. *J. Biol. Chem.* 245:2704-2708.

90. Salt,D.E., S.Hay, O.R.T.Thomas, M.Hoare, and P.Dunnill. 1995. Selective flocculation of cellular contaminants from soluble proteins using polyethyleneimine: a study of several organisms and polymer molecular weights. *Enzyme Microb. Technol.* 17:107-113.

91. Sambrook,J., E.F.Fritsch, and T.Maniatis. 1989. *Molecular cloning – a laboratory manual*, 2nd ed. Cold Spring Harbor Laboratory Press, Cold Spring Harbor, NY..

92. Sayers,J.R., D.Evans, and J.B.Thomson. 1996. Identification and eradication of a denatured DNA isolated during alkaline lysis-based plasmid purification procedures. *Anal. Biochem.* 241:186-189.

93. Schneider,B., K.Patel, and H.M.Berman. 1998. Hydration of the phosphate group in double-helical DNA. *Biophys. J.* 75:2422-2434.

94. Schorr,J., P.Moritz, T.Seddon, and M.Schleef. 1995. Plasmid DNA for human gene therapy and DNA vaccines. Production and quality assurance. *Ann. N. Y. Acad. Sci.* 772:271-273.

95. Seo,J.H. and J.E.Bailey. 1985. Effects of recombinant plasmid content on the growth properties and cloned gene product formation in E. coli. *Biotechnol. Bioeng.* 27:1668-1674.

96. Shih,Y.C., J.M.Prausnitz, and H.W.Blanch. 1992. Some characteristics of protein precipitation by salts. *Biotechnol. Bioeng.* 40:1155-1164.

97. Singer,V.L., L.J.Jones, S.T.Yue, and R.P.Haugland. 1997. Characterization of PicoGreen reagent and development of a fluorescence-based solution assay for double-stranded DNA quantitation. *Anal. Biochem.* 249:228-238.

98. Sizemore,D.R., A.A.Branstrom, and J.C.Sadoff. 1997. Attenuated bacteria as a DNA delivery vehicle for DNA-mediated immunization. *Vaccine* 15:804-807.

99. Smoluchowski,M. 1917. Versuch einer mathematischen Theorie der Koagulationskinetic kolloider Lsungen. *Z. Physik. Chem.* 92:129-168.

100. Tang,D.C., M.DeVit, and S.A.Johnston. 1992. Genetic immunization is a simple method for eliciting an immune response. *Nature* 356:152-154.

101. USFDA Center for Biologics Evaluation and Research. Points to consider in the characterization of cell lines used to produce biologicals. 1993.

102. Varley,D.L., A.G.Hitchcock, A.M.Weiss, W.A.Horler, R.Cowell, L.Peddie, G.S.Sharpe, D.R.Thatcher, and J.A.Hanak. 1999. Production of plasmid DNA for human gene therapy using modified alkaline cell lysis and expanded bed anion exchange chromatography. *Bioseparation.* 8:209-217.

103. Vasilevskaya,V.V., A.R.Khokhlov, Y.Matsuzawa, and K.Yoshikawa. 1995. Collapse of single DNA molecule in poly(ethylene glycol) solutions. *J. Chem. Phys.* 102:6595-6602.

104. Verwey,E.J. and J.T.G.Overbeek. 1948. Theory of the stability of lyophobic colloids. Elsevier, Amsterdam.

105. Vile,R.G. and S.J.Russell. 1995. Retroviruses as vectors. *Br. Med. Bull.* 51:12-30.

106. Vipond,I.B., G.S.Baldwin, and S.E.Halford. 1995. Divalent metal ions at the active sites of the EcoRV and EcoRI restriction endonucleases. *Biochemistry* 34:697-704.

107. Votavova,H., D.Kucerova, J.Felsberg, and J.Sponar. 1986. Changes in conformation, stability and condensation of DNA by univalent and divalent cations in methanol-water mixtures. *J. Biomol. Struct. Dyn.* 4:477-489.

108. Watson,J.D. and F.H.C.Crick. 1953. Molecular structure of nucleic acids. *Nature* 171:737-738.

109. Wilkins,M.H., A.R.Strokes, and H.R.Wilson. 1953. Molecular structure of deoxypentose nucleic acids. *Nature* 171:738-740.

110. Wilson,G.G. and N.E.Murray. 1991. Restriction and modification systems. *Annu. Rev. Genet.* 25:585-627.

111. Wilson,R.W. and V.A.Bloomfield. 1979. Counterion-induced condesation of deoxyribonucleic acid. a light-scattering study. *Biochemistry* 18:2192-2196.

112. Wolff,J.A., R.W.Malone, P.Williams, W.Chong, G.Acsadi, A.Jani, and P.L.Felgner. 1990. Direct gene transfer into mouse muscle in vivo. *Science* 247:1465-1468.

113. Yang,W.K. and D.C.Henley. 1991. A simple and economical procedure for large-scale plasmid DNA isolation. *Nucleic Acids Res.* 19:2507-2508.

APPENDIX I. EXAMPLE TEMPLATE FOR SINGLE-COMPONENT SOLUBILIY EXPERIMENTS

chromosomal DNA in CaCl2 - Experimental Protocol

Stock Solutions:	[NA] =	398 µg/ mL
	source lot	PMM2-105
	[High Salt Stock] =	1000 mM
	[Low Salt Stock] =	100 mM
Final Formulation Volume =		200 µL

Effect of Salt Concentration

[Final NA] =	50	µg/ mL
NA Vol =	25	µL
pH =	8	

Solubility Sample Series :

[Salt] =	**-**	**mM**
Low Salt Vol =	-	µL
10 mM Tris =	175	µL
[Salt] =	**1**	**mM**
Low Salt Vol =	2	µL
10 mM Tris =	173	µL
[Salt] =	**5**	**mM**
Low Salt Vol =	10	µL
10 mM Tris =	165	µL
[Salt] =	**10**	**mM**
Low Salt Vol =	20	µL
10 mM Tris =	155	µL
[Salt] =	**50**	**mM**
Low Salt Vol =	100	µL
10 mM Tris =	75	µL
[Salt] =	**100**	**mM**
High Salt Vol =	20	µL
10 mM Tris =	155	µL
[Salt] =	**200**	**mM**
High Salt Vol =	40	µL
10 mM Tris =	135	µL
[Salt] =	**500**	**mM**
High Salt Vol =	100	µL
10 mM Tris =	75	µL

APPENDIX II. REACTION KINETICS RATE LAWS

For the reaction $N \rightarrow P$

(e.g. in a precipitation reaction N is the soluble form and P the precipitated form)

differential and integrated rate laws for different order reactions are shown in the following table:

Reaction Order	Differential Rate Law	Integrated Rate Law	Characteristic Kinetic Plot
0	$-d[N] / dt = k$	$[N(t)] = [N(0)] - kt$	[N] vs. t
1	$-d[N] / dt = k[N]$	$[N(t)] = [N(0)]e^{-kt}$	ln[N] vs. t
2	$-d[N] / dt = k[N]^2$	$[N(t)] = [N(0)] / (1 + [N(0)] kt)$	1/[N] vs. t